Impact of Cdr1as and miR-7 network on synaptic transmission of mouse cortical neurons

Inaugural-Dissertation

to obtain the academic degree

Doctor rerum naturalium (Dr. rer. nat.)

submitted to the Department of Biology, Chemistry, Pharmacy

of Freie Universität Berlin

by

Cledi Alicia Cerda Jara

2023

The present work was carried out under the supervision of Prof. Dr. Nikolaus Rajewsky from February 2016 to February 2023 at the Berlin Institute for medical Systems Biology in the Max Delbrück Center for Molecular Medicine in the Helmholtz Association.

I declare that the work presented here is entirely my own, this thesis has been composed solely by myself and that it has not been submitted in any previous application for a degree.

1st reviewer: Prof. Dr. Nikolaus Rajewsky

2nd reviewer: Prof. Dr. Markus Wahl

date of defense: 14th of December 2023

Table of Contents

Abstract

The correct development and connectivity of synapses is essential for the function of the central nervous system especially for synaptic plasticity, the brain capacity to adjust to changes through the development of post-natal synapses that ensure the long-term storage of sensory experiences. To guarantee that the inputs are translated into long-lasting changes in synapse structure and function, gene expression programs must be tightly regulated. The brain is characterized by abundant expression of several types of regulatory RNA species, such as lncRNAs, miRNAs and circular RNAs (circRNAs), which would regulate local and coordinated transcriptional and post-transcriptional regulation of gene expression.

Cdr1as, is a mammalian-conserved, highly expressed, brain-enriched circRNA. It is predominantly expressed in excitatory neurons across cortex and moreover, strong evidence has shown a role of Cdr1as in normal brain function, arising as the most interesting candidate to study circRNA-exclusive action in brain. Cdr1as is regulated by a complex RNA network, that include several other non-coding RNAs. miR-7 is the main interactor in Cdr1as ncRNA network, is also evolutionarily conserved across vertebrates and considered to be a prototypical neuroendocrine miRNA. Nonetheless, the molecular interplay between Cdr1as and mir-7 in cortex neurons and their exact role in synaptic function is not yet understood.

Here, we demonstrate that sustained neuronal depolarization induces the transcriptional up-regulation of Cdr1as and post-transcriptional stabilization of mature miR-7. We reveal a direct link between Cdr1as expression and regulation of glutamatergic transmission, which translated into dysfunctional bursting and network activity. We show how long-term overexpression of miR-7 is sufficient to rescue abnormal glutamate release and neuronal activity and decreases the number of Cdr1as molecules in neuronal projections. The lack of Cdr1as enhances direct and indirect global transcriptomic changes caused by miR-7 overexpression and specifically regulates secretion and synaptic plasticity pathways. Together, our results reveal that in cortical neurons miR-7 has a conserved role influencing secretion pathways, that is surveilled by Cdr1as, and the imbalance of Cdr1as-miR-7 buffer system directly affects glutamate transmission and neuronal connectivity, responsible for long-lasting alterations and plastic synaptic adaptations.

__Zusammenfassung__

Die korrekte Entwicklung und Vernetzung von Synapsen ist für die Funktion des Zentralnervensystems von entscheidender Bedeutung. Insbesondere für die synaptische Plastizität, der Fähigkeit des Gehirns, sich durch die Entwicklung von post-natalen Synapsen an Veränderungen anzupassen, die die langfristige Speicherung sensorischer Erfahrungen gewährleisten, spielt dies einen bedeutende Rolle. Um sicherzustellen, dass Signale in dauerhafte Veränderungen der Synapsenstruktur und -funktion umgesetzt werden, müssen die Genexpressionsprogramme streng reguliert werden. Das Gehirn ist bekannt für die hohe Expression verschiedener Arten von regulatorischen RNAs, wie lncRNAs, miRNAs und zirkuläre RNAs (circRNAs), die die lokale und koordinierte, transkriptionelle und post-transkriptionelle Regulierung der Genexpression steuern.

Cdr1as ist eine bei Säugetieren konservierte, hoch exprimierte und im Gehirn angereicherte circRNA. Es wurde gezeigt, dass sie vorwiegend in exzitatorischen Neuronen im Vorderhirn exprimiert wird, und darüber hinaus gibt es starke Hinweise auf eine Rolle von Cdr1as bei der normalen Gehirnfunktion, was sie zum interessantesten Kandidaten für die Untersuchung der circRNA-exklusiven Wirkung im Gehirn macht. Cdr1as wird durch ein komplexes RNA-Netzwerk reguliert, zu dem auch mehrere andere nicht-kodierende RNAs gehören. miR-7 als der wichtigste Interaktionspartner im ncRNA-Netzwerk von Cdr1as, ist evolutionär über alle Wirbeltiere hinweg konserviert und gilt als prototypische neuroendokrine miRNA, obwohl die Rolle von miR-7 in nicht-endokrinen Drüsen nur rudimentär untersucht wurde. Das molekulare Zusammenspiel zwischen Cdr1as und mir-7 in Neuronen des Vorderhirns und ihre genaue Rolle bei der synaptischen Funktion sind noch ungeklärt.

Hier zeigen wir, dass eine anhaltende neuronale Depolarisation den transkriptionellen Anstieg von Cdr1as und die post-transkriptionelle Stabilisierung von der reifen miR-7 induziert. Wir können zum ersten Mal eine direkte Verbindung zwischen der Cdr1as-Expression und der Regulierung der glutamatergen Übertragung demonstrieren, die sich in dysfunktionalen neuronalen Ausbrüchen und Netzwerkaktivitäten niederschlägt. Wir zeigen, dass eine langfristige Überexpression von miR-7 ausreicht, um abnormale Glutamatfreisetzung und neuronale Aktivität zu retten, und dass die Anzahl der Cdr1as-Moleküle in neuronalen Projektionen abnimmt. Das Fehlen von Cdr1as verstärkt direkte und indirekte globale transkriptomische,Veränderungen, die durch die Überexpression von miR-7 verursacht werden, und reguliert spezifisch Sekretions- und synaptische Plastizitätswege. Unsere Ergebnisse zeigen, dass miR-7 in den Neuronen des Vorderhirns eine konservierte Rolle bei der Beeinflussung der Sekretionswege spielt, die von Cdr1as überwacht wird. Das Ungleichgewicht des Cdr1as-miR-7-Puffersystems wirkt sich direkt auf die Glutamatübertragung und die neuronale Konnektivität aus und ist für langanhaltende Veränderungen und plastische synaptische Anpassungen verantwortlich.

Abbreviations

3'UTR	three prime untranslated region
AAV	Adeno-associated virus
AGO	Argonaute
AMPAR	α-amino-3-hydroxy-5-methyl-4-isoxazolepropionic acid receptor
AP	Action potential
AP5	(2R)-amino-5-phosphonovaleric acid
bp	Base pairs
C57BL/6N	C57 black 6N - inbred strain of laboratory mouse
Ca2+	Calcium ions
CamKII	Ca2+/calmodulin-dependent protein kinase II
Cdr1	Cerebellar degeneration-related protein 1
Cdr1as	Cerebellar degeneration-related protein 1 antisense RNA
Cdr1os	Cerebellar degeneration-related protein 1 opposite strand
circRNA	Circular ribonucleic acid
Cl-	chloride ion
CNS	Central nervous system
CNXQ	cyanquixaline
CREB	cAMP response element-binding protein
DGCR8	DiGeorge syndrome critical region 8 (micropossesor subunit)
DIV	days in vitro
dpi	days post infection
DRB	5,6-Dichloro-1-β-D-ribofuranosylbenzimidazole
EPSC	excitatory post-synaptic currents
EZH2	Enhancer of zeste homolog 2
FISH	fluorescent *in situ* hybridization
FMR1	Fragile X Messenger Ribonucleoprotein 1
GABA	γ-Aminobutyric acid
Gli3	Zinc finger protein
GluSnFR	Glutamate-sensitive fluorescent reporter
GO	gene ontology
HIT-CLIP	High-throughput sequencing of RNA isolated by crosslinking immunoprecipitation
hSyn	human synapsin
HuR	human antigen R
Hz	hertz
IEG	Immediate early gene
IGF2BP3	Insulin Like Growth Factor 2 MRNA Binding Protein 3,
Igsf8	Immunoglobulin Superfamily Member
ISI CoV	Interspike coefficient of variation
K+	Potassium ion
KAR	Kainic acid receptor
KCl	potassium clohoride
KO	Knock out
L2FC	log2 fold change
lncRNA	long non-coding ribounucleic acid
LTP	long-term potentiation
MAPK	Mitogen-activated protein kinase

MEF2	myocyte enhancer factor-2
mGluR	Metabotropic glutamate receptor
miR-671	MicroRNA-671
miR-7	MicroRNA-7
miRNA	micro ribonucleic acid
MNN	mutital nearests neighbours
mRNA	messenger ribonucleic acid
Na+	Sodium ion
ncRNA	Non-coding RNA
nk2.1	NK2 homeobox 1
NMDAR	N-methyl-D-aspartate receptor
NT	neurotransmitter
nt	nucleotides
nt	nucleotides
OIP5-AS1	Opa Interacting Protein 5 antisense RNA 1
otp	Orthopedia Homeobox
P0	post natal day 0
p53	cellular tumor antigen p53
PCR	polymerase chain reaction
PI3K	Phosphoinositide 3-kinase
PKC	Protein Kinase C
PLL	Poly-L-Lysine
PMA	phorbol 12-myristate 13-acetate
PNK	polynucleotide 5'-hydroxyl-kinase
PRC2	polycomb repressive complex 2
qPCR	quantitative real time PCR
Rbfox	Fox-1 homolog
RLU	Relative light unit
RNA	Ribonucleic acid
RNA-Seq	RNA sequeicing
RNP	Ribonucleoprotein
rx	Retinal homeobox protein
Sim1	Single-minded homolog 1
SNARES	Soluble N-ethylmaleimide-Sensitive Factor Attachment Protein Receptor
Snca	Synuclein Alpha gene
snRNP	small nuclear ribonucleoproteins
TF	transcription factor
TTX	Tetrodotoxin
UBE2A	ubiquitin protein ligase A
UNG	Uracil-DNA glycosylase
UTR	untraslated region
VAMP2	Vesicle Associated Membrane Protein 2
WT	wild type

List of Figures

Introduction

1. Brain Plasticity Regulation

1.1 Nerve Cells and synaptic transmission

The human brain possesses ~86 billion neurons that communicate with one another through very precise connections (Herculano-Houzel, 2012). The correct development and connectivity of synapses are essential for the function of the central nervous system (CNS).

Nerve cells or neurons are the functional unit of the nervous system where the main signal is electrical within the cell, and chemical among them. Neurons are highly specialized cells that are very variable in size, shape, and electrical properties (Kandel et al., 2021). In mammals, neurons main anatomical components are: (1) a condensed cell body (soma), where transcription and most of protein translation occurs. (2) Dendrites, which are branched out cellular extensions where most of the inputs form other cells are received, through the dendritic spines. (3) The axon, a single projection that can extend the longest and where the electrical signal is carried away from the soma to other neurons, muscles or glands through terminal buttons, where junctions with other cells are formed (Donato et al., 2019; Kandel et al., 2021).

In these projections, the neurons possess specialized receptors which receive the input from other cells or other external signals, that activate an electrical all-or-none impulse called action potential (AP), which can be propagated along the axon to release a chemical neurotransmitter (NT), at its target site, the synapse (Kandel et al., 2021). In brief, a pre-synaptic AP triggers the release of NT through exocytosis, these NT diffuse across synaptic clefts to bind and activate receptors in post-synaptic cells, allowing the amplification of the pre-synaptic signal (Burns & Augustine, 1995).

Each neuron is part of a circuit modulating larger behavioral functions, therefore understanding the way these circuits are elaborated will allow us to explain more complex processes. The strength of neuronal connection can vary and be modified by behavior, experience, and context, throughout a variety of mechanisms, resulting from the activity of the synapses itself or extrinsic modulator factors (Kandel et al., 2021).

Another type of cells in the nervous system are glial cells, which support neurons by several means: (1) provide insulation to allow proper propagation of the AP, (2) control

the environment for the neurons to operate and (3) couple neural activity to the vascular system. The largest difference between cells in the nervous system is at the molecular level such as the different expression of ionotropic and metabotropic receptors, enzymes, ion channels and neurotransmitters. These differences are the foundation for understanding why some diseases affect some cells and not others (Araque & Navarrete, 2010).

1.2 Synaptic integration and modulation

Generally, central neurons integrate excitatory and inhibitory synaptic inputs throughout the whole nervous system. Glutamate is the most abundant excitatory NT while gamma-Aminobutyric acid (GABA) constitutes most of the inhibitory signals. Glutamate signals through ionotropic (AMPAR, NMDAR, KAR) and metabotropic receptors (mGluR) activation. For ionotropic receptors glutamate opens a non-selective cation channel permeable equally to potassium (K^+) and sodium cations (Na^+). In particular, NMDAR only conducts signals when glutamate is released and the post-synaptic membrane is sufficiently depolarized. As a result, Ca^{2+} influx during strong synaptic activation can trigger intracellular signaling cascades leading to long term potentiation (LTP) and memory storage in neurons (Figure 1a). Concerning inhibitory signals, GABA, actions through ionotropic ($GABA_A$, $GABA_B$) and metabotropic receptors ($GABA_C$). The binding of GABA activates chloride (Cl^-) selective channels, which hyperpolarize the cell membrane away from an AP threshold (Figure 1b) (Kandel et al., 2021).

a
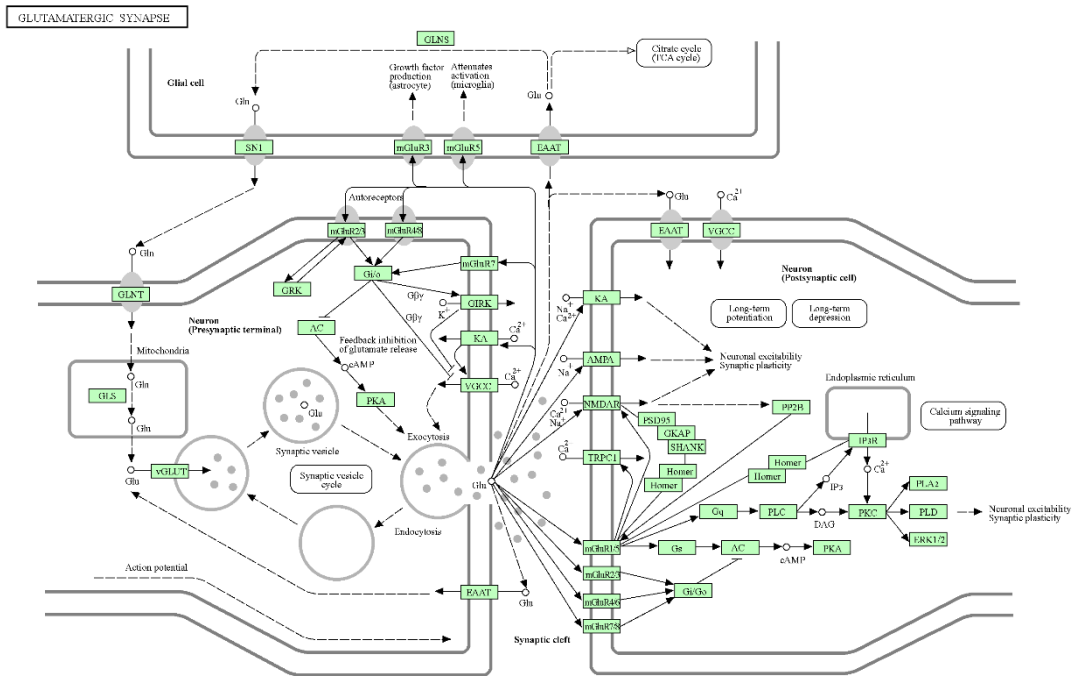
b
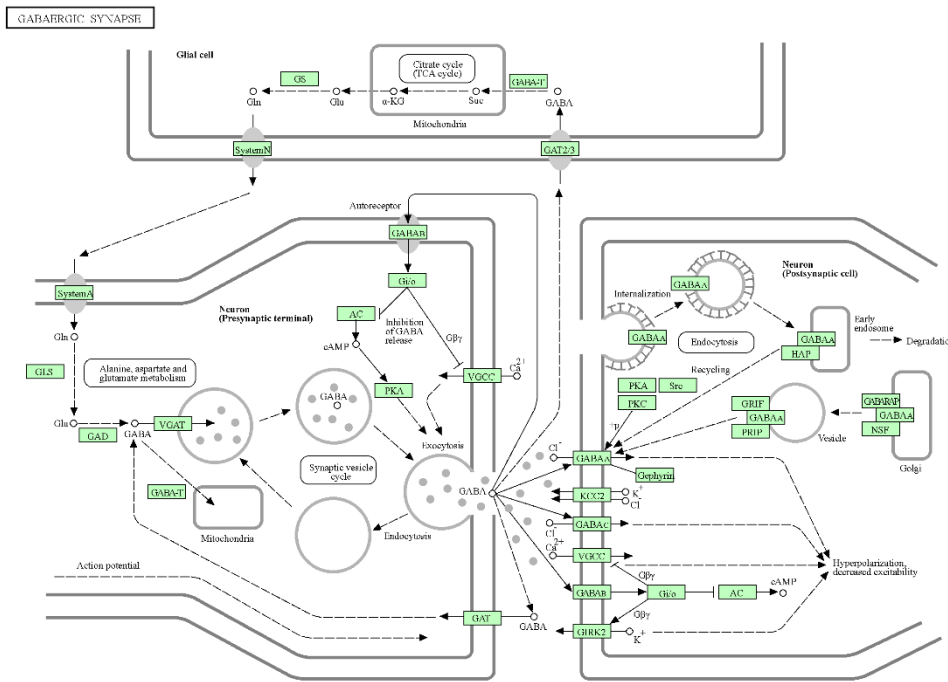
Figure 1. Main neuronal signaling pathways in cortex.
(a) Glutamatergic and (b) GABAergic synapses activations, main CNS chemical connections.
Highlighted in green all involved receptors, ion channels and vesicle transporters.
Adapted from Kegg Pathways database.
Green: all relevant enzymes, receptors and channels involved in synaptic transmission.
Black arrows indicate canonical pathways of pre and post-synaptic intracellular signaling cascades.

The NT that are not reabsorbed by the pre-synaptic receptors nor metabolized, are consider as neuromodulators (histamine, dopamine, serotonin, norepinephrine, nitric oxide), which bind to metabotropic receptors and alter neuronal excitability, NT release or functional state of post-synaptic receptors. They activate second messengers to influence ion channels and other targets from distance release, in order to regulate diverse neural populations and produce long-lasting signals (Etherington et al., 2010; Spruston, 2008).

Therefore, the decision for the firing of an AP depends heavily on spatial and temporal summation of various inputs and is determined by the depolarization at the axon.

1.3. Neurotransmitter Release

While AP is controlled by Na^+ and K^+ conductance, NT release depends on depolarization of the pre-synaptic terminal, not ion channel opening. Depolarization opens voltage-gated Ca^{2+} channels concentrated in pre-synaptic active zones, close to the release sites, resulting in Ca^{2+} influx. Therefore, Ca^{2+} influx and NT release are tightly coupled: the peak of Ca^{2+} entry lags the AP and rapidly produce NT release in quantal packets, corresponding to a single synaptic vesicle, homogeneous in size and NT content. The unitary events are driven by the fusion of individual synaptic vesicles, which contain thousands of NT molecules. A typical pre-synaptic terminal involved in fast synaptic transmission contains 100-200 vesicles and most of the ready to use vesicles are docked to the pre-synaptic membrane of the active zone. After release, the vesicle can go back to the pre-synaptic terminal through endocytosis, which allows fast recycling and continuous supply during prolonged stimulation (Fon & Edwards, 2001; Henley, 2021; Kandel et al., 2021).

Exocytosis of synaptic vesicles occurs in rapid succession and is mediated by evolutionary conserved SNARE complex composed by pre-synaptic plasma membrane (Syntaxin and SNAP-25) and synaptic vesicle membrane (Synaptobrevin) proteins. Sinaptotagmins, are other critical players for NT release. These vesicular proteins act as Ca^{2+} sensors of release regulation and bind to the SNARE complex to enable quick fusion. Vesicle exocytosis is precise and rapid due to the action of active zone protein scaffolds that (1) tether vesicles to plasma membrane, (2) recruit Ca^{2+} channels, (3) facilitate SNARE complex assembly and (4) mediate short and long synaptic plasticity. Active zone scaffolding differs across synapses and species as well as Ca^{2+} channels expression and Synaptotagmins (Kandel et al., 2021).

Most importantly, NT release can be modulated intrinsically or extrinsically as part of synaptic plasticity. Intrinsic changes, as the firing pattern, cause diversity in synaptic strengths, known as synaptic depression or synaptic facilitation. On the other hand, extrinsic neuromodulator affects NT release dynamics, mainly on Ca^{2+} channel regulation or Ca^{2+}-dependent downstream events (Kandel et al., 2021).

1.4. Synaptic plasticity

All nerve cells have very similar intrinsic signaling properties. Therefore, differences and alterations in function must arise from the pattern of functional connections of these cells and how those are affected by environmental stimuli. Synaptic plasticity is the term used to describe the brain's capability to adjust to changes, through the development of post-natal synapses that will ensure the long-term storage of sensory experiences (Kandel, 2001).

The concept was introduced first by Donald Hebb and his theory claims that the repeated and persistent activation of a pre-synaptic cell tends to induce long-lasting cellular changes that will stabilize the correspondent connection with the post-synaptic cell (Morris, 1999). This mechanism would explain brain adaptation during learning and memory processes and is summarized by "Cells that fire together, wire together" (Hebb, 1949). Furthermore, this property has been later desaturated to guarantees that the inputs are translated into long-lasting changes in synaptic structure and function (Citri & Malenka, 2008; Kandel, 2001).

Elementary forms of synaptic plasticity, like memory or learning, are common to all animals with an evolved nervous system. Therefore, the underlying mechanisms must be conserved at the cell and molecular level and can be observed effectively in simple model systems. For example, each type of known learning or memory storage has two phases, a transient phase that lasts minutes and an enduring phase that lasts days. Subsequently, the conversion of short-term to long-term memory requires a precise spaced repetition. In addition, long-term memory differs from short-term memory in requiring the synthesis of new proteins, a biochemical mechanism that is conserved from very simple organisms until complex vertebrates. In general, short-term synaptic plasticity changes involve covalent modification of pre-existing proteins, leading to modification of pre-existing synaptic connections, whereas, long-term synaptic changes involve activation of gene expression, new protein synthesis and subsequent formation of new connections (Abraham & Bear, 1996; Kandel, 2001).

Learning processes involve synaptic signaling function recruiting different neuromodulators, which activate second messenger signaling pathways that induce transcriptional programs for neuronal growth and long-term changes. Additionally, these neuromodulators can mark specific synapses for long-term activation process and then regulate local protein synthesis for stabilization (Kandel, 2001).

According to Kandel studies, supporting Ramon y Cajal hypotheses, plasticity results from changes in the strength of the synaptic connections between precisely interconnected neurons. While the developmental program of an organism ensures that connections among neurons are invariant, it does not specify their strength. On the other hand, experience alters the effectiveness of these preexisting biochemical connections. For this reason, synaptic plasticity emerged as a fundamental mechanism for information storage by the CNS, built into the molecular architecture of synapses (Kandel, 2001).

In long-term plasticity processes the response of a synapse is not determined simply by its history of activity, but also by the history of transcriptional activation in the nucleus, due to the extensive dialog between synapses and nucleus. Therefore, local and coordinated transcriptional and post-transcriptional regulation of gene expression are critical mechanisms to guarantee the effectiveness of plasticity modifications. In this regard, the brain is well recognized by its abundant expression of several types of regulatory RNA species, such as lncRNAs, miRNAs and circular RNAs (circRNAs) (Schratt, 2009).

2.Transcriptional regulation and neuronal activity

2.1. Eukaryotic transcriptional regulation

Eukaryotic cells regulate their gene expression in many ways. Tight, space- and time-controlled gene regulation is key for successful development and differentiation programs in all kinds of cellular systems, especially in multicellular eukaryotic organisms, where different types of cells co-exist. The most widespread form of gene regulation happens at the level of transcription, where the concentration and rate of mRNA production are determined. Differential expression of cell type-specific proteins is mainly regulated by controlling transcription of corresponding genes in different tissues.

Transcriptional control operates at three levels: modulation of activators and repressors, changes in chromatin structure and assembly of initiation complexes. Eukaryotic transcription is controlled by transcription factors (TF), which can stimulate or repress transcription, by association with regulatory DNA sequences often located far away from the gene promoter elements (Lodish et al., 2008).

One promoter might be regulated by several TFs bound to alternative transcriptional control elements, which overall generate an intricate gene expression arrangement. Then, RNA Polymerase II enzyme will recognize several of these trans-acting interactions to locate the transcription start site, assemble the transcription complex and proceed with RNA synthesis (Lodish et al., 2008).

2.2. Neuronal activity-dependent genes

The brain expresses a larger number of genes than any other organ and different populations of neurons express diverse set of these genes. Therefore, the selective regulation of RNA expression allows a fixed number of genes to generate a much larger number of neuronal cell types and neuronal connections (Kandel et al., 2021).

The control of gene expression is especially relevant in response to extracellular or environmental stimuli, where genes are regulated by neuronal activity. Activity-mediated transcriptional gene regulation occurs as a result of: (1) NT release and subsequent synaptic signaling, (2) post-synaptic APs that induce the increase of intracellular Ca^{2+}, (3) ion channel activation resulting in changes in membrane signaling (Lyons & West, 2011; G. Schratt, 2009).

The genes upregulated by external neuronal stimulations are defined as immediate early genes (IEGs) and are the product of a first wave of transcriptional activation not altered by the presence of translation inhibitors (Cochran et al., 1983). Several studies demonstrated that IEGs can range from TFs to structural proteins and can be activated in very short (minutes) or larger time scales (hours) after stimulation. These genes are in control of normalizing neuronal activity or facilitating homeostasis, by regulating functions such as synaptic maturation, maintenance of synaptic plasticity or neuronal phenotype determination (Dudek, 2008). Even though many IEGs have been identified (i.e., c-Jun, c-Fos, FosB, Arc, Homer, MKP1, RGS2, BDNF, Cox2, Secretogranin), programs of induced genes expression are very diverse and highly dynamic, especially genes regulated as part of the plasticity transcriptome (Barth and Yassin, 2008).

2.3. Plasticity transcriptome

The subset of genes activated by neuronal activity depends on prior activity history of the neurons and likely, on developmental or maturation state and cell type. The cellular context in which activity occurs can change the content of the response and alter the downstream candidates that are induced (Guzowski et al., 2006).

Some regulatory models suggest that genes within the plasticity transcriptome may be temporarily upregulated and then suppressed by constant elevated neural activity (James et al., 2005, 2006). Additionally, different IEGs appear to have different thresholds of induction, depending on the duration and intensity of a stimulus. Different subsets of genes may be activated with the consequential cascades of gene expression resulting in diverse perturbations of cell function. Among all reported genes, c-fos has been shown to be the most consistent IEG, upregulated under mostly all conditions (Gallo et al., 2018; Guan et al., 2005), although, some specific neurons (cerebral cortex layer 5) show very high firing rates compared to other cells in different brain regions, without expressing c-fos *in vivo* under basal conditions of neural firing (Barth et al., 2004). These results imply that there is not a common activity-induced gene expression program and that the particular type of activity as well as the genetic background can significantly influence the genes that define the plasticity transcriptome (Barth and Yassin, 2008).

2.4. Transcription at the synapses

Activity-dependent transcriptional events happening in the nucleus can directly affect the neuronal function. Firstly, nuclear events such as phosphorylation of the activity-dependent transcription factors, can be detected within seconds to minutes of synaptic stimulation or depolarization, and transcription can occur within minutes following stimulation (Deisseroth et al., 1996). Processed mRNAs can travel at rates of 0.1mm/s (Köhrmann et al., 1999), and fast dendritic transport can range from 2–5 mm/s, meaning that the products of activity-dependent gene expression could conceivably reach synaptic sites within 15 minutes following stimulation (Barth & Yassin, 2008). For gene products that are active in the soma, timing from stimulus to change in cell function is accelerated, but many RNAs are have been found present at the synapses, implying that their transport might be constitutive or that new RNA transcripts accumulate at synaptic sites after stimulation (Middleton et al., 2019). The activity-regulated transcription may thus affect synaptic transmission site-specifically, by local

retaining of newly synthesized mRNAs in synapses or by a mechanism where newly synthesized mRNAs are broadly available to all synapses (Marie et al., 2005). Many of these activity-dependent genes do not have a clear synaptic function, but rather appear to alter cellular metabolism, protein stability, or neuronal excitability (Barth et al., 2004; Dudek, 2008; James et al., 2006).

In summary, nuclear transcription primes the cell to respond to future stimuli in a pathway-specific manner, combining local control of translation without the requirement of a specific mechanism for sorting mRNAs to individual synapses (Dudek, 2008).

3. Eukaryotic Post-transcriptional regulation in neurons

The initial primary RNA transcripts produced in eukaryotic nuclei are not functional, and require several processing steps including splicing, capping ends, editing to achieve their mature functional form and then be actively transported to cytoplasm. When in the cytoplasm, transcripts can be additionally regulated by controlling their stability, localization, and rate of translation. Post-transcriptional regulatory mechanisms, such as: RNA modifications, RNA binding proteins and RNPs complexes, miRNA-driven mRNA regulation, canonical and non-canonical splicing, provide intricate and precise layers of gene control beyond transcription rates (Lodish et al., 1999). Within mammalian cellular systems, the most complex and post-transcriptionally tightly regulated tissue is the brain (Bak et al., 2008; Morris & Mattick, 2014; Quattrone et al., 2001). The most influencing post-transcriptional regulations in the brain are the following:

3.1. Long 3'UTR in neurons

mRNAs consist in translated (coding) and untranslated regions at the 5' and 3' ends, which contain important regulatory elements necessary for RNA metabolic processes like localization, translation, degradation (Proudfoot & Brownlee, 1976). One relevant characteristic feature from brain RNA transcripts is their long 3'-untranslated regions (3'UTRs) (Hilgers et al., 2011; Miura et al., 2013).

In mammals, 3'UTRs are much longer in the brain, when compared to other tissues (Mayr, 2016). Even more, in the brain some 3'UTRs can exceed 20000 nucleotides (Miura et al., 2013). Specifically, neurons express the most variable and longest 3'-

ends among all cell types. The shift from short to long 3'UTRs happens during brain development and indicates a transition from transcriptional regulation of gene expression to mostly post-transcriptional mechanisms, as newly born neurons mature into post-mitotic highly specialized cells (Miura et al., 2013). This huge diversity in 3'-ends contributes to the fine regulation of relevant genes related to neuronal functions. It has been shown that in hippocampal neurons, enhanced neuronal activity promotes the expression of shorter 3'UTRs in some genes targeted by a TF of synapse development (Flavell & Greenberg, 2008).

This occurs by changing the canonical polyadenylation site choice in these target genes (Flavell et al., 2008). In 2013, the Dreyfuss lab showed that deletion of a single ribonucleoprotein (U1) recapitulated the activity-dependent signature of 3'UTR and proximal 3' exon shortening in mRNAs, characteristic of functionally activated neuronal cells. This observation demonstrated that splicing is a key regulatory factor for activity-dependent neuronal responses (Berg et al., 2012).

3'UTRs play an essential role in dendritic and axonal localization of transcripts and are used to activate RNA transport or local translation far away from neuronal soma or in response to specific stimuli. Longer 3'UTR harbor more miRNA binding sites, which are used as negative regulators of protein translation, therefore, abundance of miRNA binding sites, imply a decreased of the protein pool from these long 3'UTR RNA isoforms (Bae & Miura, 2020; Pereira et al., 2017; Rodrigues et al., 2016).

3.2. Ribonucleoprotein particles

The brain hosts diverse complexes of RNA and proteins, participating in post-transcriptional modifications in the form of neuronal granules, large ribonucleoprotein assemblies containing complexes of multiple proteins and RNA molecules (coding and non-coding). These complexes act as signals of communication that allow efficient transport of multiple RNAs along neurites, ensuring that the necessary components for synapsis modulation are placed in the right subcellular compartment at the appropriate time (Carson et al., 2008).

Other types of RNA-protein assemblies in the cell are: (1) processing bodies, thought to be the major sites of mRNA degradation, and (2) stress granules, transient structures formed upon stress conditions, protect cellular RNAs from degradation and liberating the translation machinery. (Anderson & Kedersha, 2006).

3.3. Alternative splicing

Alternative splicing consists in the precise selection of diverse 5'- and 3-'splice site pairs, that will generate a variable pool of mRNAs and proteins (Figure 2a). Splicing concerns approximately 95% of human multi exonic genes (Pan et al., 2008) and is highly conserved in the nervous system of vertebrates, which certainly contributes to the functional complexity of these tissues (Barbosa-Morais et al., 2012).

Cis- regulatory elements like 5'- and 3'-splice sites and poly-pyrimidine tract, guide the interaction between RNA and spliceosome machinery, but are not sufficient for correct alternative splicing regulation. Trans-regulatory splicing factors, such as splicing enhancers and silencers, are as well required for precise splicing control. Most of these splicing factors are widely expressed among tissues, but enriched in neural systems (Darnell, 2010). Regions in close proximity to splice sites (~300nt) have most of the predicted cis-regulatory features, are also enriched in RNA binding protein's binding sites and are more evolutionary conserved (Barash et al., 2010). Therefore, by understanding the combination of cis- and trans-regulatory features we could comprehend tissue-dependent alternative splicing patterns.

Alternative splicing is fundamental during neuronal development, and for the establishment and function of gene networks in many regulatory pathways in the CNS. Among them, neuronal migration, axonal and dendritic outgrowth, synaptic connections and neuronal plasticity are all refined and coordinated by spatio-temporal cross-talk among those gene networks. For example, protein from genes associated with axon guidance and synaptic roles, i.e. *Rbfox*, display different spatial and temporal patterns in brain development, thanks to the dynamic inclusion of neuronal-specific exons (Licatalosi & Darnell, 2010). Another example is the neuronal splicing factor Nova, which coordinates specific subsets of co-regulated exons within functionally related genes, known as splicing regulatory networks. Nova regulates neurotransmitter receptors, cation channels, adhesion and scaffold proteins, among others, in order to ensure the proper function of RNAs encoding proteins that interact at the synapse (Ule et al., 2005). Furthermore, mutations in RNA binding proteins involved in alternative splicing regulation or aberrant alternative splicing patterns in neurons have been linked to many neurological disorders, such us familial amyotrophic lateral sclerosis, paraneoplastic neurodegenerative disorders, spinal muscular atrophy, among others (Licatalosi & Darnell, 2006).

Brain-specific alternative splicing is the result from cumulative effects of several splicing factors and unique cis-regulatory elements, that include distally located sequences. Splicing regulators acting together in antagonist or synergistic ways might also contribute to alternative splicing differences between neuronal subtypes. Nevertheless, how specifically neural splice variants impact neuronal differentiation, morphology, maturation and synaptic activity and the extent of how neural alternative splicing events are functional is not yet fully understood (Q. Li et al., 2007).
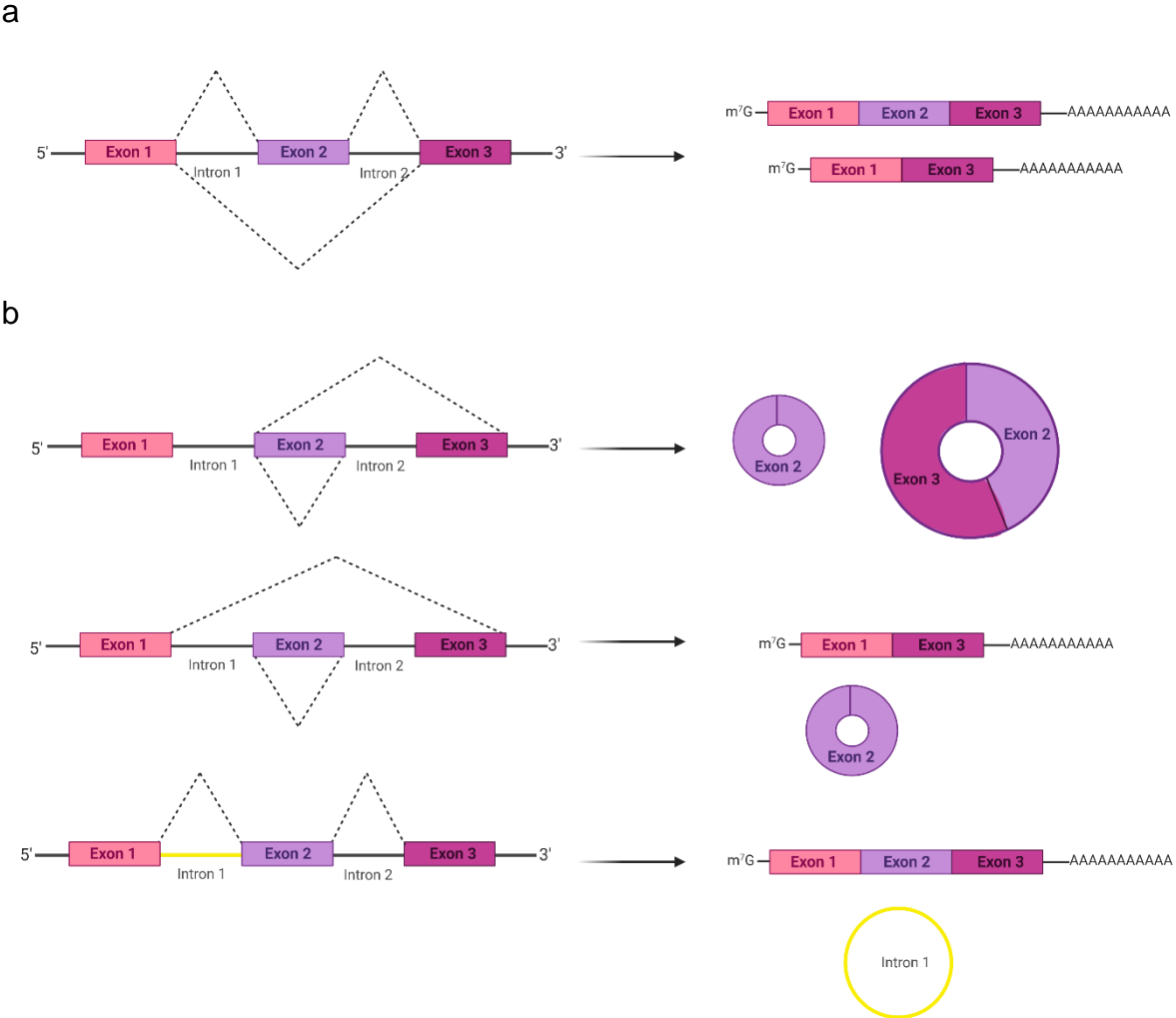
Figure 2. Alternative Splicing. Schematic representation of diverse 5'- and 3'-splice site pairs selection (dotted lines) during: (a) linear RNA alternative splicing and (b) circRNA alternative back-splicing and all possible resulting products.

3.4. Circular RNAs

Circular RNAs (CircRNAs) are an abundant and stable class of covalently closed RNAs, first observed in eukaryotic cells in the late 70's (M.-T. Hsu & Coca-Prados, 1979), and which oftentimes are tissue- and developmental stage-specifically expressed (Memczak et al. 2013). However, the actual biological role of only a handful of circRNAs has been deciphered so far.

3.4.1 circRNA biogenesis

circRNAs are generated by back-splicing of exons and introns from protein coding and non-coding precursor transcripts and their splicing is facilitated by flanking of long introns with conserved repetitive elements (Figure 2b) (Cocquerelle et al., 1992; Kristensen et al., 2019; Nigro et al., 1991).

Specifically, back-splicing occurs co-transcriptionally when an upstream branch point generates the looping of the intron and the base pairing between the inverted repeat elements (i.e Alu sequences in human). Alternatively, back-splicing can result from dimerization of RNA binding proteins (i.e QK1, ADAR). Both mechanisms bring a downstream splice-donor site into close proximity with an upstream splice-acceptor site. Subsequently, the splice-donor site attacks an upstream splice-acceptor site which results in the formation of exon–intron circRNAs or exonic circRNAs. This association is facilitated by the canonical splicing machinery and competes with linear mRNA splicing (Ashwal-Fluss et al., 2014; Conn et al., 2015; Ivanov et al., 2015; Jeck et al., 2013; X.-O. Zhang et al., 2014). Alternatively, circRNAs can also be formed from intronic lariat precursors that escape from the debranching step of canonical linear splicing (Y. Zhang et al., 2013).

3.4.2. Expression in nervous system

circRNAs have been described across most of the animal kingdom, are oftentimes evolutionary conserved among species (Rybak-Wolf et al., 2015; Wu et al., 2020). circRNAs are expressed in a tissue- and developmental stage-specific manner (Barrett & Salzman, 2016; Salzman et al., 2012; Xia et al., 2017), and are particularly enriched and conserved in mammalian and non-mammalian brains (Venø et al., 2015; Westholm et al., 2014; Xia et al., 2017).

Around 20% of all brain protein-coding RNA, in particular the ones transcribed from genes related to synaptic function, produce circRNAs (You et al., 2015).

However, the circRNA expression of these coding genes fluctuate between different regions of the brain and oftentimes are dynamically regulated during neuronal maturation, showing expression patterns independent of their linear isoforms (Rybak-Wolf et al., 2015). Within neurons, circRNAs have been found in both somas and dendrites, some of them being enriched in synaptoneurosomes (Rybak-Wolf et al., 2015; You et al., 2015). These observations together with circRNAs high stability, due to their covalently closed structure, might indicate an important role as regulators of neuronal activity and therefore synaptic plasticity.

In addition, circRNAs expression show significant and progressive age-dependent upregulation independent from their host mRNAs, especially in elderly brain, compared to other non-neuronal organs, where no accumulation occurs. The aging-related accumulation of circRNAs can be accredited to the high post-mitotic cell composition of aging neural tissues and to the high stability of circRNAs. (Gruner et al., 2016); (Cortés-López et al., 2018; K. Xu et al., 2018).

3.4.3. Functions in nervous system

The nervous system is composed of polarized and complex cells, in which it is particularly critical to coordinate gene expression in a robust but dynamic manner.

In this regard non-coding RNA including circRNAs might play a strategical role to control cell-type specific gene expression.

A few of the brain-enriched circRNAs have been reliable associated with neurological diseases and injuries. (1) In rat cellular Alzheimer disease model, circ_0000950 was found to promote neuronal apoptosis, suppress neurite outgrowth and the inflammatory response, *via* multiple complementary binding sites to miR-103 (miRNA sponge), therefore constraining the miRNA action on its mRNA targets (Yang et al., 2019). (2) In human neurons it has been shown that beta-amyloid treatments triggered a significant perturbation of the circHDAC9/miR-142 axis, and that beta-amyloid-related neurotoxicity is rescued by the up-regulation of circHDAC9 after drug treatment to reduce extracellular amyloid plaques (N. Zhang et al., 2020). (3) In hippocampal tissues of temporal lobe epilepsy patients, it was shown that circSatb1 is significantly down-regulated and *in vitro* studies demonstrated that this leads to dendritic spine morphology defects, typically observed in epilepsy development (Gomes-Duarte et al., 2022). (4) Furthermore, circRNAs transcriptomic changes independent from their linear

transcripts have been described, among others, in cortical regions from patients with multiple system atrophy (α-synucleinopathies) (B. J. Chen et al., 2016), *substancia nigra* of Parkinson disease patients, where the age-related circRNA accumulation is lost and the total number of circRNAs is reduced (Hanan et al., 2020), and in brain injury or ischemia (Lin et al., 2016; L. Zhang et al., 2022).

Recently, it has been demonstrated that some circRNAs have a clear function on normal brain functions: (1) In 2020, Suenkel et al. described that circSlc45a4 knockdown depletes the basal progenitor pool in developing mouse cortex and increases the expression of neurogenic regulators, demonstrating that the conserved circRNA is necessary to maintain the pool of neural progenitors *in vitro* and *in vivo* (Suenkel et al., 2020). (2) Studies in male rhesus macaque brain showed that the circRNA circGRIA1 negatively regulates *Gria1* mRNA and protein levels, in an age-dependent manner. By doing so, circGRIA1 regulates synaptogenesis and GluR1 activity-dependent synaptic plasticity in hippocampal neurons (K. Xu et al., 2020). (3)

In aging neurons of same primates, it was found that two voltage-dependent calcium channel gene-derived circRNAs: circCACNA2D1 and circCACNA1E, negatively regulate their host mRNA expression (K. Xu et al., 2018). (4) Interestingly, up- and down-regulation of circRNAs expression, independently from their host mRNA transcripts, have been shown to occur in hippocampal neurons following excitatory neural activity. For example, circHomer1 is up-regulated after induction of synaptic plasticity, which might regulate neuronal response to larger excitatory inputs, by competing with the transcription of homer1 mRNA (Fei et al., 2014; You et al., 2015).

3.5. miRNAs in neurons

One of the most important mechanisms of post-transcriptional regulation in brain is the repression of mRNA mediated by miRNAs. These are small non-coding regulatory RNAs that recognize and bind to partially complementary sites usually in the 3′ untranslated regions of target genes and act as fine regulators of gene expression (Ambros, 2004; Bartel, 2004).

3.5.1. miRNA biogenesis

In metazoans, most canonical miRNAs are derived from introns or exons of non-coding primary transcripts, some of which harbor hairpins for more than one miRNA while in other cases miRNAs derive from introns of pre-mRNAs. The biogenesis of miRNA starts with miRNA genes transcribed by RNA Polymerase II followed by the cleavage of polyadenylated pri-miRNA transcript by the microprocessor complex (Drosha-DGCR8) in the nucleus (Figure 3a). Then the 5'-phosporylated pre-miRNA hairpin is exported to the cytoplasm via exportin 5 complex and then cleaved by Dicer.

This second cleavage generates a miRNA duplex, where one strand is loaded into the Argonaute (AGO) silencing complex, while the other strand is degraded (Figure 3b). Mature miRNAs consist of a 22 nt long molecule that will be loaded into the guide-strand channel of AGO. They can interact with their target RNAs in different ways depending on their pairing structure. The most common and stable way of interaction is through their 8 nt long 'seed sequence' (usually bases 2 to 10), which anneal with their complementary mRNA target and leads to slicing of the target RNAs (Figure 3c). In other cases, miRNA targets get repressed by inhibition of the translation complex.

In these cases, poised miRNAs loaded into the silencing complex associates with translation machinery and recruits deadenylases, which shorten mRNA poly-A tails, thus destabilizing the complex, and therefore reduces translation initiation (Figure 3c). Ultimately, this will lead to the degradation of the mRNA (Bartel, 2004, 2018).
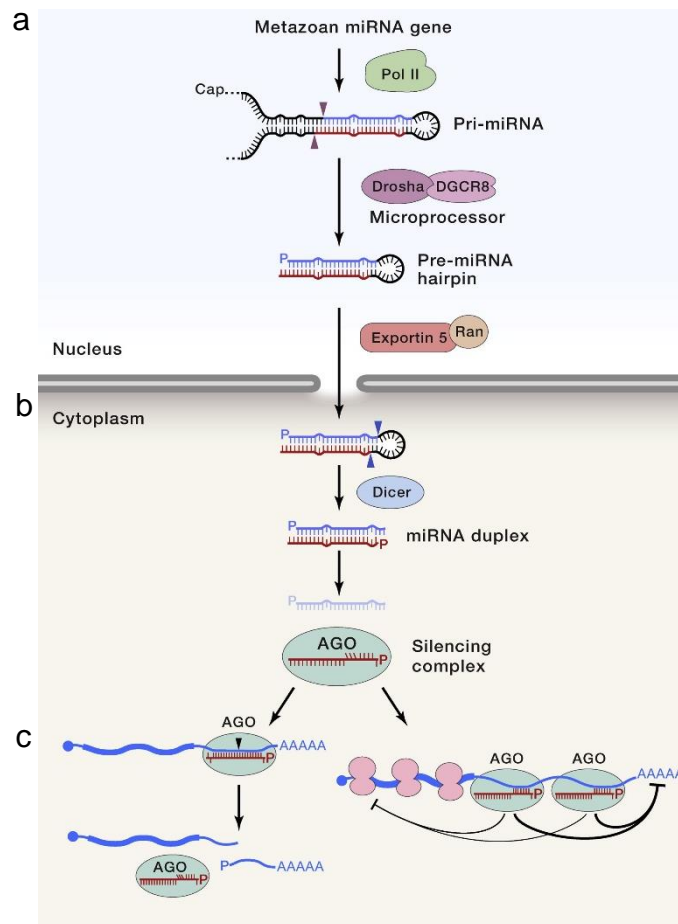
Figure 3. Schematic representation of biogenesis and processing of canonical miRNAs in metazoans.
Figure modified from Bartel, 2018 "Metazoan miRNAs".
(a) RNA Polymerase II (Pol II) transcription and cleavage o pri-miRNA by microprocessor in nucleus.
(b) pre-miRNA hairpin is exported to cytoplasm and cleaved by Dicer which generates miRNA duplex, one strand is loaded into Ago2 silencing complex while the other strand is degraded.
(c) Loaded mature miRNAs can interact with target RNAs by slicing of the mRNAs or dominantly by inhibition of translation complex.

3.5.2. Local translation regulation

miRNAs do not act as on/off switches, but rather fine-tune the abundance of target mRNAs usually without detectable effects on global target mRNA levels. Therefore small fluctuations in proteome, produced by the action of miRNAs, are sometimes not detectable or do not lead to discernible phenotypes (G. Schratt, 2009). This is particularly true when regulations occur in discrete subcellular localities or depending on cellular activity status (Bhattacharyya et al., 2006; Karres et al., 2007; Vasudevan et al., 2007).

Hence, miRNAs that can repress translation of specific targets at the synapse, are excellent candidates to regulate complex processes like synaptic plasticity or activity-dependent neuronal responses, when a very contained but strong gene regulation is needed at the synaptic terminals.

Furthermore, an expanding number of protein-encoding RNAs, as well as miRNAs, have been shown to be actively transported to the dendrites (Glock et al., 2021; Hafner et al., 2019); (Batish et al., 2012; Mendonsa et al., 2023; Sambandan et al., 2017; Zappulo et al., 2017). However, only a few of them show both activity-dependent RNA induction and activity-dependent increases in protein levels at the synapse (G. Schratt, 2009).

For example, miR-134, a well-known dendritically expressed miRNA, has been shown to respond to extracellular stimuli in hippocampal neurons and regulate size of dendritic spine, spine development, maturation and plasticity (G. M. Schratt et al., 2006).

Processing of this pre-miRNA in dendrites might indicate that only the RNAs locally present in this compartment will be targeted. Some models postulate that miRNAs might select their target in the soma and then travel bound to their mRNA to the synaptic destination, while others proposed that miRNA travel independently from their target RNAs and will pair locally. In this case, miRNAs would select their targets from a limited RNA pool (Kosik, 2006), which will require delivery of precursor and processing machineries to dendrites. Consistently with this hypothesis, some proteins associated with miRNA regulation such as Dicer, AGO, FMR1, DDX6 and p54, are in fact found in dendrites of mature neurons (Barbee et al., 2006; Lugli et al., 2005).

Therefore, it is essential to decipher the molecular mechanism by which miRNAs control synaptic local translation and consequently neuronal activity.

3.5.3. miRNAs regulated by neuronal activity

As previously mentioned, many synaptic regulators, including miRNAs, are influenced by neuronal activity. Even more, the dynamic regulation of miRNA function in response to stimuli is a pre-requisite during plasticity or synapse development. For example, several neural miRNA promoters are occupied by activity-dependent TF, like CREB or MEF2, which are coupled to Ca2+ regulated signaling (Fiore et al., 2009; Vo et al., 2005).

Post-transcriptional regulation also occurs in dependency of neuronal activity: the cleavage of calcium-dependent proteases (Calpains) present in synaptic preparations, stimulates Dicer activity and thus production of mature miRNAs at activated synapses (Lugli et al., 2005).

It has been shown in flies, that synaptic stimulation can also lead to inactivation or destruction of the helicase MOV10, part of the fly silencing complex, which results in impairments of memory formation and storage (Ashraf et al., 2006). Similar conserved mechanisms have been observed in mammals through the local interaction of miR-26 with activity-dependent protein CamKIIα in dendrites of hippocampal neurons (Lafourcade et al., 2020). Altogether, these and many more roles described for miRNAs in synapse development, formation, maturation, neuronal type determination, migration, axonal pathfinding, dendritogenesis, and even higher order processing and neurological disorders, show how miRNAs and their associated protein complexes, could strongly coordinate adaptive processes such as synaptic plasticity (Rajman & Schratt, 2017; G. Schratt, 2009).

4. Cdr1as

4.1. Locus and expression

Cdr1as, is a circular exonic circRNA, discovered by the Kjems lab (Hansen et al., 2011). It is a vertebrate-conserved, highly-expressed, brain-enriched circRNA, with low or no expression in non-neural tissues (Hansen, Jensen, et al., 2013; Memczak et al., 2013; Rybak-Wolf et al., 2015). Cdr1as results from the back-splicing of a single exon in the antisense strand of putative *Cdr1* transcript (cerebellar degeneration-related protein 1) mapped to Chromosome X (Y. T. Chen et al., 1990; Hansen et al., 2011), embedded in a much larger host transcription unit (*Cdr1os* ; Figure 4a). Cdr1as biogenesis is promoted by flanking inverted elements from the mammalian-wide interspersed repeat family (Yoshimoto et al., 2020), which results in a covalently-closed circRNA molecule of 1485nt or 2975 nt, in human and mouse respectively. This antisense transcription product of *Cdr1*, exist exclusively in a circular RNA form (Memczak et al., 2013) and there is no evidence of transcription from the opposite strand (putative Cdr1 mRNA) (Piwecka et al., 2017).

In addition, Cdr1as is known to be up-regulated during neuronal maturation (Rybak-Wolf et al., 2015) and to be predominantly expressed in excitatory neurons in forebrain

regions of the brain and not detected in glial cells, with strong evidence of a functional role in the normal brain function (Piwecka et al., 2017). Due to all of the above-mentioned molecular characteristics, Cdr1as is one of the most studied circRNAs, and therefore, the most interesting candidate to study circRNA-exclusive action mechanisms in brain.

4.2. Cdr1as interaction with miRNAs: miR-7 and miR-671

Cdr1as expression is regulated by a complex non-coding RNA network, which includes two main interactions with miRNAs. Firstly, Cdr1as mouse sequence contains more than 120 partially complementary binding sites for miR-7 seed region (more than 70 sites in the human Cdr1as isoform), not complementary enough to be sliced by AGO (Hansen et al., 2011), and more than 60 of them are conserved among vertebrates (Hansen, Jensen, et al., 2013; Memczak et al., 2013) (Figure 4b). Morevoer,AGO2 High-throughput sequencing of RNA isolated by crosslinking immunoprecipitation (HIT-CLIP) experiments (Moore et al., 2015) demonstrated that Cdr1as binds to miR-7 *in vivo* in mouse brain and is the top ranked target interactor of this miRNA in this tissue (Piwecka et al., 2017). Altogether, the independent observations of Hansen and Memczak et al. suggested that Cdr1as acts as sponge for miR-7 in neural tissues, due to the antagonist effect of Cdr1as in response to miR-7 downregulation. Nevertheless, the constitutive full knockout (KO) of Cdr1as locus in a mouse model, showed that Cdr1as functions as a post-transcriptional stabilizer of mature miR-7 in brain (Piwecka et al., 2017). Other studies suggested that the accumulation of miR-7, might as well prevent the accumulation of Cdr1as in the cytoplasm of neurons (Kleaveland et al., 2018). However, the precise function of the cross-stabilization between Cdr1as and miR-7 remains unknown.

The second main miRNA interactor of Cdr1as is miR-671. Cdr1as has a single binding site for miR-671 with almost full sequence complementarity (Hansen et al., 2011). This interaction function as a built-in mechanism for Cdr1as destruction, where miR-671 induces AGO2-mediated slicing of the circRNA, promoting its turnover (Figure 4b). In HEK293 cells, this turnover was proven to happen exclusively in the nucleus (Hansen et al., 2011). Furthermore, the dysregulation of miR-7 enhances the miR-671-directed slicing of Cdr1as (Kleaveland et al., 2018), by undetermined mechanisms that could involve miRNA cooperative action on closely spaced sites (Saetrom et al., 2007).

4.3. Cdr1as main counteractor: lncRNA Cyrano (OIP5-AS1)

Cdr1as functional antagonist is the long non-coding RNA Cyrano (annotated as OIP5-AS1 gene). Cyrano harbors a single, nearly perfectly complementary and highly conserved binding site for miR-7 in its third exon, and consequently, directs the destruction of miR-7 *via* target RNA-directed miRNA degradation (Figure 4b) (Kleaveland et al., 2018; Ulitsky et al., 2011). Cyrano was first described in zebrafish and is broadly conserved in vertebrates and shown to be important for normal brain and eyes development of zebrafish embryos (Ulitsky et al., 2011). In human cell lines, Cyrano has been shown to act as a sponge for the RNA-binding protein HuR, where influences cell proliferation (Kim et al., 2016). In mouse embryonic stem cells, Cyrano regulates miR-7 activity to maintain self-renewal (Smith et al., 2017), even though, this impact in pluripotency is not reproduced in Cyrano-deficient human stem cells, which retained the potential to differentiate into germ layers (Hunkler et al., 2020).

Nonetheless*, in vivo* data from fusion miRNA:mRNA transcripts of mouse brain showed lncRNA Cyrano as the second top-ranked RNA interacting with miR-7, after Cdr1as (Piwecka et al., 2017). Constitutive Cyrano-deficient mice do not present obvious abnormalities in standard neurobehavioral tests; however, it did show a very specific molecular phenotype. The main transcriptomic regulation in brain samples of Cyrano-deficient mouse was the significant and specific up-regulation of mature miR-7, which consequently prevented the accumulation of Cdr1as in cytoplasm of neurons (Kleaveland et al., 2018).

4.4. Cdr1as non-neuronal function

Lately, there is increasing evidence that Cdr1as expression is regulated in many tumors, such as colorectal cancer, hepatocellular carcinoma, melanoma, breast cancer, glioma, among others (Jiang et al., 2020; Kristensen et al., 2018). Suggesting that Cdr1as might play a role in the development of cancer, affecting tumor growth, metastasis and even tumor chemoresistance.

Most of the observations are based on the strong capacity of Cdr1as to stabilize miR-7, a known onco-miRNA. For example, in colorectal cancer, studies show that Cdr1as up-regulation positively impact the cell cycle by enhancing the epidermal growth factor receptor/RAF1 pathway through inhibition of miR-7 activity. Even more, the high expression of Cdr1as was associated with poor patient survival (Weng et al., 2017).

In other example, the analyzes of gliomas cell lines and brain samples from patients, uncovered an up-regulation of miR-671 that correlated with a down-regulation of Cdr1as (Barbagallo et al., 2015).

A particularly interesting observation of a miR-7 independent Cdr1as role in cancer was recently discovered in melanoma. It was shown that Cdr1as is a hallmark of melanoma progression and the loss of Cdr1as promotes melanoma invasion *in vitro* and metastasis *in vivo* through an IGF2BP3-mediated mechanism. Specifically, Cdr1as depletion results from the epigenetic silencing of its originating long non-coding RNA (host transcription unit: Cdr1os), by EZH2/PRC2. In addition, Cdr1as levels mirror cellular states associated with distinct therapeutic responses (Hanniford et al., 2020).

4.5. Cdr1as function in the central nervous system

Due to its specific and high expression in brain, most of the studied functions of Cdr1as have been discovered in the central nervous system. In 2013, Memczak et al. described that both the knockdown of miR-7 or the exogenous expression of human CDR1as in zebrafish, causes a reduction in midbrain size. This suggested that the biological role of CDR1as is in part associated with the interaction between the circRNA and miR-7 (Memczak et al., 2013).

Years after this observation, Piwecka et al. generated the first complete KO organism for a circRNA, consisting in the constitutive deletion of the 3000 nt long DNA locus comprising the full length of Cdr1as sequence in mouse (Cdr1as-KO). The animal model uncovered very specific functional phenotypes such as, dysfunctional excitatory synaptic neurotransmission in hippocampal autapses, including: (1) high frequency of spontaneous post-synaptic currents and (2) stronger depression in the synaptic response of evoked signals (Figure 4c, upper panel). In addition, a stronger sensorimotor gating deficit was observed in Cdr1as-KO mice (Figure 4c, lower panel). This is a neuropsychiatric-like alteration of behavior, that consist in the inability to effectively attenuate the intrinsic startle response to redundant stimuli (Castellanos et al., 1996; Powell et al., 2012). Clinically sensorimotor gating deficits correlate with symptoms such as disorder and distractibility in schizophrenia, ADHD, Tourette's syndrome and bipolar disorders (Castellanos et al., 1996; Swerdlow & Light, 2018).

The transcriptomic analysis of Cdr1as-KO mice also showed a robust molecular phenotype in all analyzed brain regions (cortex, hippocampus, cerebellum, and olfactory bulb). miR-7 and miR-671 were specifically and post-transcriptionally misregulated (Figure 4d, left panel), additionally, the expression of several IEGs was enhanced in Cdr1as-KO brains (Figure 4d, right panel), providing a possible molecular link to the functional phenotype. Some possible cellular mechanisms proposed by Piwecka et al. to explain Cdr1as-KO phenotypes include, changes in expression of synaptic proteins, malformation of synaptic specialization, or alteration in synaptic calcium homeostasis (Piwecka et al., 2017).

Cdr1as has also been studied in the context of disorders of the nervous system. The first observation showed a down-regulation of Cdr1as in hippocampal CA1 regions of sporadic Alzheimer disease (AD) patients (Lukiw, 2013). Later on, the same research group showed that the expression of miR-7 is significantly increased in brains of sporadic AD patients. This miR-7 up-regulation positively correlates with the down-regulation of UBE2A protein, the main effector of the ubiquitin-mediated proteolysis that removes amyloid peptides and a direct mRNA target of miR-7 (Y. Zhao et al., 2016).

Further *in vitro* studies of the role for Cdr1as in AD, showed that the overexpressed Cdr1as promotes the degradation of β-amyloid precursor protein and β-secretase 1, *via* the proteasome and lysosome, without alteration of their mRNA levels. Consequently, overexpression of Cdr1as reduces the generation of the β-amyloid peptide, a key pathogenic factor in AD, indicating a potential neuro-protective role of the circRNA. Inversely, β-amyloid precursor protein decreases the expression of Cdr1as, revealing a mutual regulation of both (Shi et al., 2017).

Nevertheless, the actual molecular and cellular mechanisms for the reported functions of Cdr1as in normal brain function. The importance of its regulation for health and disease of the nervous system and how miR-7 and other interaction partners mediate these roles, remains elusive. It will be crucial to assess the relevance of this non-coding RNA network, especially in the context of specific neuronal plasticity.
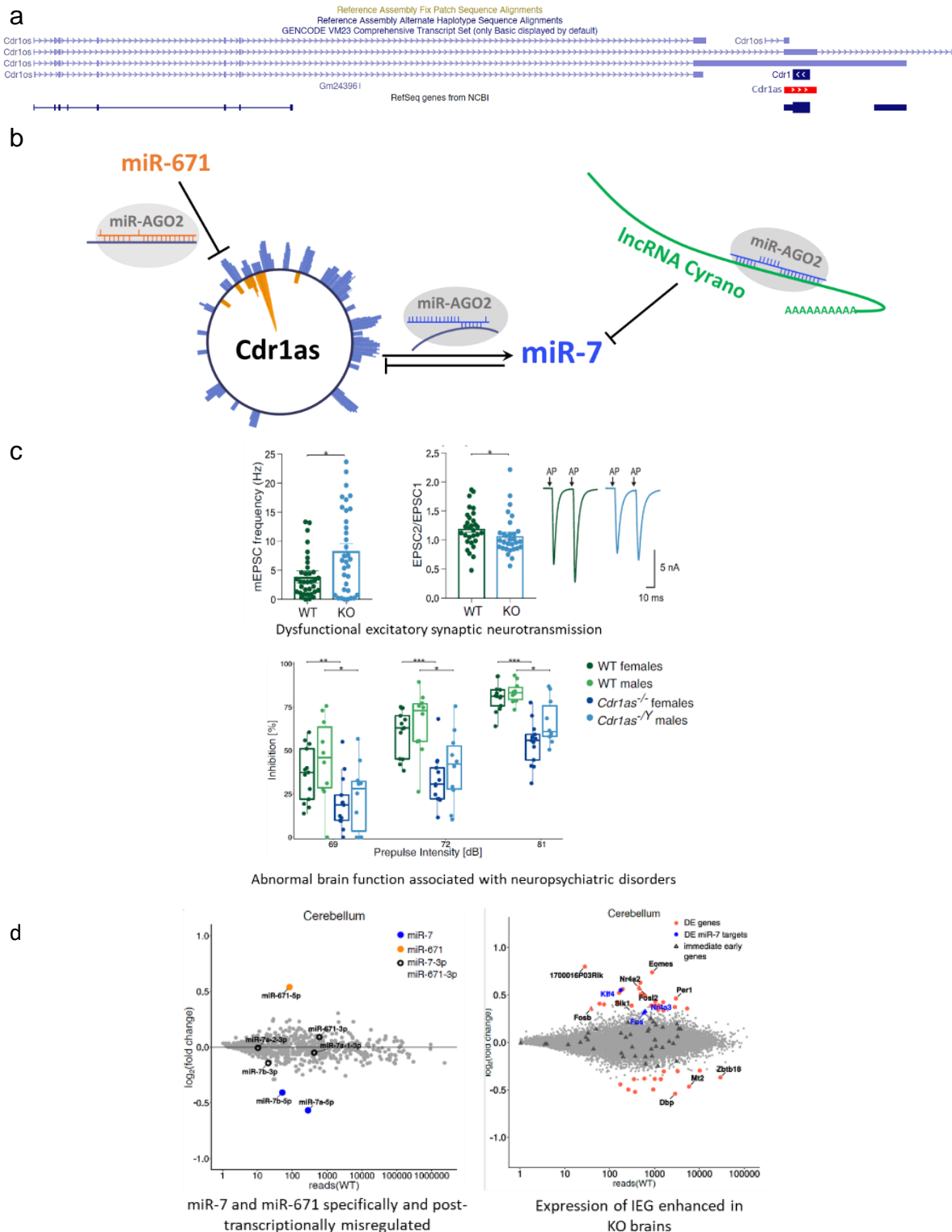
Figure 4. Cdr1as phenotypes in central nervous system

(a) Cdr1os, host transcript of circRNA Cdr1as (red). Reference sequence alignments from Genome Browser (GENCODEVM23).

(b) Schematic model of Cdr1as non-coding RNAs regulatory network including sites of miRNA interaction: miR-671(orange) and mir-7 (blue) and their diverse pairing complementarities. together with miR-7 counter interacto lncRNA Cyrano (green).

(c) Functional phenotypes of Cdr1as-KO animals. Dysfunctional synaptic transmission (top) and impaired sensorimotor gating response (bottom), figure adapted from Piwecka et al. 2017.

(d) Molecular phenotype of Cdr1as-KO animals. Cerebellum as example of bulk RNA-sequencing for small RNAs (left) and poly-A transcripts (right) showed a specific post-transcriptional dysregulation of miR-7 and miR-671 and a enhanced expression of IEGs, figure adapted from Piwecka et al. 2017.

5. miR-7

5.1. Evolutionary origin

miR-7, the central interactor in Cdr1as ncRNA network, is also an ancient miRNA, with a mature sequence evolutionarily conserved across bilaterians, from annelids to humans (Figure 5a) (*MiRNA Gene Family*, 2007). All these species are characterized by a centralized nervous system, that integrates and processes sensory information coming from the periphery, and initiates responses *via* neurosecretion or direct stimulation of the body musculature (Arendt et al., 2008). Extensive evolutionary comparative data indicates that miR-7 evolved in neurosecretory brain of vertebrate and invertebrate animals as a nervous system-restricted microRNA (Tessmar-Raible et al., 2007).

Additionally, miR-7 is a prototypical neuroendocrine miRNA and is a crucial part of the molecular circuit that ensures precise control of endocrine cell differentiation. Specific spatiotemporal localization studies of miR-7 in human samples showed a restricted expression in fetal and adult endocrine cells, indicating a potential role for miR-7 in endocrine cell differentiation and/or function (Correa-Medina et al., 2009; Kredo-Russo et al., 2012; Latreille et al., 2014). In parallel, other studies demonstrated that neuronal and pancreatic differentiation lineages are closely related, suggesting that pancreatic endocrine cells co-opted a regulatory signature from an ancestral neuron already present in an early-branched deuterostome (Perillo et al., 2018; W. Zhao et al., 2007).

5.2. Biogenesis in mammals

In mammals, miR-7 family is transcribed from 3 different genomic loci: (1) pri-miR-7-1, resides in intron 15 of the hnRNP K pre-mRNA, (2) pri-miR-7-2 is in its own transcriptional unit, and (3) pri-miR-7-3 miR-7-3 is part of the intron of PIT1 gene (Choudhury et al., 2013). All three primary miRNA transcripts are process into hairpin precursors and then into mature isoform with the same seed sequence, and therefore they can regulate the same collection of targets (Figure 5b).

Despite the ubiquitous expression of its three host pre-mRNAs, mature miR-7 is enriched in specific brain regions, neuroendocrine glands and pancreatic tissues, (Bravo-Egana et al., 2008a; Choudhury et al., 2013; S.-D. Hsu et al., 2008; Landgraf et al., 2007).

The inconsistent expression of mature miR-7 and their correspondent primary sequence, suggests that there is a relevant regulatory mechanism during the processing of the primary miR-7 transcripts. In fact, Choudhury et al, demonstrated that brain-enriched expression of miR-7, is achieved by inhibition of its biogenesis in non-brain cells in both human and mouse (Choudhury et al., 2013; Lebedeva et al., 2011).
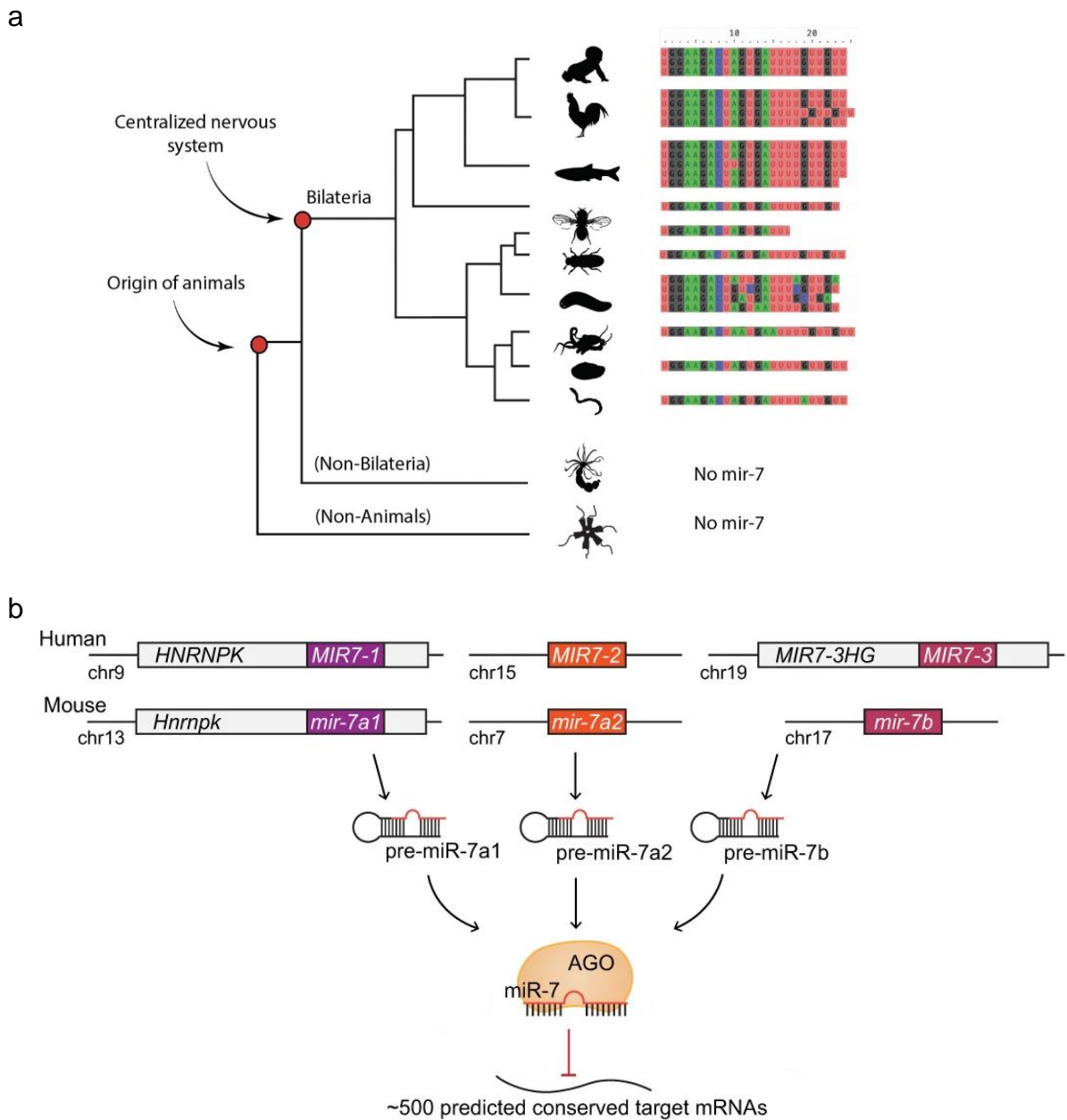
Figure 5. Evolution and biogenesis of miR-7 in mammals
(a) Evolutionary conservation of mature miR-7 in bilaterian, where same-colored boxes indicate single-base level conservation.
(b) Schematic representation of miR-7 biogenesis in human and mouse adapted from LaPierre et al. 2022. The different pre-miRNAs are transcribed from three different genomic loci and then processed into the same mature sequence, loaded into AGO proteins, and then delivered to bind more than 500 potential target mRNAs.

5.3. Functions in cancer

The most described role of miR-7 in mammals is as suppressor of proliferation pathways, and for this reason it has been deeply studied as a regulator of cancer development and as tumor suppressor (Hansen, Kjems, et al., 2013).

In cancer contexts, miR-7 acts mainly down-regulating PI3K and MAPK pathways, which affect diverse cell type processes of differentiation, protection from stress, chromatin remodulation, among others. In addition, recent data suggested miR-7 as a prognostic biomarker in cancer, and therefore, its regulation has been propose as targeted therapy (Gajda et al., 2021; Korać et al., 2021; Morales-Martínez & Vega, 2022, p.). In cancer types associated with the nervous system, as glioblastoma and neuroblastomas, miR-7 was found to be down-regulated compared to normal tissue, suggesting a role as tumor suppressor (Koshkin et al., 2014).

5.4. Secretory role: Diabetes and neurosecretory glands

The first full miR-7 – KO organism was developed for fruit flies. Even though these flies exhibited no apparent phenotype in non-stress conditions, internal or external stress treatments revealed that miR-7 had strong impact in determination of sensory organs and on stress handling behavior (X. Li & Carthew, 2005). When environmental perturbation was added during larval development, miR-7 mutant animals showed abnormal sensory organs development and concomitant abnormal gene expression (X. Li et al., 2009). This suggested that during development, miR-7 confers robustness against perturbations to resist transient environmental fluctuations in RNA expression (Ebert & Sharp, 2012; Herranz & Cohen, 2010).

In mice, miR-7 has been described as the first negative regulator of glucose-stimulated insulin secretion in β-cells of pancreas (Latreille et al., 2014). In β-cells, a miR-7-regulated gene network interconnects the exocytosis machinery with cell-specific transcription factors. Latreille et al. demonstrated that miR-7 directly regulates mRNAs that control late stages of insulin granules fusion with the plasma membrane.

Mice overexpressing miR-7 in β-cells developed diabetes due to impaired insulin secretion and β-cell dedifferentiation. Even more, miR-7 levels correlate with β-cell secretory activity in insulin resistant and diabetic mouse models and in human islets (Latreille et al., 2014). This mechanism of action seems to be as well conserved for insulin-producing cells in non-mammalian organisms (Agbu et al., 2019).

Later, it was shown that miR-7-2 KO mice model, presented diverse characteristics of infertility, such as low levels of sex steroid hormones, small testes or ovaries, impaired spermatogenesis, and lack of ovulation. This connected miR-7 direct gene silencing role with the control of sexual hormones synthesis and secretion (LaPierre & Stoffel, 2017).

Most recently, a targeted depletion of miR-7 in a critical cell type of the hypothalamic melanocortin pathway (Sim1-positive-neurons), generated hyperphagia, obesity and increase linear growth in mice. The direct action of miR-7 on *Snca* and *Igsf8* mRNAs, regulates body weight, related hormone axes and subsequently energy homeostasis (LaPierre et al., 2022).

The only work that relates miR-7 secretory function with Cdr1as, is the one from Xu et al. (2015). They characterized the expression of the circRNA and the miRNA in different neuroendocrine tissues and cell lines, and then use several secretagogues (molecules that induce secretion) to assess the activation of the RNA network in mouse pancreatic cells. They found that the extremely low basal expression of Cdr1as in mouse islets is down-regulated by short treatments with forskolin (activator of adenylate cyclase) and PMA (activator of PKC), but up-regulated by long-term treatment with the same molecules. This suggested a differential involvement of cAMP and PKC signaling cascades during different timepoints of Cdr1as regulation. This signaling activation might be derived from direct association with transcription promoter elements, like CREB, or from indirect elements of the Cdr1as-miR-7 network. The overexpression of Cdr1as in pancreatic cells didn't show any effect in the expression of miR-7 nor *vice versa*. Nevertheless, separately, both perturbations affected insulin RNA transcription, insulin content and glucose-dependent insulin secretion in opposite ways (H. Xu et al., 2015).

5.5. miR-7 during brain development

miR-7 role in non-endocrine glands remains poorly studied, mainly due to miR-7 extremely low expression under homeostatic conditions, compared to neuroendocrine cells (Correa-Medina et al., 2009; H. Xu et al., 2015).

In forebrain, only couple of directs functions of miR-7 have been described, both observed during brain development. First, it was shown that the downregulation of miR-7 in mouse embryo, results in brain defects , through the alteration of miR-7 RNA target

genes related to the p53 pathway, which leads to a decreased in expansion and survival of intermediate cortical progenitor cells (Pollock et al., 2014). A second function was shown in dopaminergic neurons, where miR-7 binds directly to the *Pax6* mRNA 3'-UTR and this regulation restricts dopaminergic spatial origin and proper morphogenesis and brain size control (de Chevigny et al., 2012; Zhang et al., 2018).

The dynamic interplay between Cdr1as and miR-7 is tightly regulated, and for both molecules their expression is the highest in brain, where both seem to have relevant roles that involved diverse molecular and functional phenotypes. Nevertheless, their coordinated molecular mechanism in post-mitotic neurons, specifically during neuronal synaptic activity remain unknown.

Aims of the study

In this study, we postulate that in cortical neurons, Cdr1as non-coding RNA act as a buffer system which monitor the direct action of miR-7 in neurotransmitter secretion. Therefore, the coordinated function of Cdr1as and miR-7 under specific external or internal perturbations would facilitate the neuronal connectivity and coordinated wiring that will translate into long-lasting alterations and plastic synaptic adaptations.

The main goal of this project is to understand how the Cdr1as - miR-7 regulatory network contributes to synaptic activity modulation in excitatory cortical neurons. To address this, we:

1. *Investigated the role of Cdr1as in neuronal activity*

Using biochemical stimulations (KCl treatments) and gene expression analysis, we l elucidated the influence of enhanced neuronal activity on the expression of Cdr1as network and its related ncRNA partners in primary cortical neuronal cultures.

2. *Evaluated Cdr1as impact on the regulation of synaptic neurotransmitter release dependent on miR-7*

Using real-time measurements of excitatory neurotransmitter glutamate secretion, under spontaneous and stimulated conditions, together with *in vivo* recordings of synaptic activity through neuronal maturation, we evaluated how Cdr1as loss and miR-7 expression perturbation affects synaptic function of primary cortical neuronal cultures.

3. *Analyze transcriptome-wide changes dependent on Cdr1as and miR-7 expression*

Using bulk polyA+ RNA-sequencing methods, we assessed neuronal transcriptomic changes after mir-7 overexpression in wild type and Cdr1as-KO neurons and uncovered specific cellular pathways or molecular targets involved in the observed synaptic phenotypes.

Materials

All items listed below were purchased from the given company and stored according to the manufacturer's recommendations.

1. **Chemicals and Reagents**

Name	Supplier
20X SSC	Sigma-Aldrich, Germany
Acetic acid	Sigma-Aldrich, Germany
Acidic Phenol Chloroform	Thermo Fisher Scientific, USA
Agar-Agar, Kobe I, pulv. 500 g	Carl Roth, Germany
Agarose NEEO Ultrapure	Carl Roth, Germany
Ampicillin 97% bio-grade	Carl Roth, Germany
Bactotryptone	Thermo Fisher Scientific, USA
Bovine Serum Albumin (BSA)	New England Biolabs, USA
CaCl2	Sigma-Aldrich, Germany
Calcium chloride	Carl Roth, Germany
Chloroform 99%	Sigma-Aldrich, Germany
CNQX	BioTrend, Germany
DAPI	Sigma-Aldrich, Germany
Deionized formamide	Applichem Panreac
Dextran sulfate	Sigma-Aldrich, Germany
Dimethyl sulphoxide (DMSO)	Sigma-Aldrich, Germany
Dithiothreitol (DTT)	Sigma-Aldrich, Germany
DL-AP5	Biomol, Germany
DNA gel loading dye (6x)	Thermo Scientific
dNTPs	Thermo Scientific
dNTPs 100mM	Thermo Fisher Scientific, USA
EDTA	Carl Roth, Germany
Ethanol absolute	Merck, Germany
Ethidium bromide	Merck, Germany
FastDigest Green Buffer (10X)	Thermo Scientific
Fetal bovine serum (FBS)	Invitrogen, USA
Fromaldehyde 37%	Carl Roth, Germany
GeneRuler 100 bp Plus DNA Ladder	Thermo Fisher Scientific, USA
GeneRuler 1kb Plus DNA Ladder	Thermo Fisher Scientific, USA
Glucose	Sigma-Aldrich, Germany
Glycerol	VWR, Germany
GlycoBlue Co-precipitant	Thermo Fisher Scientific, USA
HCl 37%	Carl Roth, Germany
HNO3 65%	Carl Roth, Germany
Isoflurane	CP Pharma, Germany

KCl	Sigma-Aldrich, Germany
Laminin	Biolamina
Lipofectamine 2000	Thermo Fisher Scientific, USA
Magnesium acetate	Sigma-Aldrich, Germany
Methanol	Carl Roth, Germany
MgCl$_2$	Sigma-Aldrich, Germany
Mix&Go Competent Cells	Zymo Research
NaCl	Sigma-Aldrich, Germany
NaOH 10 M	Sigma-Aldrich, Germany
OCT cryo-embedding compound	Tissue-Tek
Paraformaldehyde 42%	Electron Microscopy Sciences
Penicillin-Streptomycin 10,000 U/mL	Thermo Fisher Scientific, USA
phorbol 12-myristate 13-acetate (PMA)	Sigma-Aldrich, Germany
Phosphate-buffered saline	Thermo Fisher Scientific, USA
Poly-D-Lysine	Sigma-Aldrich, Germany
Poly-L-Lysine P2636	Sigma-Aldrich, Germany
Prolong Gold Antifade mounting media	Invitrogen, USA
QuickExtract DNA Extraction Solution 1.0	Biosearch Technologies
Random hexamers (50 µM)	Thermo Scientific
rCTP, rATP, rUTP, rGTP	Promega, USA
RiboLock RNase Inhibitor	Thermo Fisher Scientific, USA
RNase away	Carl Roth, Germany
RNasin Plus RNase inhibitor	Promega, USA
Sodium acetate anhydrous	Sigma-Aldrich, Germany
Sucrose	Sigma-Aldrich, Germany
Tris-HCl pH8	Invitrogen, USA
Trypan blue solution 0.4 %	Sigma-Aldrich, Germany
TTX	Enzo Life Sciences
Tween 20	Carl Roth, Germany

2. **Buffers and Media**

i) Annealing buffer for DNA oligos: 10mM Tris pH 7.5, 50 mM NaCl, 1mM EDTA

ii) PBS-T: PBS + 0.2% Tween

iii) TAE Buffer (50X): 2M Trizma (Sigma Aldrich, Germany), 250 mM acetic acid, 50 mM EDTA pH 8.0

iv) LB Medium for bacterial culture: 10 g bactotryptone, 5 g yeast extract, 10 g NaCl in 1 L H2O, adjusted to pH 7.5 and autoclaved. Media were supplemented with ampicillin or kanamycin according to standard procedures. For agar plates the LB was supplement with 1.5 % agar.

v) TRIzol: 38 % (v/v) Phenol, pH 4.5,800 mM Guanidiniumthiocyanat,400 mM Ammoniumthiocyanat, 100 mM Sodium acetate, pH 5.0 (adjust pH with acetic acid), 5 % (v/v) Glycerin.

vi) Blocking Solution: 1% BSA; 5% Horse Serum in PBS

vii) Borate Buffer: 1.24 g Boric Acid,1.90 g Na-tetraborate.10H2O (Borax) in water adjusted to pH 8.5 and f0ilter-sterilize.

viii) Tyrode Solution NaCl/KCl HEPES 0.12g, Glucose 0.09g, NaOH (to adjust pH to 7.4) 0 to 1g Sucrose to adjust osmolarity to media from cells (approx..300mOs)

ix) Evoked stimulation Solution: AP5 (1000X), CNQX (1000X), $CaCl_2$ (0.75mM), $MgCl_2$ (4mM)

x) Spontaneous recording solution: 0.5 mM TTX ,4 mM CaCl2.

xi) 100X FUDR: 8,1mM 5-fluoro-2`-deoxyuridine (Sigma F0503), Uridine (Sigma U3003) in DMEM (Gibco 31 966)

xii) Dissection Solution: HBSS, 1/100 anti-biotic/anti mycotic, 1/100 1M Hepes,1/100 2 glucose

xiii) Enzymatic Solution: DMEM (Gibco 31966), Cysteine 20mg/100ml (Sigma), CaCl2 1mM, EDTA 0.5mM.

xiv) Stop Solution: DMEM (Gibco 31966), 10%FBS (Gibco 26140), 0.1%PenStrep, Albumin (Sigma A2153), Trypsin-Inhibitor (Sigma T9253)

xv) Primary Neurons culture media: Neurobasal-A (Gibco 10888022), 1/1000 Pen Strep, 1/100 Glutamax (Gibco 35050061), 1/50 B-27 (Gibco 17504044)

xvi) Primary Neurons activity measurements: BrainPhys Neuronal Medium (StemCell 05790), 1/50 B-27 (Gibco 17504044), 1/1000 Pen Strep

xvii) Primary Astrocytes culture media: 90% DMEM (Gibco 31966), 10% FBS (Gibco 26140),10 U/ml Pen/,1µg/ml Strep.

3. Enzymes

Name	Supplier
T4 Ligase	NEB
2x Blue S'Green + ROX	Biozym
Catalase	Sigma-Aldrich, Germany
DreamTaq DNA Polymerase	Thermo Fisher Scientific, USA
FastAP	Thermo Fisher Scientific, USA
FastDigest restriction Enzymes	Thermo Fisher Scientific, USA
Glucose Oxidase *(aspergillus niger)*	Sigma-Aldrich, Germany
Kapa Hifi HotStart ready mix	Roche
Maxima H minus Reverse Transcriptase	Thermo Fisher Scientific, USA
Papain	Worthington Biochemical Corp.
Protease K	Invitrogen, USA
SuperScript III	Invitrogen, USA
T4 PNK	Thermo Fisher Scientific, USA
TaqMan Universal master Mix, no UNG-1	Applied Biosystems
Trypsin-EDTA (0.05%), phenol red	Thermo Fisher Scientific, USA

4. Commercial Kits

Name	Supplier
Zymoclean Gel DNA Recovery Kit	Zymo Research
ZymoPURE Plasmid Miniprep Kit	Zymo Research
ZymoPURE™ II Plasmid Midiprep Kit	Zymo Research
nCounter Sprint Reagents kit (72-plex)	NanostringTechnologies, USA
Direct-zol™ RNA MiniPrep	Zymo Research
ViewRNA™ Cell Plus Assay Kit	Invitrogen, USA
Glutamate-Glo Assay	Promega
Truseq Stranded mRNA Library Prep kit	Illumina
Truseq small RNA Library Prep kit	Illumina
Nextseq 500 High Output Kit v2 (150 cycles)	Illumina
AMPure RNA clean beads	Beckmann Coultier
AMPure XP beads	Beckmann Coultier
Bioanalyzer High sensitivity DNA Chip kit	Agilent
Bioanalyzer RNA Pico 6000 Chip Kit	Agilent
Bioanalyzer RNA Nano 6000 Chip Kit	Agilent
Qubit dsDNA HS Assay Kit	Invitrogen, USA
Tapestation High sensitivity D5000 Ladder	Agilent

Tapestation High sensitivity D5000 Reagents	Agilent
High sensitivity D5000 Screen Tape	Agilent
Nuclei EZ lysis buffer	Sigma-Aldrich, Germany
Ribominus eukaryote kit v2	Thermo Fisher Scientific, USA

5. **Devices**

Name	Supplier
ABI StepOne Plus	Thermo Fisher Scientific, USA
Bioanalyzer 2100	Agilent
BZ-9000 microscope (60xOil (CFI Plan Apo λ, 972036 objective)	Keyence
Nanodrop 1000	Thermo Fisher Scientific, USA
microscope Ti-E, 60x Oil (Plan Apo λ, MRD01605) and Andor iXonUltra888	Nikon
Qubit 4	Thermo Fisher Scientific, USA
Tabletop centrifuges 5415R,5415D,5804	Eppendorf
TapeStation 4200	Agilent
nCounter SPRINT^{TM} Profiler	NanostringTechnologies, USA
Lightcycler 96	Roche
Thermal cycler PTC200	MJ Research
Master cycler X50s	Eppendrof
NextSeq500 system	Illumina
Hiseq4000 system	Illumina
M200 infinite Pro plate reader	Tecan
Microscope Eclipse Ti (95B scientific CMOS-Photometrics) 60x, 1.49 NA	Nikon
Pulse generator HSE-HA	Harvard Apparatus
Trinocular stereozoom microscope STEMI 2000-C	Zeiss
Cold Light Source KL1500 LCD	Zeiss
Cell culture incubator HeraCell 160i	Thermo Fisher Scientific, USA
Cell culture hood HeraSafe 2030i	
Electrophoresis Power Supply	Bio-Rad
ImageQuant LAS 4000	GE Healthcare Life Sciences, UK
Maestro Pro MEA	Axion Biosystems
Precellys Evolution Tissue Homogenizer	Bertin Instruments

6. Consumables

Name	Supplier
12-well plate, cell culture coated	Sarstedt, Germany
6-well plate, cell culture coated	Sarstedt, Germany
Greiner T-75 flasks	Sigma-Aldrich, Germany
96-well Multiply FAST PCR plate (qPCR)	Sarstedt, Germany
BZO Seal Film, Adhesive, Optical Film	Biozym
DNA/RNA LoBind Tubes 1.5 mL	Thermo Fisher Scientific, USA
18mm round glass Coverslips	Fisher Scientific
25mm round glass Coverslips	Fisher Scientific
Superfrost Plus Adhesion Microscope Slides	Thermo Fisher Scientific, USA
Filter pipet tips SafeSeal SurPhob, 10-20-300-1250µl	Biozym
Falcon tubes 15ml or 50 ml	BD Biosciences, Germany
Multiply-µStrip 0.2 mL	Sarstedt, Germany
48-well CytoView MEA plates	Axion Biosystems
nCounter sprint cartridge	NanostringTechnologies, USA
Paraffin	Th. Geyer GmbH
Dounce tissue grinder	Sigma-Aldrich, germany

7. DNA oligos

Plasmid	Purpose
pAAV-hsyn-mCherry (Addgene #114472)	Overexpression control
pAAV-hsyn-mCherry-primiR7a	miRNA overexpression

Oligo	Purpose	Sequence
Cdr1as_3SS_For	Genotyping	**GTCTTCCAGCATCTCCAGGG**
Cdr1as_3SS_Rev	Genotyping	**ACTGTTGGCCCACAAAACCT**
Cdr1as_5SS_For	Genotyping	**TCCATGGATACCATTGTTGAGGG**
Cdr1as_5SS_Rev	Genotyping	**ACATGGATCCCTTGGAAGACAA**
Primir7_For	cloning	**GTTGGCCTAGTTCTGTGTGGA**
Primir7_Rev	cloning	**TAGAGGTGGCCTGTGCCATA**

TaqMan Probe	Catalog Assay ID (Thermo Fisher Scientific)
dme-miR-7a-5p	**000268**
hsa-miR671-5p	**002322**
hsa-Let-7a-5p	**000377**
U6 snRNA	**001973**
snoRNA202	**001232**

8. Softwares

i)   Fiji (imageJ) Schindelin, J, et al. (2012). Fiji: an open-source platform for biological-image analysis. *Nature Methods*, *9*(7), 676–682. doi:10.1038/nmeth.2019

ii) GraphPad Prism 9.1.0

iii) MEA: AxIS Navigator software, Neural Metric Tool (Axion Biosystems)

iv) nSolver Analysis Software Version 4.0 (NanostringTechnologies, USA)

v)   StarSearch   https://github.com/arjunrajlaboratory/rajlabimagetools/wiki

vi) SnapGene http://www.snapgene.com (GSL Biotech)

Methods

1. Animals

1.1. Cdr1as knockout mice

The Cdr1as knockout (Cdr1as-KO) strain was generated and maintained on the pure C57BL/6N background (Piwecka et al. 2017). All animals used in this work came from intercrosses of hemizygous Cdr1as-/Y males and heterozygous Cdr1as+/- females in (F3 generation from original founder) and mutants were compared to wild type littermate controls. Animals were kept in a pathogen-free facility in a 12 h light–dark cycle with ad libitum food and water. Animal care and mouse work were conducted according to the guidelines of the Institutional Animal Care and Use Committee of the Max Delbrück Center for Molecular Medicine, the Landesamt für Gesundheit und Soziales of the federal state of Berlin (Berlin, Germany).

2. Biochemical and Molecular Biology

2.1. Cloning, transformation, and propagation of plasmids

Cloning was performed according to standard methods. Plasmids were cut using appropriate restriction enzymes (Fast Digest - Thermo Scientific), dephosphorylated with FastAP and purified from an agarose gel with a Zymoclean Gel DNA Recovery kit (Zymo Research). Inserts were either PCR amplified, then digested with the same set of restriction enzymes or oligonucleotides with fitting overhangs were annealed and phosphorylated with T4 PNK. Insert and cut plasmid were ligated with T4 DNA Ligase and subsequently transformed into chemically competent bacteria (Mix&Go Competent Cells, DH5 α) in presence of the corresponding antibiotic for selection. Finally, plasmids were isolated using ZymoPURE Plasmid Miniprep or ZymoPURE Plasmid Midiprep kit from bacterial culture. For plasmids obtain from Addgene (Addgene Plasmid #114472), same procedure of propagation and plasmid purification was used.

2.2. Genomic DNA extraction

To genotype Cdr1as KO strain, genomic DNA was extracted from tail cuts taken from newborn or adult animals. Tissue was digested using QuickExtract™ DNA Extraction Solution 1.0 at 65°C for up to 30 mins depending on the tissue size, reaction was stopped at 98°C for 2 mins and 1ul of the supernatant, containing the genomic DNA,

was used for the follow up end-point PCR detection of wild type or mutant splice sites splice sites.

2.3. Genotyping of mutant animals

Genotypes were determined by end-point PCR performed on corresponding template genomic DNA. We used a set of primers for 3'SS multiplex detection (3'SS_For + 3'SS_Rev + 5'SS+For), as it shows in the scheme below. PCR products for wild type (355bp), heterozygotes (418 and 355 bp) and knock out (418bp) animals were analyzed on a 2.5% agarose gel, as it shows in example gel below.
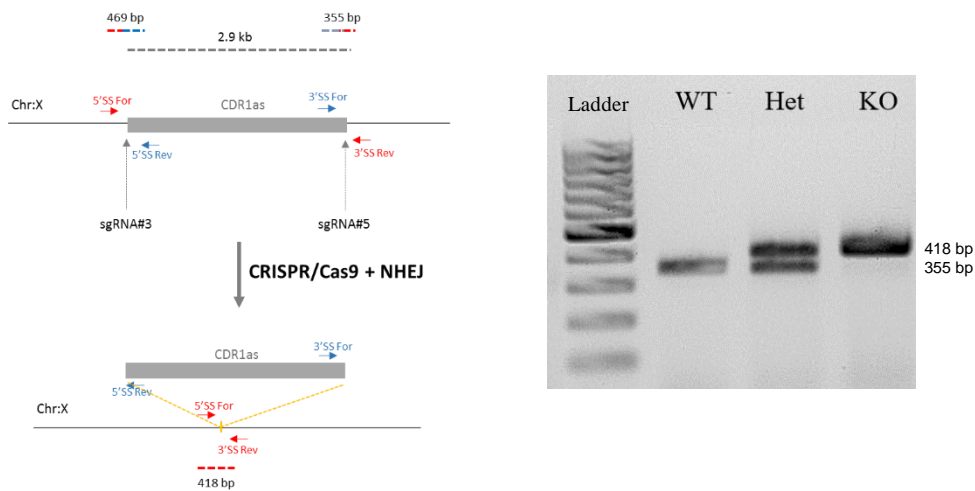
Genotyping strategy of Cdr1as locus. Right: Scheme of Cdr1as locus in WT and KO conditions. Positions and names of corresponding genotyping primers are shown in blue and red. Left: Representative agarose gel showing PCR products for wild type (WT), heterozygote (Het) and knock out (KO) animals (3'SS multiplex).

2.4. Nanostring

To achieve direct quantification of targeted single RNA molecules in a sample of total RNA. 100ng of RNA was incubated with a 72-plex Core Tag set, custom-made probe mix (reporter + capture probes) and corresponding hybridization buffer at 67°C for 18h, followed by a cool down step at 4°C for 10mins. All samples were diluted to a final volume of 30ul and loaded in a nCounter gene expression cartridge (12 sample panel). Quantification of RNA molecules was done using nCounter SPRINT™ Profiler instrument (NanostringTechnologies, USA) according with manufacturer instructions. Normalized counts of RNA molecules were obtained using nSolver™ Data analysis software.

2.5. miR-7 overexpression

To study miR-7 related effects in wild type and Cdr1as-KO neurons, we designed a miRNA overexpression strategy based on Adeno-associated viruses (AAV). The sequence of pri-miR-7a was amplified from mouse brain tissue and cloned into an AAV vector (Addgene Plasmid #114472), driven by a neuronal promoter (hSyn1) and expressed together with mCherry fluorescent reporter. The final viral particles (AAV serotype 9 and mutated versions of Serotype 9) were generated by Charité Viral Core Facility. An AAV that only expressed the mCherry protein under the same neuronal promoter was use as control condition (Addgene Plasmid #114472). wild type and Cdr1as-KO neurons were infected at DIV4-6 by directly adding the viral particles into the culturing media at a titer of 10^9 VG/ml. half of the media was exchange after 5 days of infection and then once a week. At DIV21, cells were fixed or harvested in Trizol according to the different downstream experiments.

2.6. Reverse Transcription of miRNAs

To reverse transcribed miRNAs some considerations are needed: (1) their short size, typically around 20-22 nt and (2) the lack of a polyA-tail. Therefore, instead of normal random hexamers, gene-specific stem loop primers (Taqman RT primers) were used. These primers only need a short overlap with the miRNAs 3'end. First, 100 ng of total RNA was reverse transcribed using SuperScript III (Invitrogen) (100 U/reaction), 1 mM dNTPs, 20 U Ribolock (40U/µl), 1x TaqMan RT primer per each gene of interest (miR-7a, miR-671, Let-7a, snoRNA202, U6 snRNA) (Applied Biosystems) and 1x first-strand synthesis buffer were filled up to 20 µl reaction volume with ddH2O and mixed. The gene-specific cDNA synthesis was carried out as follows: 30 min at 16°C, 30 min at 42°C and terminated for 5 min at 85°C.

2.7. Quantitative real time PCR (qPCR) using TaqMan probes (miRNAs)

Quantitative real time PCR experiments were conducted on an ABI StepOne Plus instrument or on a Roche LightCycler 96 System. For miRNA expression analysis, cDNA was diluted 3X with ddH2O and mixed with: miRNA specific TaqMan probes with an attached FAM dye (Applied Biosystems) and with TaqMan Universal master Mix II, no UNG-1 (Applied Biosystems), according to manufacturer protocol. All measurements were conducted at least in 3 technical replicates. Relative quantification of miRNA expression was performed using the comparative ΔΔCT method (Pfaffl, 2001).

2.8. RNA extraction

Total RNA from primary neurons was generally extracted using home-made TRIzol reagent in combination with Direct-zol RNA Kit (Zymo Research). The samples were fixed in cold methanol for 10 mins at -20C, then washed in cold PBS, TRIzol was directly added to each well and cells were scraped away to ensure full detachment of all neuronal processes. The dissociated sample was collected in a tube with silica beads and homogenized at 5500 rpm 2x for 20secs. Then equal volume of 100% Ethanol was added directly to the sample and then transferred to a Zymo-Spin™ IIICG Column and centrifuged (30secs x 16000g). The flowthrough was discarded and DNAse I (Zymo Research) treatment followed, incubating the column with 6U/ul for 15 mins at room temperature. Afterwards, 3 consecutive washing steps were performed and finally the RNA was eluted from the Column in DNAse/RNAse-free water.

3. Imaging techniques and analysis

3.1. smRNA FISH (Stellaris) (Raj et al., 2008)

Single molecule fluorescent in situ hybridization (smFISH) protocol was performed in wild type and Cdr1as-KO primary neurons after 14-21 DIV. Stellaris oligonucleotide probes complementary to Cdr1as, Cyrano (Oip5-as1), Hprt, circHipk3 or linHipk3 were designed using the Stellaris Probe Designer (LGC Biosearch Technologies) as conjugates coupled to Quasar 670 or Quasar 570. Neurons were fixed in 4% Formaldehyde for 10 mins. and probes hybridized overnight in 10% formamide at 37°C and 100 nM, washed according to Stellaris protocol (Biosearch Technologies), DAPI 5 ng/ml in second wash and mounted with Gloxy buffer. Images were acquired on an inverted Nikon Ti-E microscope with 60x oil NA1.4 objective and Andor iXON Ultra DU-888 camera; Z stacks had 0.3 µm spacing and were merged by maximum intensity projection. Dot detection was performed using StarSearch software from Raj Lab (https://github.com/arjunrajlaboratory/rajlabimagetools/wiki) on manually segmented neurons (somas and neurites). Posterior quantification analysis was done counting the number of dots of Cdr1as or Cyrano molecules normalized by area and per compartment. All statistics were calculated using Mann-Whitney test, nonparametric rank comparisons, between different conditions (GraphPad Prism 9.1.0), statistical significance was assigned for $P<0.05$.

3.2. Single-molecule miRNA FISH (ViewRNA Cell Plus)

Single molecule miRNA fluorescent in situ hybridization (miRNA smFISH) protocol was performed in wild type and Cdr1as-KO using (1) primary neurons after 14-21 DIV and (2) coronal brain slices from P66 animals. miRNA probes for mature sequence of miR-7a-5p, miR-671-5p, Let-7a-5p and snoU6 were obtain from available commercial catalog (Thermo scientific) and label probes for A546, A670 or A488 were used. miRNA smFISH protocol was performed according to manufacturer protocol (ViewRNA Cell Plus – ThermoFisher) plus the addition of protease K (Invitrogen) treatment in a dilution 1/1000 for 10 mins before miRNA probe hybridization step. Finally, the samples were mounted with Prolong Gold Antifade mounting media (Invitrogen) and imaged using Keyence BZ 9000 or Leica Sp8 confocal microscope. Image processing was done using Fiji-imagej.

3.3. smRNA FISH colocalization analyses

To address the spatial relation and significant association between Cdr1as and lncRNA Cyrano molecules within neurons, we performed colocalization analyses of single molecules based on MNN distances and probability of random association calculation. smRNA FISH (stellaris) images of Cdr1as and Cyrano were used as the test condition, Cdr1as and Tfrc (transferrin receptor C) as negative control and images of two probes within the same RNA molecule (linHipk3 and circHipk3) as positive control of true colocalization. Dot detection was performed using StarSearch software from Raj Lab (https://github.com/arjunrajlaboratory/rajlabimagetools/wiki) on manually segmented neurons (somas and neurites). The analyses to measure intermolecular distances and determining the significance of association, were done based on the work of (Eliscovich et al., 2017), but rewrite in a new R script according to our requirements.

3.4. Synaptic Glutamate Release

i) iGluSnFR

To study glutamate synaptic release, AAV1 particles containing a glutamate sensor under the human synapsin-1 promoter (pAAV.hSyn.iGluSnFr.WPRE.SV40 (Borghuis et al., 2013) were obtain from A.W Lab at MDC Berlin. Primary neuronal cultures were infected at DIV 4-6 with the AAV particles to express the glutamate sensor at the cell surface and then recorded at DIV17-21.

ii) Image acquisition

All image acquisition was done as previously described in Farsi et al. (2021) (Farsi et al., 2021) using same instruments, solutions and recording protocols. In brief, neurons were incubated at room temperature in Tyrode's buffer (120 mM NaCl, 2.5mM KCl, 10 mM glucose, 10 mM HEPES, pH 7.4, osmolality was adjusted to that of the culture medium with sucrose). Action potential-evoked glutamate release was recorded in a chamber with two electrodes for electrical stimulation, mounted on a Nikon Eclipse Ti inverted microscope equipped with a PFS focus controller, a prime 95B scientific CMOS (Photometrics) camera and a pulse generator (HSE-HA, Harvard Apparatus). Emission was collected with a 60x, 1.49 NA Nikon objective. Evoked glutamate release was performed by continuous imaging at 20 Hz after application of 20 field stimuli at 0.5 Hz in the presence of 50 µM AP5 (l-2-amino-5-phosphonovaleric acid) and 10 µM CNQX, to block post-synaptic, imaging solution was supplemented with 2 mM $CaCl_2$ and 2 mM $MgCl_2$. Spontaneous events were then captured by 5-min continuous imaging at 20 Hz at 4mM $CaCl_2$, in the presence of 0.5 µM TTX to block action potential firing.

iii) Image analysis

All image analysis was done as previously described in Farsi et al. 2021. In brief, time-lapse images were loaded in MATLAB (Mathworks, Natick, MA) and after de-noising and filtering, active synapses were detected as local maxima on the first derivative over time of the image stack. Regions of interest (ROIs) were defined by stretching the maxima to a radius of 4 pixels (700 nm). Taking the first derivative over time allowed to resolve fluorescence changes associated with evoked or spontaneous release and localize release sites.

iv) Release probability calculation

As previously described in Farsi et al. 2021, to characterize the release properties of individual synapses, filtered fluorescence traces were used for peak detection. Peaks with the amplitude seven times greater than standard deviation of baseline trace during spontaneous imaging were counted as a successful glutamate release event. Spontaneous frequency was calculated from the total number of events detected during 5-min acquisition. Evoked probability for each synapse was obtained by dividing the number of events happening within one frame after stimulation by the total number of stimulations.

v)   Kernel Density Estimation

All release probability calculations were plotted using the Kernel-Density-Estimate and creating a curve of the distribution of individual measurements. The curve is calculated by weighing the distance of all the points in each specific location along the distribution. Each data point is replaced with a weighting function to estimate the probability density function. The resulting probability density function is a summation of every kernel.

4. Cell Culture Methods

4.1. Primary Neuronal culture

Primary cortical neurons were prepared from C57BL/6N mouse pups (P0) as previously described in Kaech and Banker, 2007 (Kaech & Banker, 2006). In brief, cortices were isolated from P0 C57BL/6N mice from wild type and Cdr1as-KO genotypes. The tissue was dissociated in papain at 37C and then the single cell suspension was seeded in a previously coated glass coverslips, to finally place them on top of a monolayer of feeder astroglia. The cells were maintained in culture during 14-21 days in Neurobasal-A medium (Invotrogen) supplemented with 2% B-27(Gibco), 0.1% Pen-Strep (10 kU/ml Pen; 10 mg/ml Strep) and 0.5 mM GlutaMAX-I (Gibco) at 37ºC and 5% CO_2.

4.2. K$^+$ treatments

To understand how the Cdr1as network responds to neuronal stimulation, we treated wild type primary neuronal cultures with 60mM KCl. To recognize if Cdr1as regulation upon stimulation is dependent on transcriptional changes, we added the transcription inhibitor DRB (5,6-Dichloro-1-β-D-ribofuranosylbenzimidazole) to the treatments.

On DIV13 neurons were incubated over night with a mix of: 0.5μM TTX (tetrodotoxin), 100μM AP5 (l-2-amino-5-phosphonovaleric acid) and 10 μM CNQX, to silence all spontaneous neuronal responses. On DIV14 neuronal media was exchange for stimulation media (170mM NaCl, 10mM HEPES pH7.4, 1mM MgCl2, 2mM CaCl2), containing whether (1) 60mM KCl, (2) 50μM DRB (5,6-Dichloro-1-β-D-ribofuranosylbenzimidazole) or just (3) NaCl as osmolarity control.

Cells (neuronal cultures and astrocyte-feeder layer) were incubated at 37ºC; 5%CO2 for 1 hour, fixed with cold methanol for 10 mins. and used immediately for RNA extraction and following RNA-sequencing and Nanostring runs.

4.3. Glutamate Secretion assay (Glutamate-Glo™, Promega)

To assess the levels of extracellular glutamate in primary wild type and Cdr1as-KO neurons, with or without miR-7 overexpression, we implemented the luciferase-based Glutamate-Glo™ assay. Glutamate dehydrogenase catalyzes the oxidation of glutamate with consequent reduction of NAD+ to NADH. In the presence of NADH, Reductase enzymatically reduces a pro-luciferin to luciferin and then luciferin is detected in a luminescence reaction using Ultra-Glo™ rLuciferase and ATP. The amount of light produced would be proportional to the amount of glutamate in the sample. Neurons from all conditions were plated in 48-well CytoView MEA plates (Axion Biosystems) and media from each well was collected at DIV18-21 and saved at -20°C until ready to perform the assay.

25µl of media from each sample (or glutamate control) were transferred into a 96-well plate to perform the final reaction. A negative control of only buffer was included for determining assay background and a control of no-cells media was used to determine basal levels of glutamate. Samples were mixed with Glutamate detection reagent prepared according to manufacturer instructions and the plate incubated for 60 minutes at room temperature. Recording of luminescence was done using a plate-reading luminometer (Tecan M200 infinite Pro plate reader) following manufacturer protocol.

A stock solution of glutamate 10mM was used to create the standard curve (100µM to 1.28×10^{-3}µM) and as positive control. All glutamate concentrations of the test samples were estimated based on standard curve linear regression.

Analyses were done by comparison of RLU values across conditions and all statistics were calculated using two-way ANOVA, between different conditions (GraphPad Prism 9.1.0), and $P < 0.05$ was considered as statistically significant.

4.4. Multi-Electrode Array (MEA) Recordings

To measure neuronal network activity in primary wild type and Cdr1as-KO neurons, with or without miR-7 overexpression, we used a multi-electrode array system (MEA; Axion Biosystems, Atlanta, GA, USA) and recorded spontaneous extracellular field potentials in neurons from DIV 7 to DIV21.

 i) MEA cell cultures

Cells were seeded in 48-well CytoView MEA plates with 16 poly-3,4-ethylendioxythiophen (PEDOT) electrodes per well (Axion Biosystems). Each well was

coated with 100 μg/mL poly-D-Lysine and cells were seeded to a density of 100-150K mixed with 1 μg/mL laminin (FUDR was added to the media one day after seeding). Neurons were grown in supplemented Neurobasal-A media for the first 7 days, then half of the media was changed to BrainPhys™, supplemented with B-27, one day before each recording.

ii)   MEA recordings

Recordings were performed using a Maestro MEA system and AxIS Software with Spontaneous Neural Configuration (Axion Biosystems). Spikes were detected using an adaptive threshold set to 6 times the standard deviation of the estimated noise. The plate was first allowed to ambient in the Maestro device for 3 minutes and then 10 minutes of data was acquired for analysis.

iii)   Data analysis

For MEA data analysis we used a sampling frequency of 12.5 kHz and the active electrode selection criteria was 5 spikes/minute. (1) Mean firing rate (MFR): action potentials (APs) frequency per electrode. (2) Burst Frequency: Total number of single-electrode bursts divided by the duration of the analysis, in Hz. (3) Burst Duration: Average time (sec) from the first spike to last spike in a single-electrode burst. (4) Network Asynchrony: Area under the well-wide pooled inter-electrode cross-correlation, according to (Halliday et al., 2006). (5) Network Oscillation: Average across network bursts of the Inter Spike Interval Coefficient of Variation (standard deviation/mean of the inter-spike interval) within network bursts. (6) Burst Peak: peak of the Average Network Burst Histogram divided by the histogram bin size to yield spikes per sec (Hz). All statistics were calculated using 2-way ANOVA mixed model with Bonferroni correction for multiple measurements, between different conditions, statistical significance was assigned for $P<0.05$

5.   **Bulk polyA+ RNA-Sequencing**

5.1. Total RNA libraries and sequencing (circRNA detection)

 1 μg of total RNA was used as starting material for total RNA libraries and spiked with from wild type and Cdr1as-KO neurons. Then, ribosomal RNA (rRNA) was depleted with the Ribominus Eukaryote Kit v2 or with a RNase H approach (Adiconis et al., 2013). Successful ribodepletion was assessed by Bioanalyzer RNA 6000 Pico Chip. RNA was fragmented and subsequently prepared for sequencing using Illumina

Truseq Stranded Total RNA Library Prep kit. Libraries were sequenced on a Nextseq 500, at 1x150 nt.

5.2. PolyA+ libraries and Sequencing

All samples from wild type and Cdr1as-KO neurons, control and miR-7 overexpression, were prepared as described in the Illumina TruSeq Stranded RNA sample preparation v2 guide. In brief, 500ng of RNA were fragmented, reverse transcribed and adapter-ligated, followed by a pilot qPCR to determine the optimal PCR amplification. Library quality was assessed using Tapestation (DNA1000 kit) and Qubit. Samples were sequenced on an Illumina NextSeq 500 with 1x150 bp.

5.3. Small RNA libraries

All samples from wild type and Cdr1as-KO neurons were prepared from total RNA as described in Illumina TruSeq Small RNA Sample Prep Kit and sequenced on a NextSeq 500 with 1x50 bp.

5.4. RNA-Seq analysis

RNA-seq reads were mapped to the mouse mm10 genome assembly using STAR v2.7.0a (Dobin et al., 2013). Aligned reads were assigned to genes using annotations from Ensembl (Mus_musculus, release 96) and featureCounts v1.6.0 () with the parameter reverse stranded mode (-s=2). Differential gene expression analysis was done using DESeq2 v 1.30.1(Love et al., 2014), taking both batch effects and nested effect into account. Specifically, we used multi-factor design that consider the batch effect to WT vs KO and WT vs KOm7oe (design = ~ 0 + group + batch), while used nested effect to WT vs WTm7oe and KO vs KOm7oe in paired experiments (design = ~genotype+genotype:batch+genotype:cond). Significance threshold of differential expression genes was set to adjusted P-value of 0.05 and log2-fold-change of 0.5.

5.5. miR-7-5p target regulation analysis

To test if log2FoldChange distribution of miR-7 targets are significantly different to other genes used in differential expression genes analysis, we performed a two-sided Mann-Whitney U-test for each comparison. A list of predicted conserved targets of miR-7-5p and miR-122 as a control were downloaded from TargetScan Mouse, release 7.2 (Agarwal et al., 2015) and miRDB (Y. Chen & Wang, 2020). We only used targets exist in both databases.

5.6. Gene ontology (GO) analysis

Gene ontology enrichment analysis was done using topGOtable function in the pcaExplorer (Marini & Binder, 2019). In GO analysis, genes showing average log2 fold change of 0.5 and adjusted p value less than 0.05 were considered significant and all expressed genes were used as background. We used the elim algorithm instead of the classic method to be more conservative and excluded broad GO terms with more than 1000 listed reference genes.

Results

1. <u>Sustained neuronal depolarization transcriptionally induces Cdr1as and post- transcriptionally stabilizes miR-7</u>

We hypothesized that miR-7 might be involved in cortical neurotransmitter secretion in similar ways as it is participating in stimulus-regulated secretion of insulin in pancreatic cells (LaPierre et al., 2022; Latreille et al., 2014). Additionally, as some circRNAs subcellular localization were shown to be modulated specifically by neuronal activity (You et al., 2015). We tested the response of both, Cdr1as and miR-7, to sustained neuronal depolarization in primary cortical neurons from mice (**Figure 6a**). Elevated extracellular potassium (K^+) generates a global neuronal depolarization. Therefore, extracellular KCl treatments are useful for elucidating transcriptional and plasticity-related events. This events are associated with homeostasis, and long-term potentiation, which controls neuronal recruitment for sensory stimuli, learning, memory, etc. (Rienecker et al., 2020).

A fast, primary response to neuronal stimulation is activation of immediate early genes (IEGs), which expression depends on the duration of the stimulation (Bartel et al., 1989; Tyssowski et al., 2018). IEGs are mostly transcription factors and DNA-binding proteins which are primary transcriptional, rapid, and transient response to neuronal activation and depolarization stimuli (Curran & Morgan, 1987; Herdegen & Leah, 1998; Lanahan & Worley, 1998; Tischmeyer & Grimm, 1999). Therefore, to inhibit spontaneous neuronal responses generated by Na^+-dependent depolarization or neurotransmitter release, we pre-treated primary neurons at DIV13 with TTX, CNQX and AP5 overnight. These compounds inhibit spontaneous neuronal responses generated by Na^+-dependent depolarization or glutamate release. On DIV14, the culture media was exchanged with media containing high extracellular concentrations of potassium (KCl 60 mM). This treatment was performed for 1 hour (control condition: media with the same osmolarity as the high K^+ media) (**Figure 6a, right**).

The observed significant up-regulation of IEGs in K^+ treated neurons (including master neuronal activity regulators such as *Fos, Fosb, Jun, Junb, Egr2, Nr4a1, Nr4a2* , **Figure 6b blue dots**) is consistent with previously described gene expression changes for

one hour of sustained K$^+$ treatment (Bartel et al., 1989; Rienecker et al., 2020). Genes not expected to react to stimulation were indeed not changing in expression. For example, housekeeping genes (*Actb, Vinculin, Tubb5*), other transcription factors (*Klf13, Atf3, Zic1*) and cell-cycle related genes (*Dusp1, Dusp5, Dusp6, IGF1R*) (**Figure 6b, black and grey dots, respectively**).

Together with upregulation of activity-dependent IEGs, we observed a robust and significant up-regulation of Cdr1as in magnitude similar to what we have seen for IEG. In fact, the absolute expression levels of Cdr1as was the highest observed across all IEG tested (**Figure 6b, red label**). Moreover, of all circRNAs detected by total RNA sequencing, Cdr1as was the most highly expressed and induced circRNA after K$^+$ stimulation (**Figure 6c**). Similarly, mature miR-7 isoforms (miR-7a and miR-7b), were also strongly up-regulated after K$^+$ stimulation, compared to the control (**Figure 6d, left panel**). No changes were observed in the expression of mature miR-671, involved in Cdr1as turnover, or in highly expressed neuronal miRNA Let-7a (**Figure 6d, middle and right panels**).

Interestingly, none of the primary transcripts of miR-7 (pri-miR-7-1, pri-miR-7-2, pri-miR-7b) changed after K$^+$ stimulation (**Figure 6e**). This demonstrated that the regulation of mature miR-7 occurred post-transcriptionally. We further probed the dependence on transcription using inhibitor of transcription elongation (5,6-Dichlorobenzimidazole - DRB, methods). We incubated neurons with DRB before K$^+$ treatment and compared them with neurons treated only with K$^+$. For none of the genes of interest (Cdr1as, miR-7, mR-671) significant up-regulation was observed (**Figure 7a-b**). Down-regulation was observed for some IEG and primary miR-7 isoforms, probably due to their short half-life times (**Figure 7c-d, respectively**). Specifically, Cdr1as levels were unperturbed (**Figure 7a, left panel)**, as well as mature miR-7 levels were unchanged (**Figure 7a, right panel**). This is likely explained by the known high stability and half-life of Cdr1as (Memczak et al., 2013) and the known stability of miR-7 bound to AGO complex (Bartel, 2018).

We also tested the response of the Cdr1as RNA network to the same sustained depolarization in primary astrocytes exposed to the neuronal culture (glial feeder layer). We did not observe any response after K$^+$ stimulation, with or without DRB pre-treatment, compared to the control.
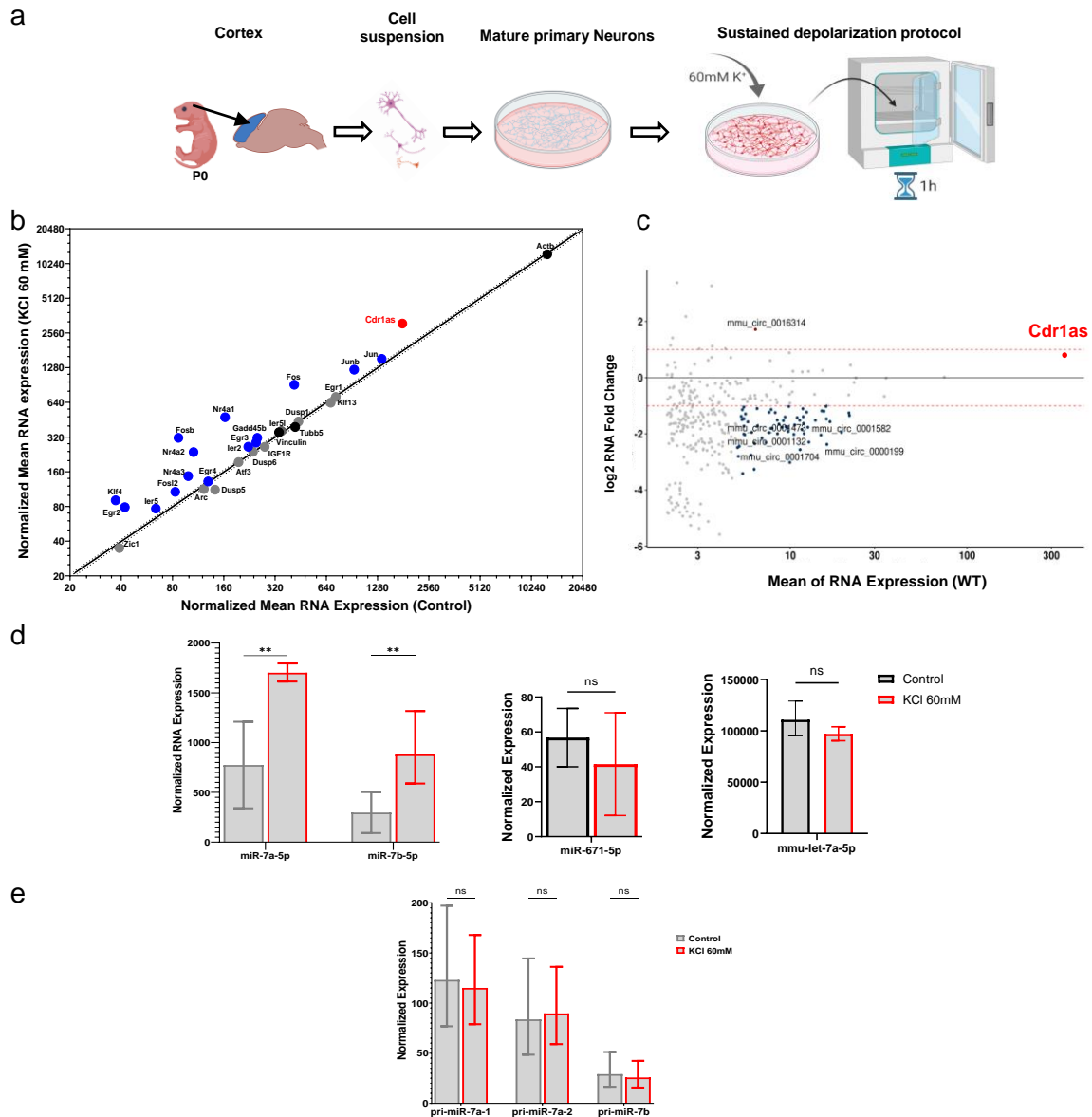
Figure 6. Sustained neuronal depolarization causes transcriptional up-regulation of Cdr1as and post-transcriptional stabilization of miR-7.

(a)Protocol to culture primary cortical neurons (modified from Keach and Banker,2006: Methods). DIV14 neurons, pretreated with TTX, CNQX and AP5, were stimulated with 1 hour of KCl (60mM).

(b) RNA quantification before and after KCl treatment (Nanostring nCounter, Methods). Statistically significantly upregulated RNA levels are shown in blue (IEGs) and in red (Cdr1as). Housekeeping genes: black. RNA counts are normalized to housekeeping genes (*Actb, Tubb5 and Vinculin*). Each dot represents the mean of 4 biological replicates (4 independent primary cultures from 4 animals). Black line: linear regression; dotted line: 95% confidence interval.

(c) RNA Quantification before and after K+ treatment depolarization plus pre-incubation with transcription inhibitor (DRB) (Nanostring nCounter, methods). Cdr1as and Cyrano shown in red. RNA counts are normalized to housekeeping genes (*Actb, Tubb5 and Vinculin*). Each dot represents the mean of 3 biological replicates (3 independent primary cultures from 3 animals). Grey line: linear regression.

(d)) Expression levels of mature miR-7, miR-671 and Let-7a, quantified by small RNA-seq for 3 independent primary cultures, before and after sustained depolarization. Bar plot represents the geometric mean. P value: ratio paired t-test (significance: p value < 0.002). Error: SD

(e) Quantification of primary miRNAs (Nanostring nCounter, methods), before and after sustained depolarization. RNA counts are normalized to housekeeping genes (*Actb, Tubb5 and Vinculin*). Bar plot represents the mean of 4 biological replicates (4 independent primary cultures from 4 animals). P value: ratio paired t-test. Error: SD.
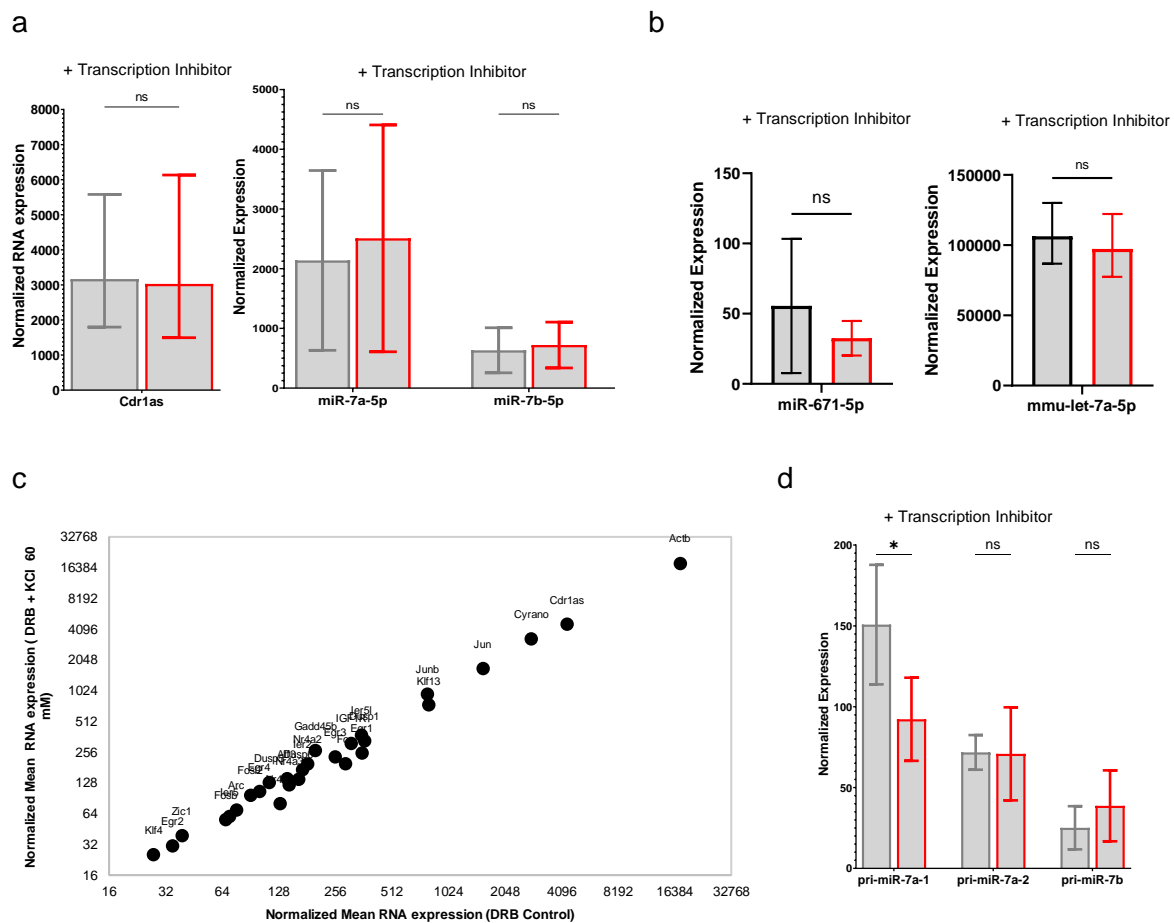
Figure 7. Pre-incubation with transcription inhibitor DRB avoids Cdr1as network induction.
(a) Quantification of Cdr1as (Nanostring nCounter, methods) and mature miR-7 isoforms (small RNA-seq, methods), before and after sustained depolarization plus pre-incubation with transcription inhibitor (DRB). Nanostring RNA counts are normalized to housekeeping genes (*Actb, Tubb5 and Vinculin*). Bar plot represents the mean of 3 biological replicates (3 independent primary cultures from 3 animals). P value: ratio paired t-test. Error: SD.
(b) Expression levels of mature miR-671 (left) and let-7a (right) quantified by small RNA-seq for 3 independent primary cultures, before and after sustained depolarization. Bar plot represents the mean. P value: ratio paired t-test. Error: SD.
(c) RNA Quantification before and after K+ treatment depolarization plus pre-incubation with transcription inhibitor (DRB) (Nanostring nCounter, methods). Cdr1as and Cyrano shown in red. RNA counts are normalized to housekeeping genes (*Actb, Tubb5 and Vinculin*). Each dot represents the mean of 3 biological replicates (3 independent primary cultures from 3 animals).
(d) Quantification of primary miRNAs (Nanostring nCounter, methods), before and after sustained depolarization plus pre-incubation with transcription inhibitor (DRB). RNA counts are normalized to housekeeping genes (*Actb, Tubb5 and Vinculin*). Bar plot represents the mean of 3 biological replicates (3 independent primary cultures from 3 animals). P value: ratio paired t-test. Error: SD.

Interestingly, we also did not observe any up-regulation of IEGs (**Figure 8a**), Cdr1as, Cyrano, pri- or mature miR-7 or of any other miRNAs tested (**Figure 8b and c**). This suggests that Cdr1as and mir-7 activity-dependent regulation is part of a neuronal specific response mechanism.

Together our observations demonstrate that miR-7 is post-transcriptionally regulated in likely neuronal-specific way. This either occurs by regulation of maturation of the miR-7 precursor or by stabilization via interaction with Cdr1as.
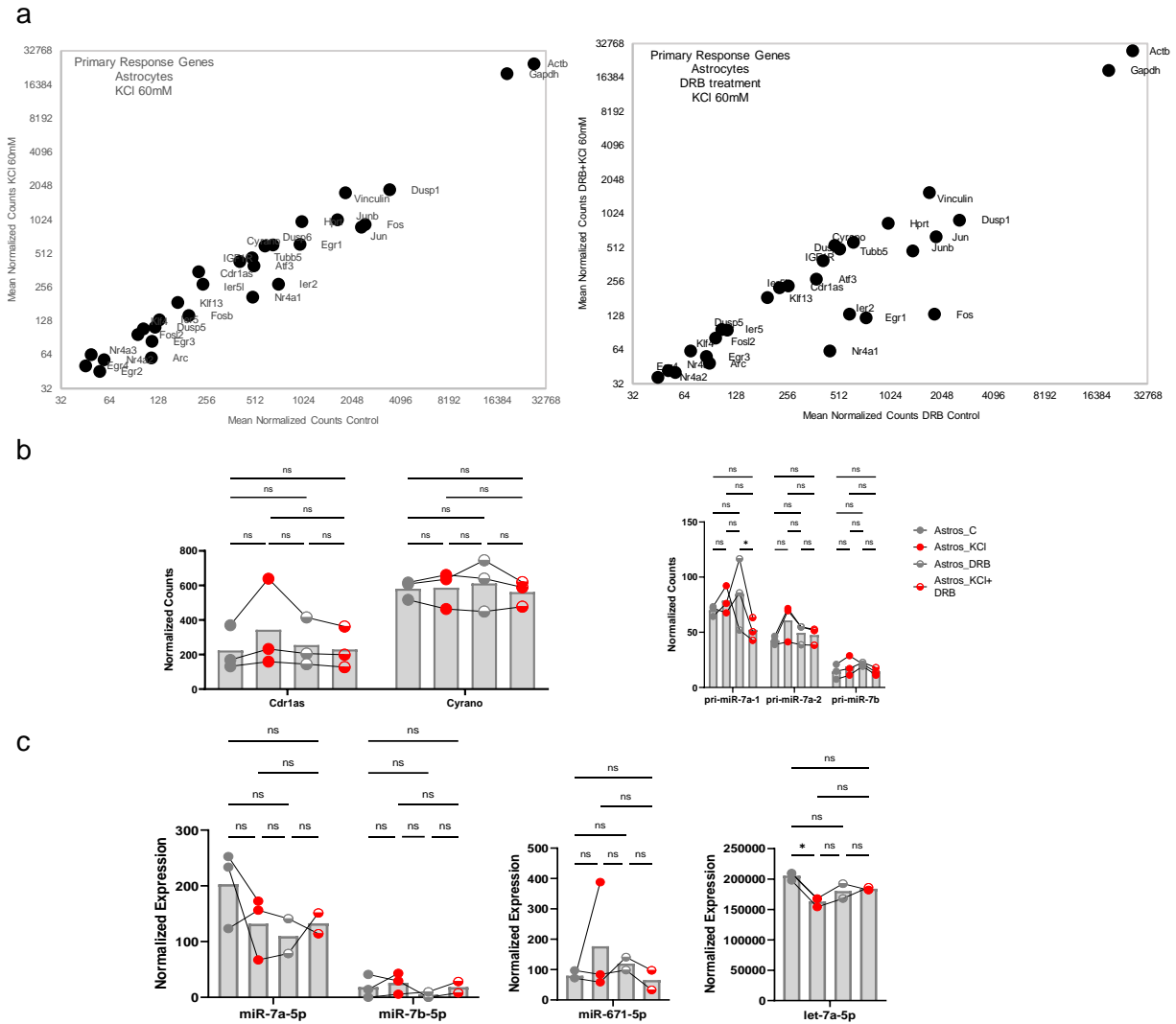
Figure 8. Sustained depolarization does not affect Cdr1as network or immediate early genes in primary astrocytes.

(a) RNA quantification in primary astrocytes exposed to neuronal culture (feeder layer) before and after sustained depolarization (left) plus pre-incubation with transcription inhibitor (DRB) (right) (Nanostring nCounter, methods). Cdr1as and Cyrano shown in red. RNA counts are normalized to housekeeping genes (Actb, Tubb5 and Vinculin). Each dot represents the mean of 3 biological replicates (3 independent primary cultures from 3 animals).

(b) Quantification of Cdr1as, Cyrano and primary miRNAs (Nanostring nCounter, methods), in primary astrocytes exposed to neuronal culture (feeder layer) before and after sustained depolarization plus pre-incubation with transcription inhibitor (DRB). RNA counts are normalized to housekeeping genes (*Actb, Tubb5 and Vinculin*). Bar plot represents the mean of 3 biological replicates (3 independent primary cultures from 3 animals). P value: two-way ANOVA.

(c) Expression levels of mature miR-7 isoforms (left) miR-671 (middle) and let-7a (right) quantified by small RNA-seq for 3 independent primary cultures, in primary astrocytes exposed to neuronal culture (feeder layer) before and after sustained depolarization plus pre-incubation with transcription inhibitor (DRB. Bar plot represents the mean. P value: ratio paired t-test.

2. <u>Sub-cellular localization of Cdr1as ncRNA network in neurons</u>

Importantly, while mostly all IEGs up-regulated by depolarization are TFs encoding nuclear proteins, Cdr1as and Cyrano are lncRNAs enriched in the neuronal cytoplasm. We demonstrated the cytoplasmic enrichment of both lncRNAs by doing nuclear versus cytoplasmatic sub-cellular fractionations in DIV21 WT neurons and measuring relative RNA expression in both compartments **(Figure 9a, green bars)**. These results showed that, as expected, all classical IEGs quantified are enriched in the nucleus (*Fos, Egr3, Junb, Fosl2, Jun, Egr1, Egr2, Fosb*; **Figure 9a, blue bars**). Identical for all primary miRNA transcripts measured (*pri-miR-7a, pri-miR-7b, pri-miR-671*; **Figure 9a, red and orange bars**). Although, mature miR-7 and miR-671, measured by miRNA TaqMan assays, are equally expressed in both nucleus and cytoplasm **(Figure 9b)**. The cytoplasmic localization of mature miR-671 differs from previous finding in HEK293 cell lines (Hansen et al., 2011), where miR-671 was only found in nucleus.

Simultaneously, using quantitative single molecule RNA FISH in DIV21 WT neurons, we demonstrated that Cdr1as and Cyrano are broadly expressed in all analyzed neuronal projections and extended far away from the cellular nucleus. Even more, both molecules are also co-expressed in the same neurons **(Figure 9c)** and distributed almost equally within sub-cellular compartments (somas and neurites). We found that, in a resting state, on average Cdr1as is express in more than 260 copies per neurons (n=80 cells – 6 animals) and is evenly distributed in the cell, ~54% in somas and ~46% in neurites. On the other hand, Cyrano is present only in half of the number of molecules (~100 molecules per cell; n= 69 cells – 5 animals), but distributed more or less equally: ~48% in somas and ~52% in neurites **(Figure 9d).**

Therefore, considering difference in Cdr1as sub-cellular distribution and the induction of Cdr1as-miR-7 axis upon neuronal activation, we hypothesize that Cdr1as can function locally in the neurites. In these subcellular compartments far away from soma, Cdr1as could interact with mature miR-7, to safeguard or buffer the action of miR-7 in stimulated neurons.
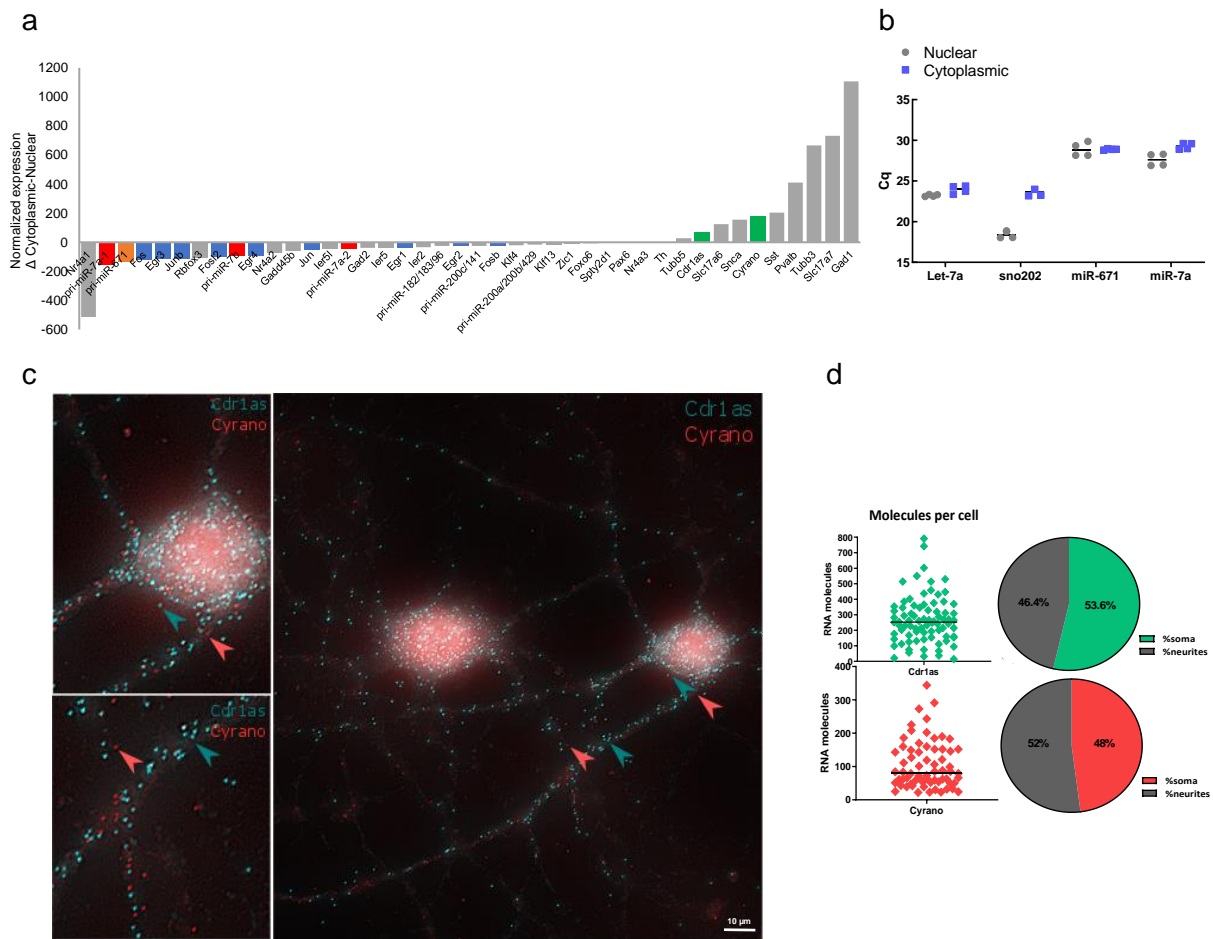
Figure 9. Cdr1as RNA network sub-cellular localization and distribution

(a) RNA Quantification of genes of interest (Nanostring nCounter, methods) in nuclear versus cytoplasmatic fractions of WT neurons DIV21. Each bar represents the mean difference of 3 independent biological replicates. Cdr1as and Cyrano: green. Primary miRNAs: red and orange. IEG: blue. RNA counts are normalized to housekeeping genes (*Actb, Tubb5 and Vinculin*).

(b) miRNA quantification (TaqMan miRNA Assay, methods) in nuclear versus cytoplasmatic fractions of WT neurons DIV21. Each dot represents an independent biological replicate. miRNA Let-7a and snoRNA-202 are used as cytoplasmic and nuclear housekeeping controls, respectively.

(c) Single molecule RNA FISH (Stellaris, Methods) of Cdr1as (cyan) and Cyrano (magenta) performed in WT neurons.

(d) Single molecule RNA FISH quantification of Cdr1as molecules (following Raj et al., 2008, methods). Each dot represents the mean number of molecules in an independent cell (soma + neurites) (Cdr1as n=6; 80 cells) (Cyrano n=5; 69 cells). Horizontal line: Median. Pie chart show molecule distribution in somas versus neurites.

3. Cdr1as-KO neurons show strongly increased pre-synaptic glutamate release after stimulation

To test if Cdr1as is involved in synaptic transmission in stimulated neurons, we used the cortical primary neurons of Cdr1as-KO animals (Piwecka et al., 2017) with their corresponding WT littermates. We compared cultured Cdr1as-KO and WT neurons at DIV21. We performed RNA quantification of marker genes and we did not observe significant differences in the expression of excitatory (**Figure 10a**), inhibitory **(Figure 10c)**, glial **(Figure 10d)**, or proliferation or maturation RNA markers **(Figure 10b)**. This indicated that, in resting state, mature Cdr1as-KO neurons don't show major difference with WT cells at cell-type specification, neither in main proliferation nor maturation regulations.

Glutamatergic neurons are the main cell type in cortex (Niciu et al., 2012). We corroborated that this is also true in our primary neuronal cultures from WT and Cdr1as-KO animals. Glutamatergic neurons were the predominant cell type *(Sclc17a7, Sclc17a6, Sclc17a8*, **Figure 10a**). Consequently, we focused on measuring the activity of glutamate, as the main neurotransmitter relevant in our primary cultures.

We used a genetically-encoded glutamate sensor (GluSnFR; Marvin et al., 2013) to perform real-time recordings of spontaneous and action potential-evoked glutamate release from individual pre-synaptic terminals in mature neurons (DIV18 to 21). Neurons were pre-treated with TTX, CNQX and AP5, to inhibit spontaneous or post-synaptic responses, methods. Separately, we calculated: (1) The frequency of spontaneous neurotransmitter release over a specific time frame (5 minutes). (2) The probability of evoked glutamate release during a sustained trend of electrical stimulations for individual synapses (20 APs at 0.5 Hz), as previously described by Farsi et al., 2021 **(Figure 10e)**.

Our data showed a mild but significant increase in spontaneous glutamate release in Cdr1as-KO pre-synaptic terminals as compared to WT neurons (**Figure 10f**). This is consistent with previously shown up-regulation of spontaneous miniature EPSC frequency in Cdr1as-KO hippocampal patch clamp experiments of single, isolated neurons (autapses, Piwecka et al., 2017).

However, we observed that the increase in glutamate release was mainly driven by the spontaneous activation of some groups of synapses, rather than by a global activation of all terminals (**Figure 10f, pink Kernel density distribution**). Strikingly, we observed much stronger up-regulation of action potential-evoked glutamate release in Cdr1as-KO neurons: 20 APs at 0.5 Hz for 40 secs. (**Figure 10g**). This, suggests that Cdr1as plays potentially important role in the modulation of excitatory transmission during sustained neuronal stimulation, in line with our hypothesis derived from K$^+$ stimulation of WT neurons (**Figure 6 and 7**). Overall, real-time recording of pre-synaptic neurotransmitter release revealed a direct link between Cdr1as-dependent regulation of glutamatergic transmission in resting and particularly in stimulated neuronal states.

How could Cdr1as regulate glutamatergic transmission? It has been proven that Cdr1as' main binding partner, miR-7, directly acts as a negative regulator of stimulus-regulated secretion in secretory glands where the miR-7 is within the top highly expressed miRNA (Bravo-Egana et al., 2008; Landgraf et al., 2007; LaPierre et al., 2022; Latreille et al., 2014). However, cortical neurons are characterized by a very low basal expression of mature miR-7 when compared to characteristic neuronal miRNAs (miR-181, let-7, miR-9, etc.). We also confirmed this by performing small RNA-sequencing of 21 days old neurons (DIV21). We found that out of 1978 mature miRNAs detected and ranked by normalized expression, both miR-7 isoforms ranked in place 216 and 340, respectively. Meanwhile, miR-671 only in position 496 (being 1 the most expressed miRNA: miR-181; **Figure 11a**)**.** Additionally, data obtained from single molecule miRNA FISH showed only ~40 copies of miR-7 per cell, in WT neurons in resting state at DIV21 **(Figure 11b)**.

Thus, we decided to induce miR-7 expression in un-stimulated WT and Cdr1as-KO neurons. This will allow us to reliably study the functions of miR-7 in cortical neurons and to molecularly mimic the increased miR-7 levels observed as consequence of neuronal stimulation (K$^+$ treatments; **Figure 6**).
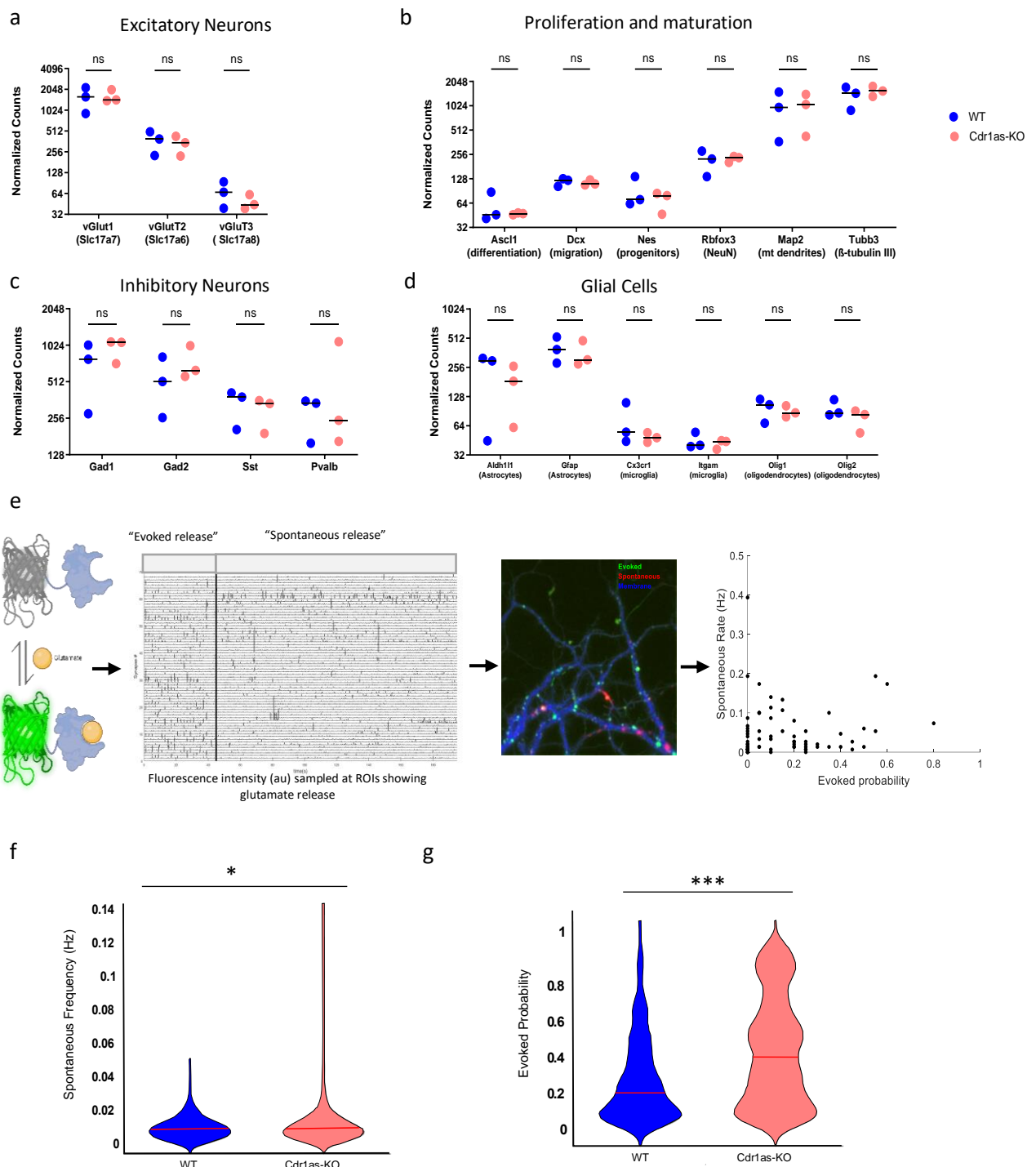
Figure 10. Cdr1as-KO pre-synaptic terminals exhibit increased glutamate release

(a-d) Quantification of cellular markers to characterize WT versus Cdr1as-KO primary cultures DIV21 (Nanostring nCounter, Methods). RNA counts are normalized to housekeeping genes (*Actb, Tubb5 and Vinculin*). Each dot represents an independent biological replicate (3 independent primary cultures from 3 animals) are plotted. P value: U Mann-Whitney test. Horizontal bar: Median. (a) Excitatory neurons (*Sclc17a7, Sclc17a6, Sclc17a8*), (b) Proliferation and maturation markers (*Ascl1, Dxc, Nes, Rbfox3, Map2, Tubb3*), (c) Inhibitory neurons (*Gad1, Gad2, Sst, Pvalb*), and (d) Glial cells markers (*Aldh1, Gfap, Cx3cr1, Itgam, Olig1, Olig2*)

(e) Transduction of a glutamate sensor (AAV, Methods) into WT and Cdr1as-KO primary neurons followed by real-time imaging of excitatory synaptic terminals during AP-evoked (20 APs at 0.5 Hz) and spontaneous (5 minutes + 500 nM TTX) release conditions.

(f) Quantification of spontaneous glutamate release calculated as spontaneous frequency. Violin plots: integration of the synapses from all animals used (WT: n = 4 animals and 662 synapses; Cdr1as-KO: n = 23 animals and 421 synapses; Methods). Synapses with fluorescence value = 0 were removed. Kernel-Density-Estimate plotted (Methods). Red line: median. P value: Unpaired t-test.

(g) Quantification of AP-evoked glutamate release calculated as evoked probability. Violin plots: integration of the synapses from all animals used (WT: n = 4 animals and 335 synapses; Cdr1as-KO: n = 3 animals and 237 synapses; Methods). Synapses with fluorescence value = 0 were removed. Kernel-Density-Estimate plotted (Methods). Red line: median. P value: Unpaired t-test.

4. Sustained miR-7 overexpression reverts increased glutamate secretion in Cd1as-KO neurons

We created a neuron-specific (human synapsin promoter; hSYN) long-term transgene overexpression system. This consist of a miR-7 precursor transcript (pre-miR-7-1) coupled to a fluorescent reporter (mCherry) and packaged into an adeno-associated virus particle (AAV) for highly efficient neuron transduction. In parallel we used a fluorescent vector control (**Figure 11c**, Methods).

We infected WT and Cdr1as-KO primary neuronal cultures on DIV7 with miR-7 or control AAV particles and then monitored mCherry as a reporter of miR-7 expression, until DIV21 when neurons are synaptically mature **(Figure 11c)**. Then, we tested miR-7 overexpression and confirmed significant induction of mature miR-7 in WT and Cdr1as-KO cultures **(Figure 11d)**. Importantly, induced miR-7 levels were very similar in strength in both cases **(**WT= 9.80 L2FC and Cdr1as-KO= 9.77 L2FC; **Figure 11d)**. Additionally, we did not observe significant change of miR-671 (WT: 0.09 L2FC, Cdr1as-KO: 0.4 L2FC), or for highly expressed neuronal miRNA let-7a (WT: -0.02 L2FC, Cdr1as-KO: 0.05 L2FC) in any genotype **(Figure 11e)**. This indicate that our neuron-specific AAV overexpression system did not interfere with the abundance of other miRNAs, therefore is efficient and specific for studying long-term effects of miR-7.

We observed that mCherry protein became visible starting from DIV14 onwards (7dpi). Using single molecule RNA *in situ* hybridization of miR-7, we demonstrate that the overexpressed miRNA is found homogenously distributed in somas and neurites of neurons from both genotypes **(Figure 11f)**. Meanwhile, in control neurons (not infected or empty control) the signal is sparse and only few molecules are captured (~40 copies per cell; **Figure 11b**). Accordingly, we kept DIV14 (7dpi) as the starting time-point to monitor neuronal activity in all following experiments.
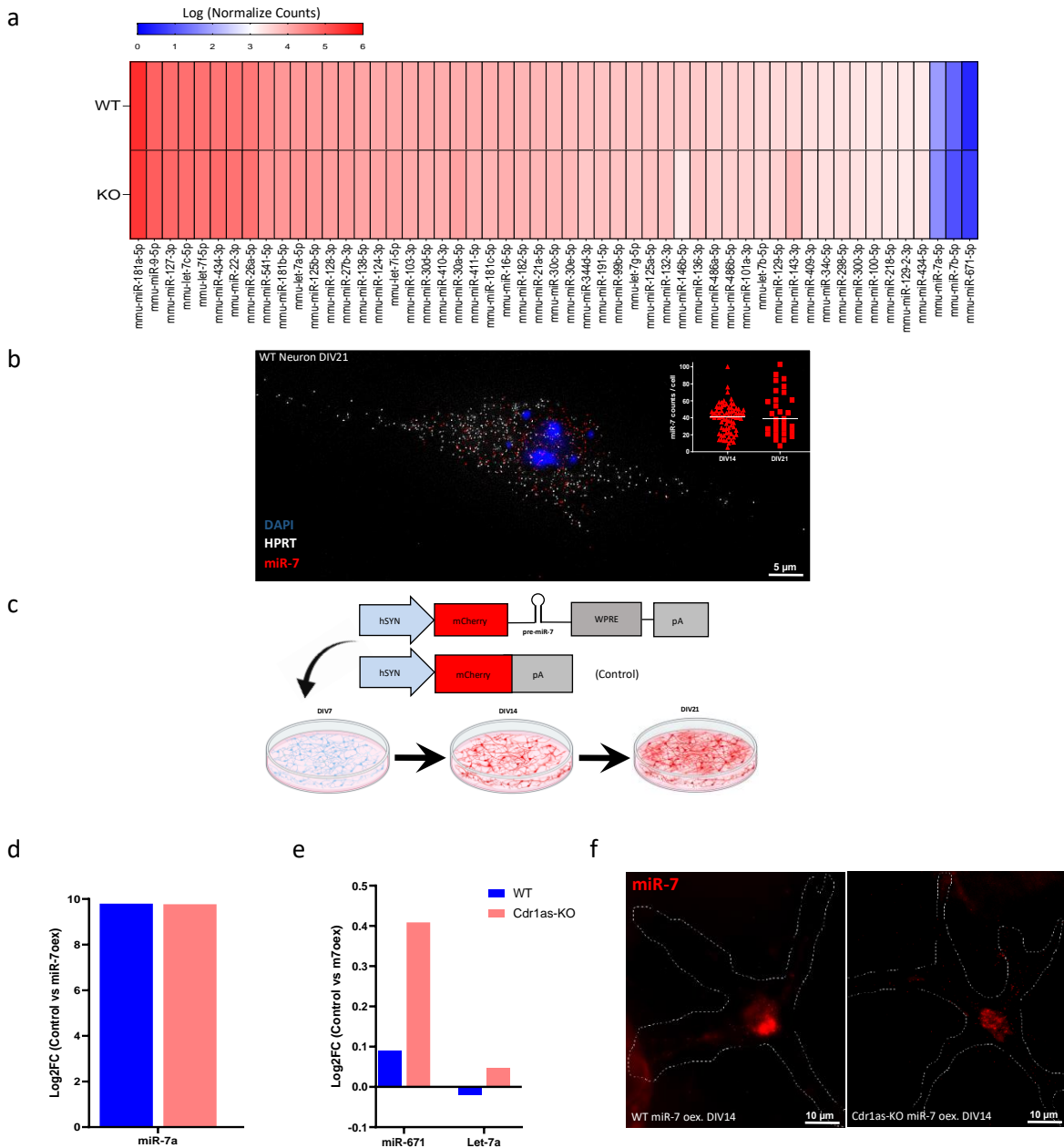
Figure 11. Long-term miR-7 overexpression system is specific and equally efficient in WT and Cdr1as-KO neurons

(a) Heat map from bulk smRNA-Seq (Methods) (1978 miRNA isoforms detected), normalized expression plotted (log.norm.counts) of top 50 mature miRNAs in WT and Cdr1as-KO primary neurons DIV21, plus miR-7, miR-7b and miR-671.

(b) Single molecule RNA FISH (ViewRNA Plus, Methods) of miR-7 (red) and housekeeping gene Hprt (white) performed in WT neurons DIV14 and DIV21, DAPI: blue. Insert: smRNA FISH quantification of miR-7 molecules (following Raj et al., 2008, methods). Each dot represents the mean number of molecules in an independent cell: DIV14 (n=75 cells) and DIV21 (n=30 cells).

(c) Schematic representation of the miR-7 overexpression and the mCherry control constructs. Viral transduction performed at DIV7 (AAV, Methods). mCherry became visible at DIV14 and experiments were performed at DIV21.

(d) Quantification of miR-7 up-regulation by RNA-Seq (Methods) in WT and Cdr1as-KO neurons at DIV21, 14 days post miR-7 overexpression. Bar plots represents mean of 4 independent biological replicates per genotype.

(e) Quantification of miR-671 and let-7a by RNA-Seq (Methods) after miR-7 overexpression in WT and Cdr1as-KO neurons at DIV21 (14dpi). Bar plots represents mean of 4 independent biological replicates per genotype.

(f) Single molecule miRNA *in situ* hybridization (ViewRNA Plus, Methods) of miR-7 (red), performed in WT and Cdr1as-KO neurons DIV21, (14 dpi)(Widefield microscopy; 60X).

We then measured secreted glutamate in the media of DIV18-21 WT and Cdr1as-KO neuronal cultures at resting state, in neurons infected with control or miR-7 overexpression AAV (14dpi). For this, we set up a bioluminescent enzymatic assay (Methods), based on the activity of glutamate dehydrogenase (GDH) coupled to the activity of Luciferase (Ultra-GloTM rLuciferasa, Promega). This reaction results in the production of light proportional to the concentration of glutamate in the media **(Figure 12a)**. Exact concentrations of secreted glutamate were calculated by interpolation of luminescence values (RLU) from a glutamate standard curve **(Figure 12b)**.

We detected that secreted glutamate levels were not changed in WT cells after overexpressing miR-7 **(Figure 12c)**. In contrast to other systems such as pancreatic β-cells, where specific overexpression of miR-7 induced a reduction of insulin secretion (Latreille et al., 2014). However, consistent with our previous observations from individual pre-synaptic terminals (**Figure 10f - g**), glutamate levels were strongly and significantly increased in Cdr1as-KO neurons. Strikingly, this increase was reverted to almost WT levels when miR-7 was overexpressed in the absence of Cdr1as. As Cdr1as is absent or only spuriously expressed in the pancreas (H. Xu et al., 2015). Our data suggest that Cdr1as in cortical neurons has evolved to buffer miR-7 function and that Cdr1as expression is necessary to modulate miR-7 effect in maintaining glutamate secretion under tight control.
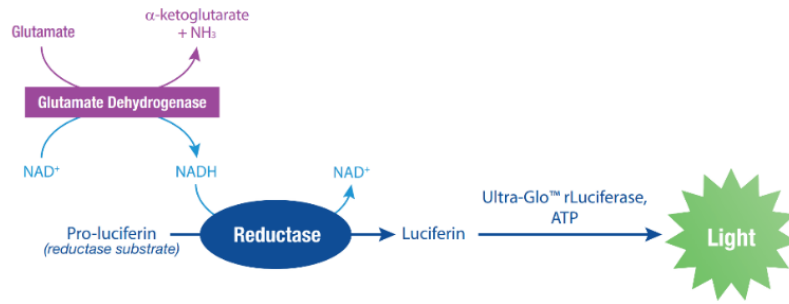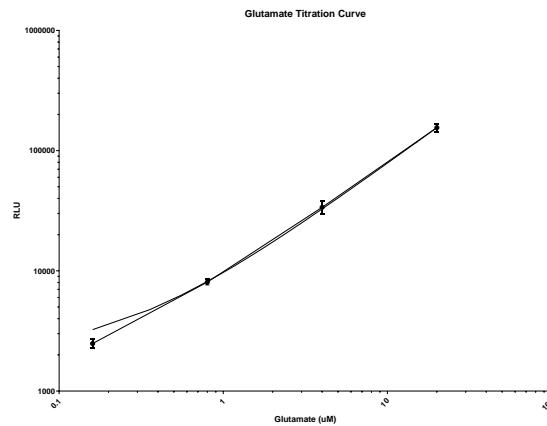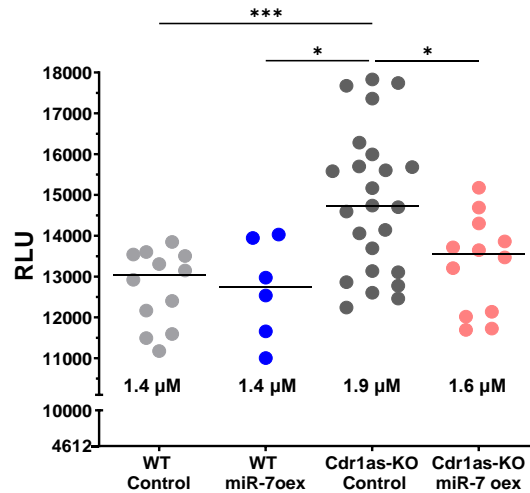
Figure 12. Long-term miR-7 overexpression rescues increased glutamate secretion in Cdr1as-KO mature neurons

(a) Schematic representation of the enzymatic principle behind glutamate secretion assay. Modified from Glutamate-Glo™ Assay (Methods). GDH enzyme catalyzes the oxidation of glutamate with associated reduction of NAD+ to NADH. In the presence of NADH, Reductase enzymatically reduces a pro-luciferin to luciferin. Luciferin using Ultra-Glo™ Luciferase and ATP, and the amount of light produced (RLU) is proportional to the amount of glutamate in the sample.

(b) Standard curve for calibration of glutamate secretion assay. Serial dilutions curve of 50uM Glutamate stock solution. Quantification of secreted glutamate concentrations for tested samples based on interpolation of RLU values.

(c) Glutamate secretion assay performed on neuronal media collected from DIV18-21 WT and Cdr1as-KO neurons infected with control or miR-7 overexpression construct. Each dot represents the glutamate concentration quantified in an independent primary culture (WT = 12; WT + miR-7 overexpression = 12; Cdr1as-KO = 12; Cdr1as-KO + mirR-7 overexpression = 24 independent replicates). Glutamate concentrations are calculated based on a glutamate titration curve (Methods, Supplementary material). Baseline concentration of glutamate in control media without cells was 0,28 uM (4612 RLU). Black line: median. P value: two-way ANOVA, all other comparisons were not statistically significant (not shown).

5. Sustained miR-7 overexpression reverted increased local neuronal bursting in Cdr1as-KO neurons.

To investigate changes in neuronal activity associated with the loss of Cdr1as and miR-7 overexpression, we recorded local and network real-time activity over neuronal maturation (DIV7 until DIV21). For this we tested WT and Cdr1as-KO cultures, with or without miR-7 overexpression. We used a multi-electrode array well-based system (MEA, Axion BioSystems) to record extracellular field APs, and ultimately network activity (**Figure 13a**).

We measured local APs recorded by an electrode placed nearby the generating neurons. We observed that throughout maturation time there are no significant changes in the frequency of firing in WT neurons overexpressing miR-7 as compared to WT controls in any of the analyzed timepoints (**Figure 13b, blue and grey-blue datapoints**). Similar to our data for glutamate secretion in media (**Figure 12c**). However, Cdr1as-KO neurons consistently showed a significant up-regulated spontaneous firing frequency (larger number of functional APs per second). This up-regulation is progressively increased from DIV7 until DIV21 as compared to WT neurons (**Fig. 13b, pink and blue datapoints**). Once more, this up-regulation was reverted to almost WT levels (or exceeding those) when overexpressing miR-7 in Cdr1as-KO neurons (**Fig. 13b pink and grey-pink datapoints**). This reversion was the strongest in more mature neurons (DIV21). Consequently, we can conclude that our observations of up-regulated glutamate secretion in Cdr1as-KO (**Figure 10**) translate into increased functional APs.

To test if changes in firing rates are linked to changes in patterns of neuronal activity, we measure neuronal burst formation (Methods). Burst we can define as rapid AP spikings followed by inactive periods, much longer than typical inter-spike intervals. In WT neurons no significant differences in bursting frequency were observed after sustained overexpression of miR-7 compared to controls, at any timepoint (**Fig. 13c, blue and grey-blue**). However, Cdr1as-KO neurons bursting activation patterns were persistently increased over maturation. This increase in bursting was as well reverted by miR-7 overexpression to WT or even lower frequencies (**Fig. 13c, pink and grey-pink datapoints**).

Cdr1as-KO neurons also showed significantly longer burst duration, (**Figure 13d, pink and blue datapoints**) and higher number of functional spikes per burst (**Figure 13e, pink and blue datapoints**). Both growing in deviation from WT as the neurons mature. Interestingly, miR-7 overexpression affected burst duration of neurons at DIV21 in opposite ways and in a genotype dependent manner. Burst duration was increased in WT neurons and decreasing it on Cdr1as-KO (**Figure 13d**).

Taking all together, the real-time recording of local neuronal activity demonstrated that AP frequencies are impaired in Cdr1as-KO neurons. All these defects were effectively rescued by sustained mir-7 overexpression. This suggests that cellular mechanisms responsible for transforming local AP into coordinated activation patterns (bursting activity) are as well affected in Cdr1as-KO neurons. Longer, more frequent, higher number of spikes per bursts are indications of stronger excitatory transmission, or of less inhibition, as it takes longer time to shut down a burst (Zeldenrust et al., 2018). Therefore, our results suggest that the effect of the interaction of Cdr1as and miR-7 on glutamatergic release might be linked to the modulation of some aspects of neuroplasticity, for example, neural coding or network synchronization.
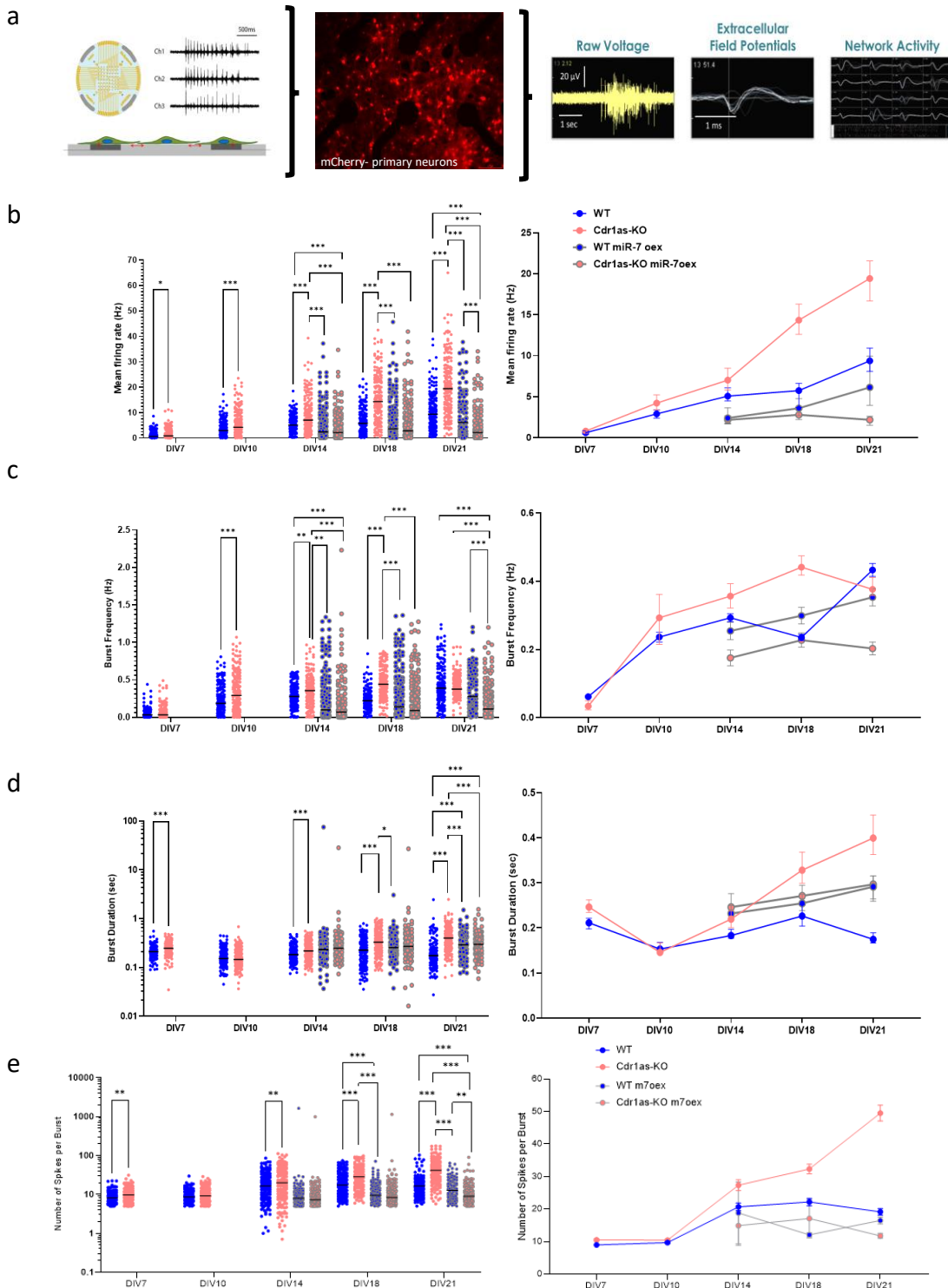
Figure 13. miR-7 overexpression rescues upregulated local neuronal bursting activity in Cdr1as-KO neurons

(a) Scheme of the Multi electrode Array recording protocol (Axion Biosystems, CytoView MEA 48, Methods). Second panel: representative image of cultured neurons DIV14 in a recording well. white: electrodes, red: mCherry reporter. Third panel: schematic representation of output data, extracellular field potentials and neuronal network activity. AP: Adaptative threshold 6 SD. Sampling frequency 12.5 kHz. Active electrode selection criteria 5 spikes/minute.

(b) Mean Firing Rate: Total number of spikes per single-electrode divided by the duration of the analysis (600s), in Hz. Left panel: each dot represents a single electrode recording from 4 independent primary cultures (WT = 187; WT + miR-7 overexpression = 194; Cdr1as-KO = 189; Cdr1as-KO + miR-7 overexpression = 200 electrodes). Horizontal line: median. Right panel: median value across timepoints with 95% confidence interval is plotted; arrows indicate transduction time (AAV, DIV7) and reporter first visualization (mCherry, DIV14), respectively. P value: two-way ANOVA, all other comparisons were not statistically significant (not shown).

(c) Burst Frequency: Total number of single-electrode bursts divided by the duration of the analysis, in Hz. Left and right panels plotted as in (b).

(d) Burst Duration: Average time (sec) from the first spike to last spike in a single-electrode burst. Left and right panels plotted as in (b).

(e) Number of Spikes per Burst: Average number of spikes in a single-electrode burst. Left and right panels plotted as in (b).

6. Sustained miR-7 up-regulation strongly affects neuronal connectivity in a Cdr1-as dependent manner

We explored various neuronal wiring parameters, such as network synchrony and AP oscillations. To investigate further how Cdr1as and miR-7 are relevant for the modulation of plasticity and neuronal network patterns.

First, we calculated network synchrony by comparing the activity profiles of two neighboring electrodes across different time delays (area under the cross correlation). When the area is 0 there is perfect synchrony, while larger area values indicate lower synchronicity. We observed a more asynchronous network in Cdr1as-KO neurons on very late states of maturation compared to WT (**Figure 14a, pink and blue datapoints and Figure 14b**). On the other hand, after miR-7 overexpression there is a significant change to a highly synchronic network activity for both genotypes (**Figure 14a, grey-blue and grey-pink datapoints**). Though, this higher synchrony could be explained as well by less neuronal activity displayed after miR-7 overexpression as showed in our local neuronal activity observations.

Second, we analyzed AP oscillations across the network and captured the distribution of action potentials. We measured the coefficient of variation of the intervals inter-spike (ISI CoV), where zero (0) values indicate perfect Poisson distribution of APs and higher values represent irregular bursting. We observed significantly higher oscillation periodicity in Cdr1as-KO network at very late points of maturation (DIV18-DIV21). In WT and Cdr1as-KO neurons, after sustained miR-7 overexpression there was a significant down-regulation of oscillatory bursting (**Figure 14c, grey-blue and grey-pink datapoints**). The size of the miR-7 dependent effect in WT neurons was much smaller compared to Cdr1as-KO, and completely disappeared at DIV21. Network oscillation differences in Cdr1as-KO, which were efficiently modulated by the sustained high expression of miR-7, is a strong indication of an imbalance between glutamatergic and inhibitory signaling in Cdr1as-KO neuronal network.

Finally, we studied timepoints where the network reaches its maximal firing peak, as proxy for maturation of the network. We measured the maximum spike frequency in the average network burst.

We did not find significant differences between WT and Cdr1as-KO neurons over time. However, we observed a significant down-regulation on the burst peak after miR-7 overexpression affecting equally both genotypes (**Figure 14d, right panel, blue and pink lines**).

These results suggest that the modulation of miR-7 expression has a great influence in neuronal network activity regulation. Yet, the extent and strength of its influence is modulated by the expression of the Cdr1as. Therefore, in constitutive absence of Cdr1as the system is more prone to the effects of miR-7, especially noticeable in very late times of synaptic maturation.
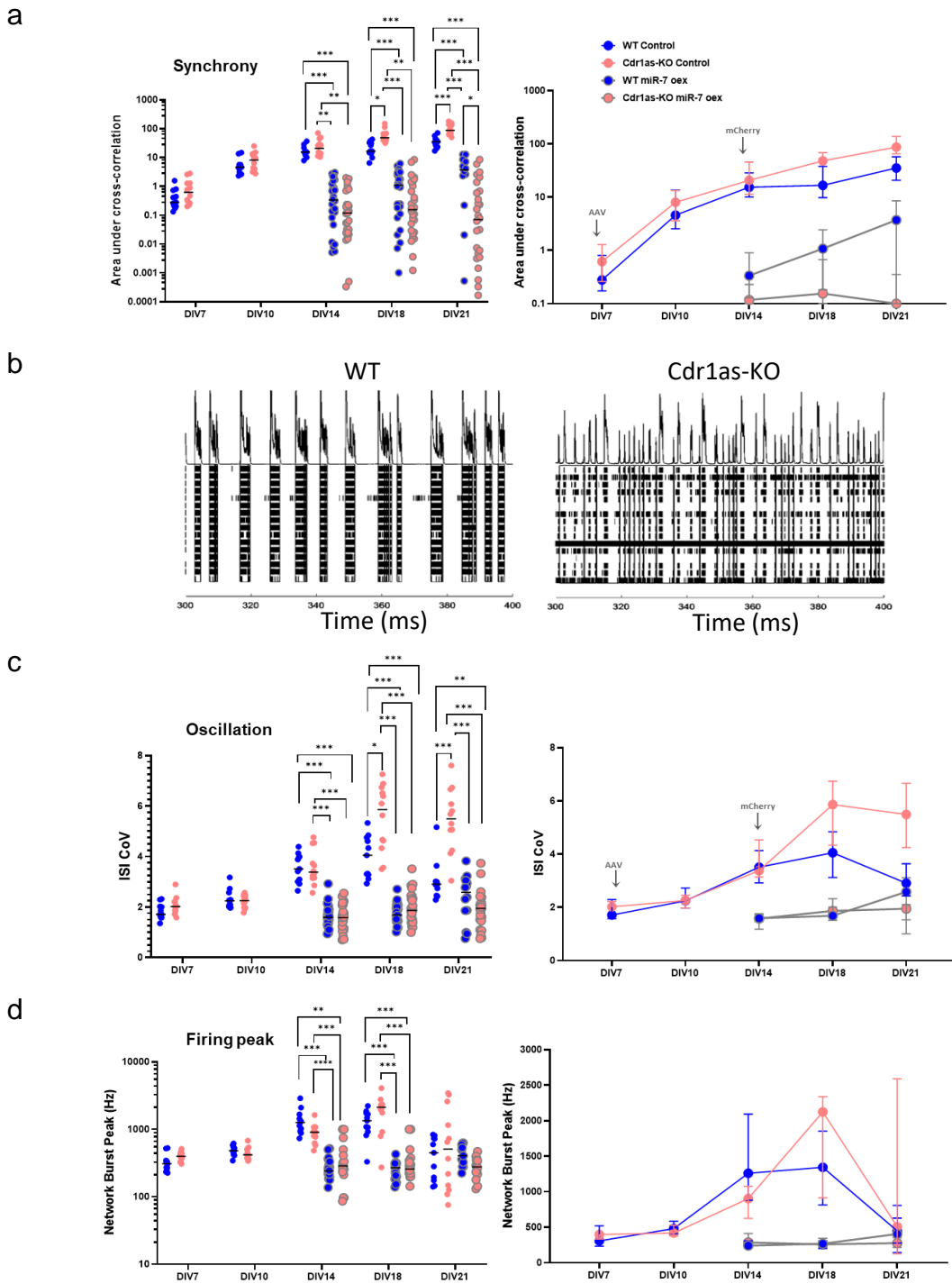
Figure 14 Removal of Cdr1as affects neuronal connectivity by changing network synchrony and oscillation. Sustained miR-7 expression reverted these effects.

(a) Synchrony: The ability of neurons to generate APs simultaneously was calculated as area under the well-wide pooled inter-electrode cross-correlation. Higher areas indicate lower synchrony (Halliday et al., 2006, Methods). Left panel: each dot represents a network recording (Methods) from 4 independent primary cultures (WT = 11; WT + miR-7 overexpression = 26; Cdr1as-KO = 12; Cdr1as-KO + miR-7 overexpression = 28 electrodes). Horizontal line: median. Right panel: median across timepoints with 95% CI plotted, arrows indicate transduction time (AAV, DIV7) and reporter first visualization (mCherry, DIV14). All metrics apply to network bursts across single wells within 20 ms. P value: two-way ANOVA, all other comparisons were not statistically significant (not shown).

(b) Example raw spikes from multi electrodes Array recording: 100 ms raw spikes of WT and Cdr1as-KO neurons DIV21. Each row represents one independent electrode (blac bars).

(c) Oscillation: Average across network bursts of the inter spike interval coefficient of variation (ISI CoV) (standard deviation/mean of the inter-spike interval) within network bursts. Oscillation is a measure of how the spikes from all of the neurons are organized in time. WT = 11-26; Cdr1as-KO: 12-28 independent network recordings. Left and right panels plotted as in (a).

(d) Burst Peak: Maximum number of spikes per second in the average network burst. The peak of the average network burst histogram divided by the histogram bin size to yield spikes per sec (Hz). WT = 11-26; Cdr1as-KO: 12-28 independent network recordings. Left and right panels plotted as in (a).

7. Sustained miR-7 overexpression down-regulates Cdr1as and restricts its residual expression to the soma

To better understand Cdr1as:miR-7 regulatory network, we decided to look into expression of Cdr1as antagonist - lncRNA Cyrano. We performed single molecule RNA *in situ* hybridization (Stellaris, Methods) for Cdr1as and Cyrano (**Figure 15a-b**), in control neurons and in neurons after sustained miR-7 overexpression. Cdr1as-KO neurons DIV21 served as technical negative controls (**Figure 15c**). Images were quantified (Methods) across biological replicates (independent cultures from different animals). We noticed that upon sustained miR-7 overexpression in WT neurons, the distribution of Cdr1as molecules was restricted to neuronal somas and close proximal space, while massively cleared from all neurites (**Figure 15a and d**). Additionally, we also observed a reduction of Cyrano molecules. However, this reduction was only significant in the soma but not in neurites (**Fig. 15b and d**).

To investigate if Cdr1as and Cyrano are spatially co-localized in control neuronal conditions or after miR-7 overexpression we used a computational pipeline (Eliscovich et al., 2017) for quantification of single-molecule spatial correlations (Methods). We measured all mutual nearest neighbor distances (MNN) of molecule associations: Cdr1as-Cyrano in comparison with positive (probes for CircHipk3-LinHipk3: probes spamming two consecutive exons in the same mRNA), and negative (probes for Cdr1as-Tfrc: probes for an housekeeper RNA unrelated to Cdr1as regulation) technical controls (Methods). The results from the cumulative distribution of MNN distances between each pair of probes showed no significant association in space between Cdr1as and Cyrano molecules neither in control neurons nor after miR-7 overexpression, as compared to positive molecule-association controls (**Figure 15e, left panel**). The association in space was tested in whole cells, neurites, and somas, separately (**Figure 15e, right panel**). We did not find significant differences between Cdr1as-Cyrano distances and the negative control in any of the tested compartments, for either of the two tested experimental conditions. Therefore, we conclude that Cdr1as and Cyrano do not co-localized in a biologically relevant distance.

We further validated the RNA expression by the Nanostring system (Methods). We confirmed statistically significant decrease of Cdr1as and Cyrano molecules in WT neurons after miR-7 overexpression. Even more, we observed that Cyrano expression is also decreased in Cdr1as-KO neurons (**Figure 15f**), after sustained miR-7 overexpression.

Altogether, these data indicate that we have identified a new layer of regulation of the Cdr1as-Cyrano-miR-7 axis. The expression changes of both lncRNAs affect miR-7 levels (Kleaveland et al., 2018; Piwecka et al., 2017). The exposure to sustained high concentrations of miR-7 generates a negative feedback loop that down-regulates both lncRNAs. Meanwhile, for Cdr1as this decrease happens mainly in neuronal projections. The molecular mechanisms responsible for this down-regulation and whether it is a direct or indirect effect of miR-7 up-regulation remains unknown.

The observations that Cdr1as is cleared out from neurites in WT neurons, may explain in part the reduced phenotype observed in local and network neuronal activity, and glutamate secretion of WT neurons after sustained miR-7 overexpression. A gradual reduction of Cdr1as from the intracellular compartments closer to synaptic zones, during the time course of miR-7 overexpression would be similar to what we observed in Cdr1as-KO neurons. The effect was however lower and depended on the time after miR-7 overexpression.
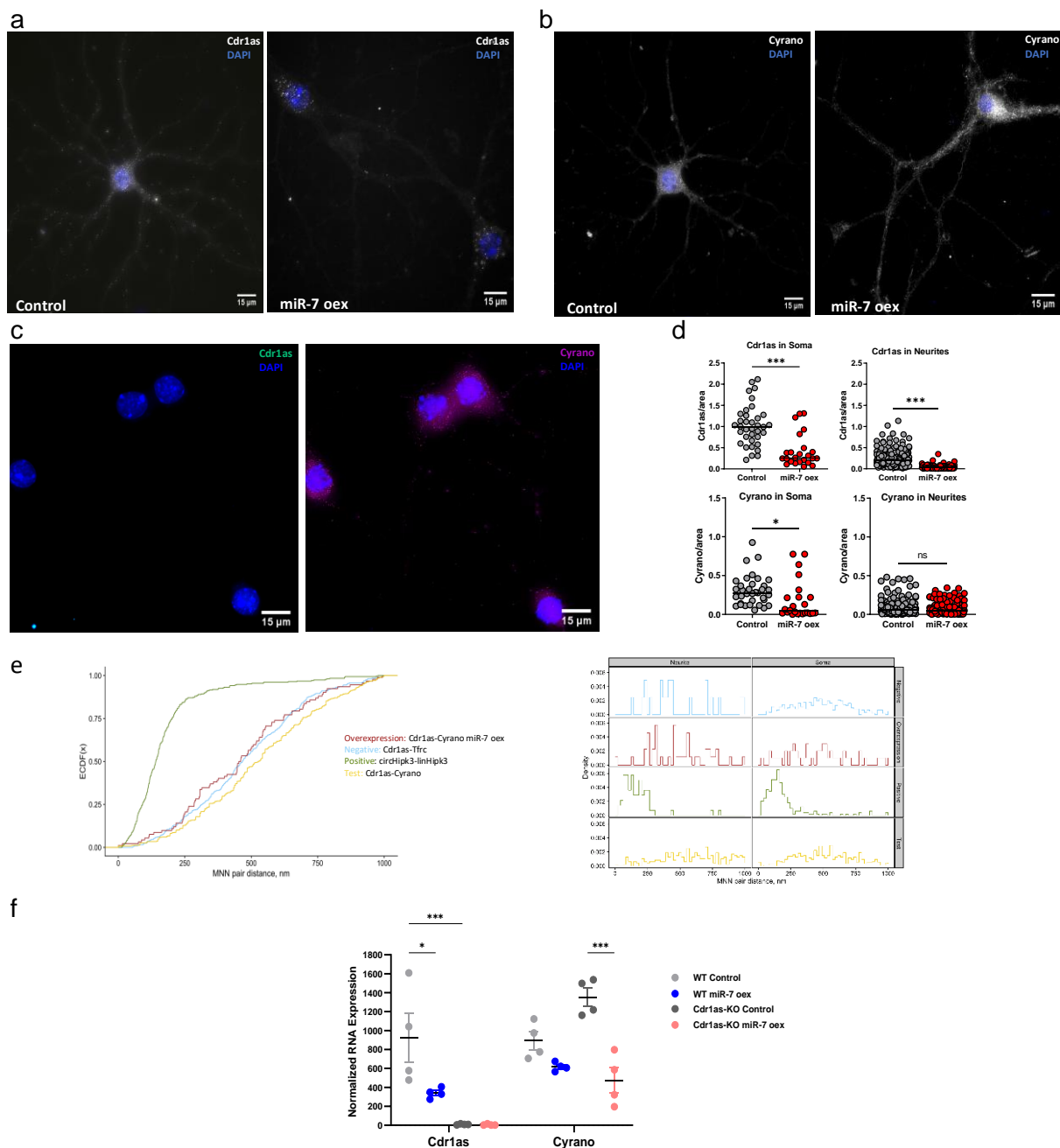
Figure 15. miR-7 overexpression downregulates Cdr1as and Cyrano, removes Cdr1as from neurites and restricts its residual expression to the soma

(a) Single molecule RNA FISH (Stellaris, Methods) of Cdr1as (white) performed in WT neurons DIV21 from neurons infected with control or miR-7 overexpression construct. DAPI: blue.

(b) Single molecule RNA FISH (Stellaris, Methods) of lncRNA Cyrano (white) performed in same conditions as (a). DAPI: blue.

(c) Single molecule RNA FISH (Stellaris, Methods) of Cdr1as (cyan) and Cyrano (magenta) performed in Cdr1as-KO neurons DIV21.DAPI: blue.

(d) smRNA FISH quantification of Cdr1as and Cyrano molecules (following Raj et al., 2008, Methods). Each dot represents the mean number ofCdr1as or Cyrano molecules in an independent cell compartment (soma or neurite) normalized by area (100 px = 21,5 um). Control neurons: 25 somas and 110 neurites (2 independent cultures from 2 animals); miR-7 overexpression neurons: 35 soma and 230 neurites (2 independent cultures from 2 animals). Horizontal line: Median. P value: unpaired t-test with Welch correction.

(e) Left: Cumulative distribution function (CDF) plot of molecule distances based on smRNA FISH images of WT neurons DIV21. before and after miR-7 overexpression (Methods) comparing all computationally predicted mutual nearest neighbors' distances in nm all conditions (MNN, Methods). Positive technical control: circHipk3-linHipk3; Negative control: Cdr1as-Tfrc; Test: Cdr1as-Cyrano; overexpression: Cdr1as-Cyrano miR-7 overexpression. 2 independent biological replicates from 2 animals. Right: Density plot molecule distances based on smRNA FISH to compare somas versus neurites for all tested conditions. Analysis conditions same as in left plot.

80

(f) Quantification of Cdr1as and Cyrano (Nanostring nCounter, Methods), performed in WT and Cdr1as-KO neurons DIV21 from neurons infected with control or miR-7 overexpression construct. RNA counts are normalized to housekeeping genes (Actb, Tubb5 and Vinculin). Each dot represents an independent biological replicate (4 independent primary cultures from 4 animals). P value: 2-way ANOVA. Error: SD. Horizontal bar: Median. P value: two-way ANOVA, all other comparisons were not statistically significant (not shown).

8. <u>Transcriptomic changes caused by sustained miR-7 overexpression are enhanced by the absence of Cdr1as</u>

Next, we investigated whether the role of Cdr1as-miR-7 network in neuronal functions and the observed molecular RNA changes are reflected in global transcriptomic patterns. For this, we performed bulk polyA+ RNA-sequencing of 4 independent primary neuronal cultures at DIV21 from WT and Cdr1as-KO animals, infected with control or miR-7 overexpression (14dpi). To identify differentially expressed genes we applied DESeq2 pipeline, while controlling for batch effects and individual effects (**Figure 16a**).

We investigated predicted miR-7 target mRNAs. To do so, a list of predicted conserved targets of miR-7-5p (and miR-122 as a control) were downloaded from TargetScan Mouse, release 7.2 (Agarwal et al., 2015) and miRDB (Y. Chen & Wang, 2020) and only targets existing in both databases were used (Methods). We did not find significant global changes of miR-7-5p predicted targets genes when comparing WT and Cdr1as-KO control neurons (**Figure 16b, grey versus yellow lines**). Nonetheless, in both WT and Cdr1as-KO neurons, we did observe a significant global decrease of predicted miR-7-5p targets compared to non-target transcripts expression, consistent with long-term miR-7 up-regulation (**Figure 16b, grey versus purple or brown lines**). However, we noticed that in Cdr1as-KO neurons, miR-7-5p predicted target genes are more strongly down-regulated, compared to WT (significant difference between the shift of cumulative fractions: p value $< 1e10^{-6}$; **Figure. 16b, purple and blue lines**). Considering that miR-7 up-regulation is equally efficient in both genotypes (**Figure 11d and f)**, suggests that the interaction between Cdr1as and miR-7 is responsible for the differences in observed miR-7 targets regulation strength. This indicates that the constitutive loss of Cdr1as is sensitizing the neurons to the action of miR-7 on its mRNA targets. Predicted targets from a control miRNA were not altered in any of the tested comparisons (i.e., miR-122-5p, miRNA not expressed brain; Figure 16c).
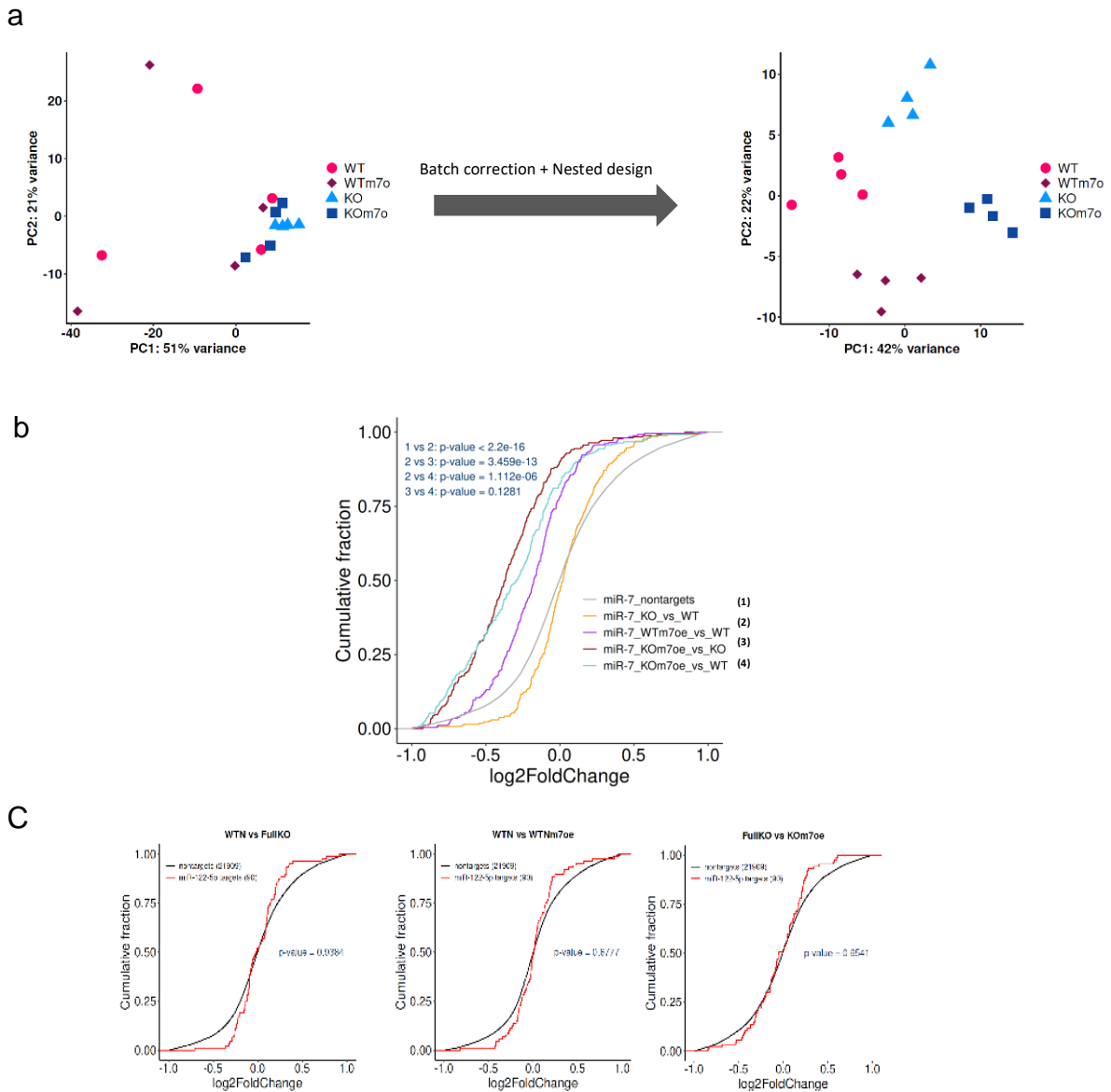
Figure 16. Loss of Cdr1as sensitized neurons to the action of miR-7 on its mRNA targets.
(a) Principal component analysis (PCA) of all data sets. Each replicate represented by one dot. Original (left) and batch corrected with nested design (right).
(b) Cumulative distribution function (CDF) plot of gene expression comparing all computationally predicted miR-7 targets (Methods) to mRNAs lacking predicted miR-7 target sites (non-targets, grey), across 4 independent biological replicates of WT, Cdr1as-KO, WT + miR-7 overexpression, Cdr1as-KO + miR-7 overexpression. P value: U Mann–Whitney test.
(c) Cumulative distribution function (CDF) plot of gene expression comparing all computationally predicted miR-122 targets (Methods, red) to mRNAs lacking predicted miR-7 target sites (non-targets, black), across 4 independent biological replicates of WT, Cdr1as-KO, WT + miR-7 overexpression, Cdr1as-KO + miR-7 overexpression. P value: U Mann–Whitney test.

Besides the strong dependence of miR-7 target genes expression on Cdr1as expression, our transcriptomic data revealed many other genes which are dysregulated upon Cdr1as and/or miR-7 perturbation (**Figure 16**). In Cdr1as-KO control neurons, we observe only a few mRNAs significantly changing compared to WT neurons (**padj<0.05; Figure 17a; panel i)**. This is expected, since the small down-regulation in homeostatically lowly expressed mature miR-7 in Cdr1as-KO neurons (**Figure 11a**) is most likely not reflected in global abundance of mRNAs of resting neurons.

Separately, we compared WT and Cdr1as-KO neuronal transcriptomes before and after miR-7 overexpression. We observed an increasing number of differentially expressed genes depending on the genotype. This suggested that global mRNA transcriptomic changes are enhanced by the complete constitutive loss of Cdr1as (**Figure 17a, panels ii and iii**).

Few of these RNA modulations are intrinsic changes of Cdr1as loss, not affected by miR-7 overexpression (*Crocc, Pisd-ps1, Cdr1os, Cd5l, Tyrobp, Vat1*; **Figure 17b**; up-regulated: 0.6% differentially expressed genes and down-regulated 0.5% of differentially expressed genes). Other RNAs appear to be down-regulated exclusively in Cdr1as-KO control neurons, (*Tagln2, Tgm2, Ucp2, Ifitm3, Mybpc1, Anxa1*; **Figure 17b, right diagram blue bubble:** 0.9% of differentially expressed genes). On the contrary, 72 genes were dysregulated by miR-7 overexpression in both genotypes independent of the expression levels of Cdr1as (**Figure 17b**; up-regulated: 3% and down-regulated 8.6% of differentially expressed genes).

Most interestingly, the largest group of transcriptomic variations occur after miR-7 overexpression exclusively when Cdr1as is constitutively absent. 24.4% of all up-regulated genes (132) are exclusively changing on Cdr1as-KO neurons after sustained miR-7 expression (**Figure 17a, panel (iii) and Figure 17b, left diagram, grey bubble**). This group of genes do not belong to predicted miR-7-5p target mRNAs and the gene ontology enrichment analyses linked them mostly with vesicle and membrane related proteins, and with membrane receptor pathways (**Figure 18a, (i)CC and (ii)ML**). This is illustrating the large indirect up-regulation of 'non-miR-7 targets genes' only in Cdr1as-KO neurons.

Similarly, 23.3% of all down-regulated genes (151) are only regulated in Cdr1as-KO and their most overrepresented ontology term associated them mostly with plasma membrane proteins with catalytic activity (**Figure 18a, (i) CC and (ii) ML**). In contrast, only a small number of genes are regulated by miR-7 specifically in WT neurons (3.9% up-regulated - 0.6% down-regulated; **Figure 17b, yellow bubbles**). Of course, indirect effects are to be expected, but the vast increase in dysregulated genes when combining miR-7 overexpression in Cdr1as-KO neurons points at a synergetic regulation exerted by both RNAs.

Cdr1os (Cdr1as precursor; **Figure 4a**), which was previously shown to be up-regulated by the loss of Cdr1as locus in bulk brain tissue (Barrett et al., 2017), was not altered by miR-7 overexpression (**Figure 17c, left panel**). We also confirmed the significant down-regulation of lncRNA Cyrano in both genotypes caused by miR-7 up-regulation, but not affected by the loss of Cdr1as itself. (**Figure 17c, right panel**).

In summary, our data suggests that global transcriptomic changes caused by miR-7 overexpression are enhanced by the constitutive loss of Cdr1as. This connects mRNA changes in neurons with changes in local and network neuronal activity and glutamate secretion. Therefore, we next turned into a more detailed analysis of specific molecular pathways that might explain these differences.
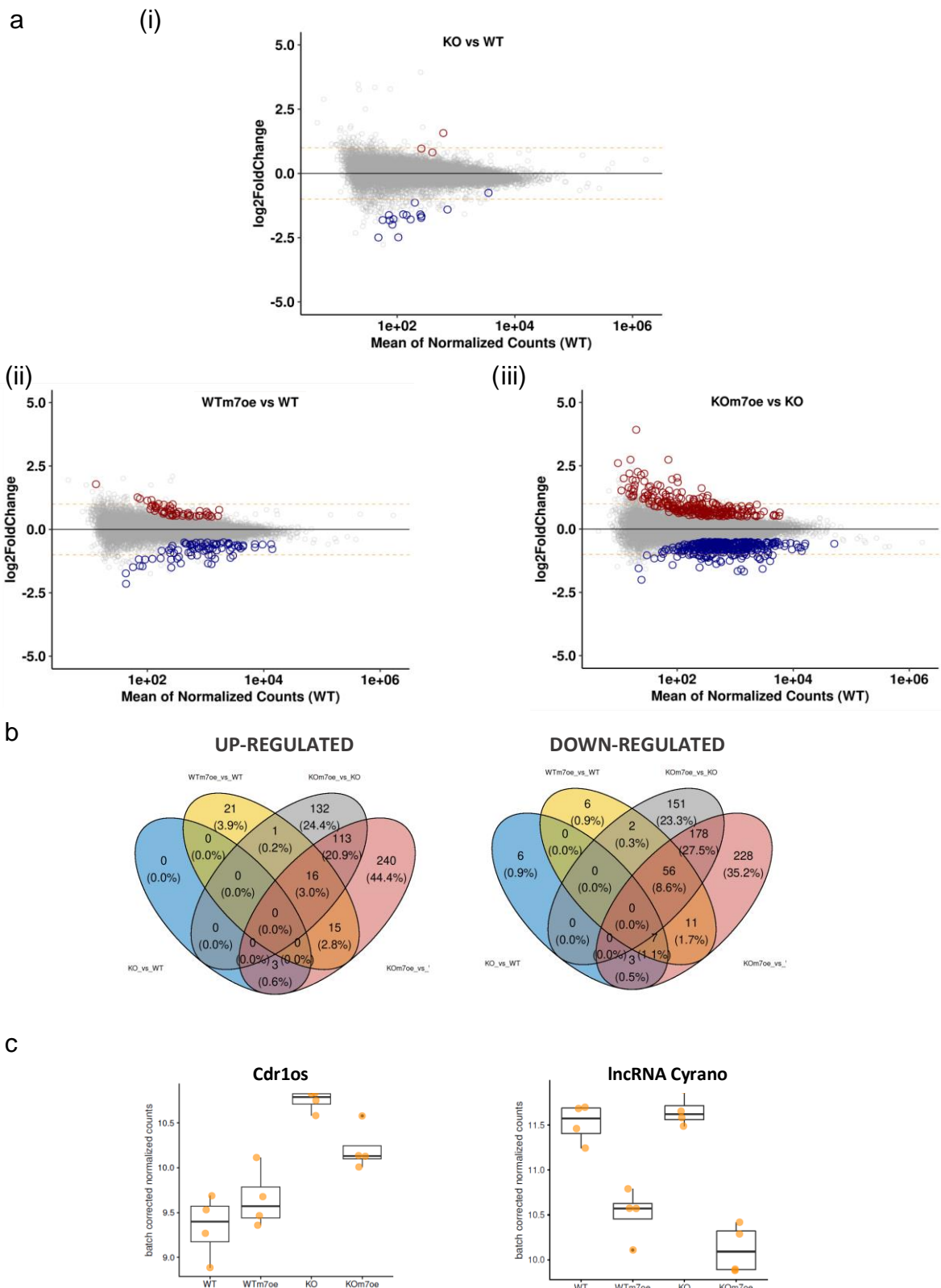
Figure 17. Transcriptomic changes resulting from miR-7 sustained overexpression are enhanced by the loss of Cdr1as.

(a) mRNA expression changes for each comparison tested: (i) Cdr1as-KO vs WT, (ii) WTmiR-7oex. vs WT, (iii) Cdr1as-KO miR-7oex.vs Cdr1as-KO). Plotted is the mean change of 4 independent biological replicates per condition. Red dots: statistically significant up-regulated genes. Blue dots: statistically significant down-regulated genes (Methods).

(b) Number of specific and commonly up-regulated and down-regulated genes from mRNA expression changes for each comparison tested (Cdr1as-KO vs WT, WTmiR-7oex. vs WT, Cdr1as-KO miR-7oex.vs Cdr1as-KO). Venn diagram, mean change of 4 independent biological replicates per condition.

(c) Gene expression of Cdr1os (left) and lncRNA Cyrano (right) in each data set. Box plots, 4 independent biological replicates per condition, for each comparison tested. (FDR < 0.05).

9. Identification of gene regulatory pathways controlled by the interaction of miR-7 and Cdr1as

Several miR-7 target genes have been validated in pancreas and hypothalamus as direct regulators of secretion. Both of this thoroughly studied neuroendocrine cell tissues are highly enriched in miR-7 expression (Bravo-Egana et al., 2008b; Kredo-Russo et al., 2012; Landgraf et al., 2007; LaPierre et al., 2022; LaPierre & Stoffel, 2017). Out of these *Snca* - a gene encoding for a pre-synaptic scaffold protein and involved in many neurodegenerative diseases, was the most down-regulated miR-7 target gene after miR-7 overexpression regardless of Cdr1as expression. While not being statically significant in controls (**Figure 18b, left panel)**. Sustained miR-7 overexpression strongly down-regulated *Snca*, regardless of Cdr1as expression level (**Figure 18b, middle and right panel**), which we did not see for other miR-7 targets.

Strikingly, we observed that previously experimentally validated secretion-related miR-7 targets that function in pancreatic insulin secretion (Latreille et al., 2014) are exclusively and significantly down-regulated in Cdr1as-KO neurons after sustained miR-7 overexpression (**Figure 18b, right panel**). Among them we found: central regulator of vesicle fusion and SNARE activity (*Cplx1*), cytoskeleton remodeler (*Pfn2*) and enzyme responsible of regulation of dendritic growth and inhibitory synapses formation (*Zdhhc9*) (**Figure 18b, middle and right panel**). Together these observations suggest that the role of miR-7 as a regulator of secretion is conserved between secretory glands (i.e insulin secretion) and cortical neurons (glutamate secretion). The crucial difference is that the strength of miR-7 action in cortical neurons depends on Cdr1as levels.

Thus, we tried to connect these context-specific gene regulations to precise cellular pathways and decipher general mechanisms of action of Cdr1as and miR-7 co-regulation. We performed gene ontology (GO) enrichment analysis with all differentially expressed genes on our transcriptomic data. We used cellular compartments, molecular functions and biological processes terms and identified statistically significant enriched or depleted GO terms in each of the 4 conditions tested (WT, Cdr1as-KO, WT + miR-7 oex and Cdr1as-KO + miR-7 oex; **Figure 18a**).

Interestingly, when we looked at the enriched GO terms of the genes exclusively up- or down- regulated after miR-7 overexpression in Cdr1as-KO (**Figure 17b, left and right diagram, red bubble:** up-regulated= 44.4% and down-regulated= 35.2% of differentially expressed genes). We found that: (1) the largest and specific enriched GO terms are related to the regulation of neuronal action potentials and gene pathways of synaptic vesicle targeting to destination membranes. (2) The depleted terms include, regulation of excitatory post-synaptic potentials, regulation of plasticity, long-term potentiation (LTP), and with regulation of GABAergic transmission and glutamatergic receptors signaling pathways (**Figure 18a, (iii) BP and Figure 18c**).

Strikingly, all those GO terms enriched or depleted in WT neurons were, conversely depleted or enriched in Cdr1as-KO neurons with miR-7 overexpression. On the other hand, WT neurons with miR-7 overexpression and Cdr1as-KO control represent intermediates between these two scenarios (**Figure 18c**). Similar to what we observed for these same conditions on neuronal activity (**Figures 13 and 14**). These results suggest that the synaptic phenotypes we observed in Cdr1as-KO neurons after miR-7 sustained up-regulation, are, in part, explained by the interaction between miR-7 and Cdr1as. miR-7, buffered by Cdr1as, modulate functional cellular pathways reflected in global transcriptomic changes, and that this interaction is essential to trigger all adequate cellular pathways.

All together our data showed that miR-7 regulates a specific set of functional pathways related to synaptic signaling dynamics and synaptic plasticity in a Cdr1as-dependent manner. All those pathway regulations are reflected in excitatory neurotransmitter release, and local and network synaptic activity of the neurons. Furthermore, we could identify gene regulatory pathways connecting these ontology terms with our functional phenotypes.
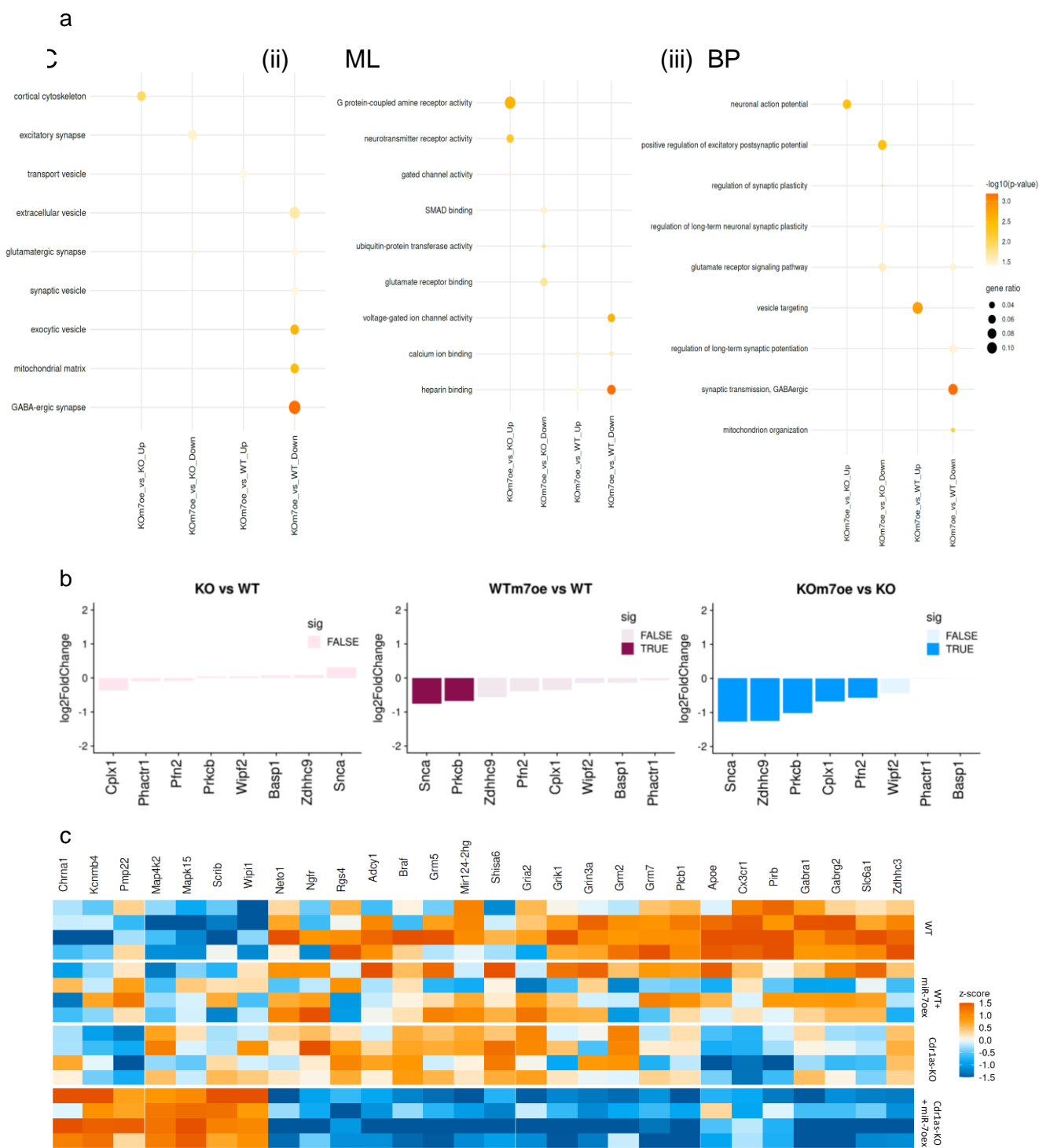
Figure 18. Sustained miR-7 overexpression (oex) are enhanced by the loss of Cdr1as and highlights miR-7 role controlled by their interaction.in exocytosis and secretion

(a) Enrichment profile from gene ontology (GO) analysis of (i) cellular compartments (CC), (ii) Molecular Functions (ML) and (iii) Biological Process (BP) Gene ontology enrichment analysis done using topGOtable function in the pcaExplorer (Marini et al., 2019, Methods). The dot size shows gene ratio and the color denotes the FDR-corrected p-value. Genes with average log2 fold change of 0.5 and adjusted p value <0.05 were considered significant and all expressed genes were used as background.

(b) miR-7 target genes involved in Insulin granules secretion, experimentally validated by Latreille et al., 2014 in pancreatic β-cells. Bar plots, the mean log2 fold change of 4 independent biological replicates per condition, for each comparison tested. Transparent bars, not significant changes (FDR > 0.05).

(c) Heatmap of statistically significant DE genes associated with GO terms significantly enriched specifically in Cdr1as-KO + miR-7 overexpression vs Cdr1as-KO comparison (specifically up- and down-regulated). Each row represents one independent biological replicate. Z-scores across samples were calculated based on normalized and batch-corrected expression values.

In summary, our data proposes a molecular model (**Figure 19**) for the mechanism by which Cdr1as and miR-7 exert their function. In resting neurons (**Figure 19a**) the removal of Cdr1as causes mild but significant reduction of mir-7 levels and minor effects on glutamate pre-synaptic release clearly reflected in neuronal network modulations. On the other hand, the low expression of miR-7 relative to the large amount of Cdr1as impede the continuous action of mir-7 on secretion targets. During strong sustained neuronal stimulation Cdr1as is transcriptionally up-regulated which prevents miR-7 degradation (**Figure 19b**). Therefore, rapidly post-transcriptionally stabilizes miR-7. Whereas long-lasting persistent increase of miR-7 expression will down-regulate Cdr1as from neurites, so that the buffer can self-regulate. Consequently, dynamically modulate glutamatergic transmission and neuronal network activity. We hypothesize that the post-transcriptional nature of this buffer system allows fast and local regulation of vesicle targeting in synapses and ultimately synaptic plasticity.
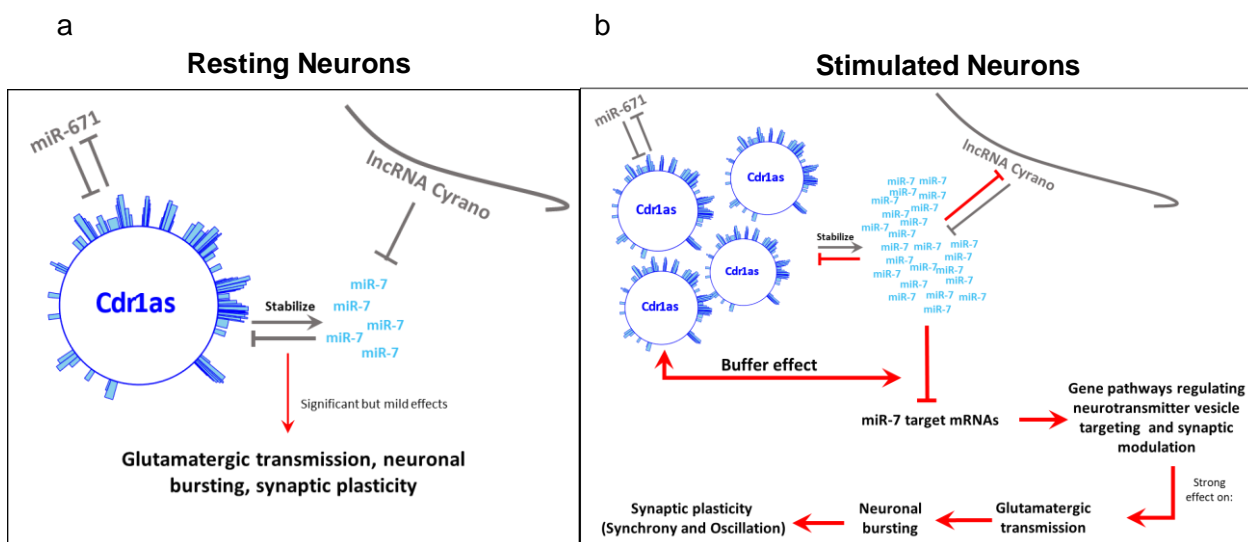
Figure 19. Proposed coordinated mechanism and function of Cdr1as and miR-7 in resting and stimulated neurons. Grey arrows: Published data (Hansen et al., 2011; Memczak et al., 2013; Hansen et al., 2013; Piwecka at al., 2017; Kleaveland et al., 2018). Red Arrows: New interactions propose in this study.

(a) Binding sites of miR-7 to Cdr1as (blue bars) are drawn following Piwecka et al. 2017. In resting neurons upon removal of Cdr1as, mir-7 levels are reduced and there are mild but significant effects on glutamate pre-synaptic release, which induce changes in synchrony and oscillation of the neuronal network. However, the low expression of miR-7 relative to the large amount of Cdr1as impede the continuous action of mir-7 on its targets.
(b) Strong sustained neuronal stimulation transcriptionally up-regulates Cdr1as which prevents miR-7 degradation and therefore rapidly post-transcriptionally stabilizes miR-7. This persistent increase in miR-7 will cause long-lasting down-regulation of Cdr1as from neurites, so that the buffer can self-regulate and therefore dynamically modulate glutamatergic transmission and neuronal network activity. We propose that the post-transcriptional nature of this buffer system allows fast and local regulation of vesicle targeting in synapses.

Discussion

Synaptic plasticity is an essential process for post-natal and adult brains, where sensory experiences will differentially wire the neuronal connections according to their external stimuli (Kandel, 2001). Understanding specific molecular mechanisms that shape synaptic plasticity in restricted neural networks and that are activated by diverse types of triggers are crucial to decipher brain connectivity. Therefore, we hypothesized that Cdr1as, one of the most highly expressed circular RNAs in the mammalian brain, might play a role during plasticity regulation. Interestingly, the miRNA miR-7, core Cdr1as interactor in mammalian brain (Hansen, Jensen, et al., 2013; Memczak et al., 2013; Piwecka et al., 2017), is deeply conserved among species and linked to ancestral proto neurosecretory organs identity. Thus, what is the function of this unusual and conserved interaction between two non-coding RNAs? And could this interaction impact on neuroplasticity?

1. **Are Cdr1as and miR-7 modulators of neuronal responses during neuronal stimulation?**

In this work we demonstrated how in murine cortical neurons Cdr1as:miR-7 network is involved in neuronal adaptation to strong stimulation (**Figure 6**), we hypothesized that the joint action of both molecules serves as a cellular surveillance system, where Cdr1as act as the coordinator that will constrain the direct action of miR-7 on its mRNA targets, and consequently modulate the neuronal response to strong depolarizations, which then would translate into long-term plasticity changes.

We observed that Cdr1as expression behaves as a IEG, strongly up-regulated by neuronal K$^+$ depolarization (**Figure 6b**), in magnitudes and time frames comparable with previously characterized IEGs. The strong stimulation of neurons will transcriptionally up-regulate Cdr1as (**Figure 7**). Consequently, Cdr1as would cause the post-transcriptional stabilization of mature miR-7 (**Figure 6c**). Nevertheless, the exact character of Cdr1as activity-dependent regulation, remains to be completely decipher, one possibility can be a direct transcription of Cdr1as in response to membrane depolarization or an indirect effect caused by the primary up-regulation of canonical IEGs encoding for transcription factors (Lanahan & Worley, 1998).

If we consider that Cdr1as expression doubles at one hour of stimulation, we could classified Cdr1as as a primary activity response gene, similar to *Fos* and *Jun,* which are genes mostly regulated by MAPK-ERK signaling pathway (Tyssowski et al., 2018). Hence, we hypothesize that this up-regulation can be a result of direct Cdr1as transcriptional activation.

It has been described that different patterns of neuronal stimulations induce different subsets of activity-dependent genes. Cdr1as increase would classified as a delayed primary respond gene, which are the RNAs induced only after sustained stimulation, that not require *de novo* translation for their induction (Dudek, 2008; Fowler et al., 2011; Tyssowski et al., 2018). Most common DNA promoter element respondent to neuronal activity is CREB (Herdegen & Leah, 1998), but so far no studies have connected Cdr1as transcription with any activity-dependent promoter element.

The stabilization of miR-7 by the pairing with Cdr1as involves loading of the miRNA in Ago2 silencing complex (Moore et al., 2015; Piwecka et al., 2017). Therefore, miR-7 post-transcriptional up-regulation caused by neuronal activity implicates that more miR-7 would be available for RNA-induced silencing. Then, could be miR-7 transported to precise sub-cellular locations, like synaptic buttons or peri-synaptic zones, where it would bind and silence target mRNAs present on site.

Another relevant aspect of Cdr1as:miR-7 coordinated role in neuronal activity is the cell-type specificity of Cdr1as expression. Even though miR-7, miR-671 and lncRNA Cyrano are highly expressed in non-neuronal tissues (Kim et al., 2016; Korać et al., 2021, p. 7; Landgraf et al., 2007; Ulitsky et al., 2011), Cdr1as remains consistently enriched throughout the mammalian brain, specifically in neurons (Piwecka et al., 2017; Wu et al., 2020).

Therefore, we strongly believe that Cdr1as could be a novel molecular regulatory player gained by mammalian brains to buffer the actions of miR-7 over the control of neuronal activity. Cdr1as would be the coordinator by post-transcriptionally stabilizing miR-7 in response to strong stimulations (**Figure 6**).

Previous studies have suggested that Cdr1as:miR-7 gene regulations might be related to specific neuronal functions. Kleaveland et al. (2018) discussed that the role of Cdr1as inhibiting neuronal activity might be partly attributed to the protection of miR-7 from degradation. Thereby, allowing increased repression of miR-7 targets. Nevertheless, the lack of significant effects on miR-7 target genes observed in resting neurons of Cdr1as-KO animals (**Figure 17**), raised a concern on the stabilization hypothesis. Here, we demonstrated that the previously proposed post-transcriptional stabilization of miR-7 by Cdr1as depends strongly in the sustained stimulations of the neurons. Therefore, we showed that Cdr1as:mR-7 axis is a robust system to control neuronal activity.

The low expression of miR-671 in murine cortical neurons does not allow us to draw any conclusions on its influence on the network regulation upon neuronal stimulation. On the other hand, we observed that lncRNA Cyrano follows a similar trend of up-regulation than Cdr1as only in the samples with the highest expression levels of both molecules. However, Cyrano does not respond to neuronal stimulation consistently. We hypothesize that the role of Cyrano on activity-dependent neuronal adaptation, might be important after miR-7 function on mRNA silencing is not longer needed. Cyrano might act as a late regulator that counteract the stabilization of miR-7. The exact involvement of miR-671 and Cyrano, remain to be uncovered. Further timepoints of analysis and a broader range of Cdr1as and Cyrano expression levels are essential to draw precise conclusions.

To decipher the specific molecular mechanism controlling Cdr1as:miR-7 activity-dependent up-regulation, it would be necessary to check: (1) Which other type of neuronal stimulation produce Cdr1as up-regulation. (2) Which intracellular signaling pathways are activated downstream the activation. (3) How Cdr1as expression and subcellular localization precisely vary over time.

2. <u>Is miR-7 controlling secretion in cortical neurons?</u>

miR-7 is particularly highly abundant in secretory glands and neurosecretory brain regions, where it has been shown to negatively regulate secretion (Ahmed et al., 2017; LaPierre et al., 2022; Latreille et al., 2014).

This means that the ancient brain already comprised miR-7 positive neurosecretory parts (Christodoulou et al., 2010). Other studies have demonstrated that pancreatic cells can dedifferentiate into neuronal precursors and recapitulate embryonic development. However, the neuronal differentiation of pancreatic cells occurs prior to endocrine differentiation and gradually becomes dominant, implying a default neuronal lineage specification (W. Zhao et al., 2007). It is intriguing to consider that a conserved mechanism of miR-7-regulated secretion exists in both cortical neurons and pancreatic tissues, which gives rise to an interesting hypothesis.

However, neurons differ from pancreatic cells in many regards, including their structure, complex intracellular functions, capacity of intercellular signal modulations and importantly for our research, in the expression proportion between Cdr1as and miR-7. In primary cortical neurons, we observed that miR-7 is expressed at very low levels (~40-60 miR-7 molecules per neuron in resting state; **Figure 11a-b**). Meanwhile, Cdr1as is very highly expressed (~250 molecules/neuron, **Figure 9d**). On the other hand, Cdr1as is extremely lowly expressed in pancreatic cells while miR-7 is the topmost highly abundant miRNA (Xu et al., 2015). How can one explain these expression patterns?

One explanation could be that in neurons released of synaptic vesicles must be extremely fast (milliseconds) and adaptive to stimuli (neuroplasticity). Therefore, the availability of miR-7 must be tightly regulated. Our data shows that pre-synaptic terminals of Cdr1as-KO cortical neurons have modestly increased release of glutamate during neuronal resting conditions (**Figure 10f**). Nonetheless, we observed strong increase of glutamate release after strong electrical stimulation trains (**Figure 10g**). This enlarged released of excitatory neurotransmitter is completely reverted by sustained miR-7 up-regulation (**Figure 12c**). Suggesting that Cdr1as:miR-7 network is directly involved in the modulation of glutamate release form electrically-stimulated cortical neurons.

The overexpression of miR-7 in Cdr1as-KO cortical neurons indicated that the role of this miRNA as negative regulator of granule secretion (Ahmed et al., 2017; LaPierre et al., 2022; Latreille et al., 2014; H. Xu et al., 2015).

Might be as well conserved in cortical neurons (**Figure 18**), but with the addition of an extra layer of modulation: Cdr1as.

3. How miR-7 affects synaptic connectivity?

We showed that the changes in glutamate release have functional consequences on real-time synaptic activity properties, both at local and at network levels (**Figures 13 and 14**).

Cortical neurons with a constitutive loss of the Cdr1as locus, and a mild, but statistically significant, down-regulation of miR-7, showed up-regulated action potential frequencies (**Figure 13b**). The augmented AP activity allows longer and more frequent neuronal bursting, increasing over time of maturation (**Figures 13c and d**). The changes in local bursts are consequently translated into globally uncoordinated network connectivity and potentially altered long-term plasticity responses (**Figure 14**). These phenotypes could be directly caused by the increased release of glutamate observed in the pre-synaptic terminals of the same Cdr1as-KO neurons (**Figure 12**). All the observed local and network phenotypes of Cdr1as-KO neurons are reverted by the sustained overexpression of miR-7, comparable to what we observed for glutamate release.

According to the description done by Rybak-Wolf et al. (2015), in primary neurons Cdr1as expression increases dramatically on DIV14 (120 FC). This suggests that the role of Cdr1as in cortical cells is relevant for neuronal functions in more mature states of synaptic connections. Moreover, our observation of increasing neuronal activity over time in Cdr1as-KO neurons, could indicate that miR-7 activity must be strongly buffered at when more intricated synaptic connections are present in the network (**Figures 13 and 14**).

Sustained miR-7 overexpression up-regulated equally (±10 folds) the number of miR-7 molecules in WT and Cdr1-KO neurons (**Figure 11d**). This is sufficient to recover the glutamate release and local AP/burst frequencies disrupted in Cdr1as-KO neurons (**Figure 12 and 13**). Meanwhile, neither of these parameters was affected in WT neurons (**Figures 12 and 13**). Furthermore, we observed that this is also true for miR-7-dependent target gene modulations (**Figure 16b**) and global transcriptomic changes

(**Figures 17a and b**). Altogether, these observations proved that miR-7 activity in cortical neurons heavily depend on the expression levels of Cdr1as.

Therefore, suggesting that a high expression of Cdr1as is critical to control miR-7-dependent effects on bursting regularity and overall the balance of excitatory and inhibitory signals (**Figure 14**). We propose that one of the potential cellular mechanisms through which miR-7, coordinated by Cdr1as, directly regulates long-term changes in neuronal connectivity can be observed in our measurements of network oscillation (**Figure 14b**).

In general, oscillation differences would account for alternating periods of high and low activity of neuronal communication and changes in network periodicity. Oscillation is a hallmark of functional neuronal networks with mixed cell populations of excitatory and inhibitory neurons, such as in cortex, composed of glutamatergic and GABAergic cells (Gonzalez et al., 2014; Onitsuka et al., 2013; Zeldenrust et al., 2018). Then, network oscillation augmentation in Cdr1as-KO, is an indication of imbalance between glutamatergic and GABAergic signaling affecting Cdr1as-KO cortical activity. We corroborated this hypothesis with the glutamate secretion assay, where we observed an increase excitatory neurosecretion in Cdr1as-KO. Interestingly, this imbalanced transmission is rescued by the sustained increase of miR-7 expression (**Figure 12c**), suggesting that miR-7 availability plays an important role to maintain proper cortical network wiring.

Some network activities tested here (oscillation and network bursting) seem equally affected by miR-7 sustained overexpression in most timepoints and for both genotypes. Nevertheless, network synchrony is the exception. Cdr1as-KO neurons appears to be extremely sensitive to miR-7 up-regulation (**Figures 14a and b**). This suggests that, even though, miR-7 has a great influence in neural network activity regulation, the extent of its influence is modulated by the expression levels of the Cdr1as. Therefore, the constitutive absence of Cdr1as sensitize this miR-7 modulating effects.

We could also infer that the signaling pathways and molecular interactors behind the control of synchrony and oscillation are the most sensitive to Cdr1as presence.

This is especially noticeable in very late time point of synaptic maturation, where activation of synapses required a tight control in order to achieve long-term synaptic changes. Therefore, the activity of miR-7 must be strongly buffered by Cdr1as.

4. Transport Hypothesis

In neuronal cortical primary cultures Cdr1as is well expressed in all neurites and detected far away from somatic compartments (**Figure 9c**). This is a special feature for a long non-coding RNA, which are mainly expressed in nucleus. Cdr1as shows also a unique expression pattern compared to other circRNAs, which are very lowly expressed compared to their linear counterpart (Rybak-Wolf et al., 2015). For the first time we showed that Cdr1as is co-expressed in the same neurons and in the same subcellular locations as lncRNA Cyrano (somas and neurites). The functional interaction of these two RNAs is clearly linked by miR-7 and probably depends heavily on the stimulated state of neurons. Nevertheless, the direct physical interaction between them needs to be more deeply investigated.

According to our analyses there is not a statistically significant co-localization between Cdr1as and Cyrano molecules to conclude that they are interacting in space, neither in somas or in neurites. However, widefield microscopy would not allow us to completely discard an interaction between these molecules. One possibility is that interaction of these two RNAs is indirect and mediated by other RNA or RNA-binding proteins, that could act as scaffold between both ncRNAs. This will ensure that both, the stabilizer and the repressor of miR-7, are present in close proximity controlling dynamic regulation of the miRNA.

We call this proposal, the transport hypothesis. For example, upon strong stimulation of neurons miR-7 is post-transcriptionally stabilized (**Figure 6**), then Cdr1as potentially could transport miR-7 to synaptic or peri-synaptic locations, where it is delivered to locally expressed miR-7 targets. Afterwards the action of miR-7 would need to be repressed by Cyrano, which has been recruited to same subcellular locations together with the circRNA-miRNA complex.

However, in resting neuronal state almost half of Cdr1as molecules are present in a cellular location far from the cell body.

Therefore, it will be crucial to evaluate if this distribution or expression levels are maintained over specific functional perturbations of the neurons.

The understanding of the subcellular localization of miR-7 and miR-671 is also critical to corroborate our transport hypothesis, nevertheless, is a much more difficult task. Imaging of molecules with very short sequence and very low expression levels in cortical neurons (**Figure 11a**; miR-7a ±66.67; miR-7b ±15.21; miR-671 ±2.75 read counts per mature miRNA normalized by depth).

It has been shown that, in HEK293 cells, mR-671 is the main facilitator of the endonucleolytical Ago2-dependent cleavage of Cdr1as (Hansen et al., 2011). miR-671 predominantly localized to the nucleus, suggesting that the directed down-regulation of Cdr1as was likely to be mediated by a nuclear mechanism (Hansen et al., 2011). Later, a mouse model with disrupted site for miR-671 in Cdr1as sequence showed 4-fold increase of Cd1as expression in cortex and hippocampus. This indicated that miR-671-dependet regulation is sufficient to alter Cdr1as levels (Kleaveland et al., 2018). Thus, we performed subcellular fractionation of nucleus versus cytoplasm, to get some more insights into the localization patterns of primary and mature transcripts of miR-671.

Our results of subcellular fractionations showed that the primary transcript of miR-671 is enriched in the nuclear compartment (**Figure 9a**). While the mature miR-671 localized equally in nuclear and cytoplasmic extracts of cortical neurons (**Figure 9b)**. This suggested that miR-671-dependent Cdr1as turnover, can as well occur in somas and neuronal projections. We hypothesize that miR-671 is potentially functioning as a local indirect regulator of miR-7 activity by reducing Cdr1as levels at specific dendritic/axonic locations. This supports the transport hypothesis.

Additionally, using smRNA FISH, we observed that Cdr1as is heavily depleted in WT neurites after miR-7 overexpression (**Figure 15a**). This might suggest that the coordinator role of Cdr1as is relevant in neuronal projections. Specifically, in neurites Cdr1as could act as a stabilizer and subsequent transporter of miR-7 to specific subcellular locations. The neurite-specific Cdr1as downregulation could also explain the differences in size-effect of glutamate release and burst frequencies between

Cdr1as-KO and WT neurons after sustained miR-7 (**Figures 12, 13 and 14**). Then, we postulate that neurons could have evolved Cdr1as:miR-7 interaction as a molecular mechanism of surveillance that can rapidly up- or down-regulate mRNAs locally in synaptic vicinities. This mechanism would shape the modulation of the corresponding synaptic terminals.

Good evidence to support this hypothesis has been presented in a very recent pre-print (Zajaczkowski et al., 2022). In this study, RNA-sequencing data of circRNAs present in synaptosomes of mouse medial prefrontal cortex, after fear extinction trainining, highlighted the presence of Cdr1as in these synaptic locations. Subsequently, local targeted knockdown of Cdr1as in neural processes, induced an *in vivo* up-regulation of miR-7 and an impaired fear extinction memory (Zajaczkowski et al., 2022). Moreover, it has been also previously demonstrated *in vitro* that some circRNAs respond to homeostatic plasticity modulations. For example, circHomer1 after bicuculine treatment (You et al., 2015).

Our observations also exposed the importance of profiling cirRNAs in brain before and after specific neuroplasticity challenges. We have shown here that Cdr1as (**Figure 6**) changed expression levels after strong depolarization and that it can be depleted from specific subcellular locations when miR-7 is overexpressed consistently over time. Therefore, is intriguing to discover which will be the molecular involvement of Cdr1as:miR-7, in specific behaviors, restricted to different brain regions or neuronal populations. The advantage of circRNA driven transport mechanism is that their stability and specific expression could lead the steadiness of cellular and subcellular neuronal activities which could enable the permanence of stable neuronal connections through space and time.

5. Cdr1as absence sensitized neurons to miR-7 activity

When we analysed whole transcriptome changes in Cdr1as-KO cortical neurons, we observed very few mRNA changes compared to WT (**Figure 17a (i)**). We attributed this to KO of Cdr1as, which generates only a mild depletion of a homeostatically lowly expressed miRNA. It is unlikely to find a global perturbation in miRNA targets upon the loss of a single competing interaction miRNA partner (Jens & Rajewsky, 2015). Especially considering that miRNA-driven regulation mostly occurs under time- and

stimulus-specific circumstances (Bushati & Cohen, 2007; Miska et al., 2007) and that miR-7 is very lowly abundant in resting cortical neurons (**Figure 11b**). Moreover, the constitutive KO of genes can produce compensatory adaptations, generating a striking difference in gene expression and phenotypes when comparing to knock downs (El-Brolosy & Stainier, 2017).

Hence, only the long-term increase of miR-7 expression allowed us to observe the activity of miR-7 on its targets and global transcriptomic changes in constitutive Cdr1as-KO neurons. It showed that the constitutive loss of Cdr1as sensitizes the neurons to the action of miR-7 on target and non-targets mRNAs (**Figures 16b and 17a**).

Then, considering the enhanced pre-synaptic glutamate release observed in Cdr1as-KO after stimulation and the reserved effect after miR-7 overexpression (**Figure 10g**). We expected that, at mRNA level, miR-7 overexpression on Cdr1as-KO neurons had opposite effects on genes related to neurotransmitter release. This is the case for *Snca* mRNA, which is the strongest regulated miR-7 target gene observed, regardless of the genotype where miR-7 was overexpressed (**Figure 18b**). *Snca* encodes for α-Synuclein protein, that functions as chaperone for SNARE function in pre-synaptic terminals, directly interacting with VAMP2 (Burré et al., 2010).

It has been described that in cortical neurons exists a positive concentration dependency between α-Synuclein expression and activity-dependent pre-synaptic glutamate release terminals (Sarafian et al., 2017). This effect depends on the level of α-synuclein expression. The possible mechanisms consider the inhibition of glutamate re-uptake by transporters localized on pre-, post-synaptic, and astrocytic endings. Alternatively, a physical disruption of synaptic vesicles on the pre-synaptic membrane (Sarafian et al., 2017). Both of these proposed mechanisms, might also explain our observations of down-regulation of *Snca* (**Figure 18b**), together with the detected enhanced glutamate release. Both of them compensated by miR-7 expression in exclusively Cdr1as-KO neurons (**Figure 12c**).

Moreover, we identified other genes that might be interesting to investigate. For example, miR-7 target *Cplx*, which encodes for a central regulator of vesicle fusion and

SNARE activity. It has been reported that the generation of a brain-specific conditional Cplx-KO mouse (López-Murcia et al., 2019) results in attenuation of spontaneous synchronous synaptic function, without affecting vesicle priming. This demonstrated that Cplx proteins are facilitators of synaptic vesicle fusion (López-Murcia et al., 2019). Our data showed similar synchronicity phenotypes in Cdr1as-KO neurons when miR-7 is up-regulated (**Figures 13 and 14**). Furthermore, we observed a significant down-regulation of *Cplx* exclusively in Cdr1as-KO neurons (**Figure 18b).**

Another interesting miR-7 target down-regulation, occurring solely in Cdr1as-KO neurons, is *Zdhhc9*. This protein specifically mediates palmitoylation of cell signaling proteins in neurons. It has been reported that Zdhhc9-KO mice exhibit increased seizure activity and network excitability, due to impaired excitatory/inhibitory synapse balance (Shimell et al., 2019). Taking into consideration our observations of impaired oscillatory frequencies in Cdr1as-KO neuronal networks (**Figure 14b**). The imbalanced synaptic output showed in *Zdhhc9*-deficient animals would explain the synaptic responses observed in Cdr1as-KO neurons.

6. Cellular pathways controlled by miR-7 and Cdr1as

In pancreatic β-cells miR-7 is a negative regulator of insulin secretion. Its removal enhances insulin secretion and improves glucose tolerance (Latreille et al., 2014). Our observations of glutamate release from cortical pre-synaptic terminals suggested a similar role for the miR-7 in cortical neurons (**Figure 12c**). The difference is that in neurons the scale of glutamate release depends on Cdr1as expression and neuronal stimulation (**Figure 10f-g**). This is the description of a brand-new function for miR-7 in cortical neurons, where the expression of Cdr1as is predominant compared to miR-7.

The capability of Cdr1as:miR-7 of regulating glutamate secretion is particularly relevant if we look at cellular pathways modulated exclusively in Cdr1as-KO after sustained miR-7 overexpression (**Figure 18**). We observed up-regulation of gene sets involved in directing newly formed vesicles to specific destination membranes and membrane receptors sensible to depolarization stimuli (**Figure 18a**). Complementary, we found strong down-regulation in genes related to glutamate singling, long term potentiation and GABAergic transmission (**Figure 18c**).

These Cdr1as-KO transcriptional regulations positively correlate with the functional phenotypes observed: (1) down-regulated glutamatergic transmission (**Figure 12c**). (2) Recovery of synchronicity observed after miR-7 overexpression (**Figure 14a**).

Nevertheless, there is one missing connection between the functional phenotypes, the observed transcriptional changes and our transport hypothesis. We lack of information about the intracellular localization of the mRNAs affected by miR-7 regulation in absence of Cdr1as. mRNA localization is very common in highly polarized cells, as neurons, and determines the function and regulation of many protein coding genes (Martin & Ephrussi, 2009). Especially, in neurons protein synthesis machinery is subcellularly localized and these translated mRNAs participate in a restricted number synaptic functions (Glock et al., 2021; Hafner et al., 2019; Sambandan et al., 2017). Most recently has been shown that also miRNAs can affect target mRNA localization (Mendonsa et al., 2023). Altogether, these precedents suggest that we should determine whether the genes groups regulated after miR-7 modulation, are differentially localized to neurites. Particularly interesting is to understand the localization of these gene sets after strong depolarization stimuli. We could be observing a molecular mechanism of neurite translation regulation, gained by mammalian cortical neurons, that could consolidate or stabilize permanentt plasticity changes.

7. <u>Potential pathological consequences of Cdr1as:miR-7 glutamatergic regulations</u>

The importance of an activity-regulated gene transcription program is heavily dependent on stimulus, cell-types and developmental stages of the brain (Lyons & West, 2011). Therefore, this newly characterized non-coding RNA regulatory network, of Cdr1as and miR-7 in an *in vivo* biological context remains to be tested.

Most of the observed changes in neuronal connectivity (**Figure 14**) are probably due to the strong alteration in glutamate release (**Figure 10f and g**). Alterations in the release of glutamate have been linked principally with alterations in long term potentiation mechanisms.

Consequently, direct associated with diminishing cognition, learning and mood disorders, all areas in which neuroplasticity is essential to adapting to environmental stressors (Reznikov et al., 2009). For example, it has been described that glutamatergic transmission plays a central role in psychiatric diseases such as major depressive disorder. In our system, miR-7 reversed the altered cortical glutamatergic transmission of Cdr1as-KO neurons (**Figure 12c**). Drugs that normalized glutamatergic neurotransmission, disrupted in patients with major depression, has been prove to reverse stress-associated structural and cellular changes in the brain (Kasper & McEwen, 2008).

Another potential consequence of the miR-7-driven phenotypes could be the reversion of the altered synchrony observed in Cdr1as-KO (**Figure 14a**). Similar alterations in cortical networks has been observed in autism spectrum disorder. It has been shown that autism-associated mutations altered network architecture and synchrony (Gutierrez et al., 2009). Moreover, synchrony of cortical waves is reduced in brain regions related with social, emotional and communication dysfunction of autistic brains (Jia et al., 2021).

Thus, an interesting endogenous scenario to test the importance of Cdr1as:miR-7 function in the brain would be: (1) Animal models trained on different learning tasks or memory challenges, where neuroplasticity can be evaluated *in vivo.* (2) Brain samples of patients with complex cortical-related disorders, such as the mentioned above, where there has been a long-term alteration of glutamatergic transmission. (3) In a dynamic cellular model where both Cdr1as and miR-7 can by acutely perturbed. And where these perturbations could be combined with neuronal challenges or stressors that will molecularly recapitulate neuropsychiatric disorders.

However, all of these described psychiatric phenotypes/diseases implicate a recruitment of several brain regions (i.e. cortex, hippocampus, amygdala). Further more, neuroplasticity alterations are related to joint changes in neurotransmitters, hormones and growth factors (Gansel, 2022). Hence, it is necessary to study the observed miR-7-driven glutamate and neuronal wiring phenotypes, not only in isolated cell-types, but in the brain as a whole. Especially, taking into consideration the brain capacity of self reorganization and dynamic multi neuronal activity.

Conclusions

In this research work, I have presented the following evidence, regarding the impact of Cdr1as and miR-7 network in synaptic transmission in mouse cortical neurons:

1.   circRNA Cdr1as, the main known regulator of miR-7 and a member of activity-dependent genes specifically modulated in neurons in response to sustained depolarization.

2.   Transcriptional up-regulation of Cdr1as after sustained neuronal depolarization leads to a post-transcriptional stabilization of miR-7.

3.   When Cdr1as locus is lost, pre-synaptic neuronal terminals exhibit increased glutamate release in spontaneous and stimulated conditions.

4.   miR-7 overexpression is sufficient to rescue glutamate secretion in Cdr1as-KO mature neurons to WT levels.

5.   Recording of spontaneous neuronal activity revealed that miR-7 modulation is sufficient to rescue spiking and bursting impairments observed in neurons with deletion of Cdr1as locus. The strength and time extent of miR-7 effects depends on the presence of the Cdr1as.

6.   The loss of Cdr1as locus directly affects the network coordination of cortical neurons, specifically changing spike frequency and burst length, that result in asynchronous and high oscillatory neuronal network.

7.   The restoration of bursting activity and network communication seen in Cdr1as-KO neurons after miR-7 expression is mediated by a modulation in excitatory neurotransmitter secretion.

8.   The effects of high concentrations of miR-7 in WT neurons showed dissimilar physiological outcomes compared to Cdr1as-KO neurons, which appear to be sensitized to the outcomes of miR-7 expression.

9.   miR-7 overexpression down-regulates Cdr1as and Cyrano restricting its spatial distribution.

10.   Transcriptomic changes caused by miR-7 overexpression are enhanced by the loss of Cdr1as. miR-7 overexpression up-regulates a set of genes enriched in neurotransmitter transduction, vesicle release, action potential modulation and synaptic plasticity pathways, only in Cdr1as-KO neurons.

References

Abraham, W. C., & Bear, M. F. (1996). Metaplasticity: The plasticity of synaptic plasticity. *Trends in Neurosciences*, *19*(4), 126–130. https://doi.org/10.1016/S0166-2236(96)80018-X

Agarwal, V., Bell, G. W., Nam, J.-W., & Bartel, D. P. (2015). Predicting effective microRNA target sites in mammalian mRNAs. *ELife*, *4*, e05005. https://doi.org/10.7554/eLife.05005

Agbu, P., Cassidy, J. J., Braverman, J., Jacobson, A., & Carthew, R. W. (2019). MicroRNA miR-7 Regulates Secretion of Insulin-Like Peptides. *Endocrinology*, *161*(2), bqz040. https://doi.org/10.1210/endocr/bqz040

Ahmed, K., LaPierre, M. P., Gasser, E., Denzler, R., Yang, Y., Rülicke, T., Kero, J., Latreille, M., & Stoffel, M. (2017). Loss of microRNA-7a2 induces hypogonadotropic hypogonadism and infertility. *The Journal of Clinical Investigation*, *127*(3), 1061–1074. https://doi.org/10.1172/JCI90031

Ambros, V. (2004). The functions of animal microRNAs. *Nature*, *431*(7006), Article 7006. https://doi.org/10.1038/nature02871

Anderson, P., & Kedersha, N. (2006). RNA granules. *The Journal of Cell Biology*, *172*(6), 803–808. https://doi.org/10.1083/jcb.200512082

Araque, A., & Navarrete, M. (2010). Glial cells in neuronal network function. *Philosophical Transactions of the Royal Society B: Biological Sciences*, *365*(1551), 2375–2381. https://doi.org/10.1098/rstb.2009.0313

Arendt, D., Denes, A. S., Jékely, G., & Tessmar-Raible, K. (2008). The evolution of nervous system centralization. *Philosophical Transactions of the Royal Society B: Biological Sciences*, *363*(1496), 1523–1528. https://doi.org/10.1098/rstb.2007.2242

Ashraf, S. I., McLoon, A. L., Sclarsic, S. M., & Kunes, S. (2006). Synaptic protein synthesis associated with memory is regulated by the RISC pathway in Drosophila. *Cell*, *124*(1), 191–205. https://doi.org/10.1016/j.cell.2005.12.017

Ashwal-Fluss, R., Meyer, M., Pamudurti, N. R., Ivanov, A., Bartok, O., Hanan, M., Evantal, N., Memczak, S., Rajewsky, N., & Kadener, S. (2014). CircRNA Biogenesis Competes with Pre-mRNA Splicing. *Molecular Cell*, *56*(1), 55–66. https://doi.org/10.1016/j.molcel.2014.08.019

Bae, B., & Miura, P. (2020). Emerging Roles for 3' UTRs in Neurons. *International Journal of Molecular Sciences*, *21*(10), 3413. https://doi.org/10.3390/ijms21103413

Bak, M., Silahtaroglu, A., Møller, M., Christensen, M., Rath, M. F., Skryabin, B., Tommerup, N., & Kauppinen, S. (2008). MicroRNA expression in the adult mouse central nervous system. *RNA*, *14*(3), 432–444. https://doi.org/10.1261/rna.783108

Barash, Y., Calarco, J. A., Gao, W., Pan, Q., Wang, X., Shai, O., Blencowe, B. J., & Frey, B. J. (2010). Deciphering the splicing code. *Nature*, *465*(7294), 53–59. https://doi.org/10.1038/nature09000

Barbagallo, D., Condorelli, A., Ragusa, M., Salito, L., Sammito, M., Banelli, B., Caltabiano, R., Barbagallo, G., Zappalà, A., Battaglia, R., Cirnigliaro, M., Lanzafame, S., Vasquez, E., Parenti, R., Cicirata, F., Di Pietro, C., Romani, M., & Purrello, M. (2015). Dysregulated miR-671-5p / CDR1-AS / CDR1 / VSNL1 axis is involved in glioblastoma multiforme. *Oncotarget*, *7*(4), 4746–4759. https://doi.org/10.18632/oncotarget.6621

Barbee, S. A., Estes, P. S., Cziko, A.-M., Hillebrand, J., Luedeman, R. A., Coller, J. M., Johnson, N., Howlett, I. C., Geng, C., Ueda, R., Brand, A. H., Newbury, S. F., Wilhelm, J. E., Levine, R. B., Nakamura, A., Parker, R., & Ramaswami, M. (2006). Staufen- and FMRP-containing neuronal RNPs are structurally and functionally related to somatic P bodies. *Neuron*, *52*(6), 997–1009. https://doi.org/10.1016/j.neuron.2006.10.028

Barbosa-Morais, N. L., Irimia, M., Pan, Q., Xiong, H. Y., Gueroussov, S., Lee, L. J., Slobodeniuc, V., Kutter, C., Watt, S., Colak, R., Kim, T., Misquitta-Ali, C. M., Wilson, M. D., Kim, P. M., Odom, D. T., Frey, B. J., & Blencowe, B. J. (2012). The evolutionary landscape of alternative splicing in vertebrate species. *Science (New York, N.Y.)*, *338*(6114), 1587–1593. https://doi.org/10.1126/science.1230612

Barrett, S. P., Parker, K. R., Horn, C., Mata, M., & Salzman, J. (2017). CiRS-7 exonic sequence is embedded in a long non-coding RNA locus. *PLoS Genetics*, *13*(12), e1007114. https://doi.org/10.1371/journal.pgen.1007114

Barrett, S. P., & Salzman, J. (2016). Circular RNAs: Analysis, expression and potential functions. *Development (Cambridge, England)*, *143*(11), 1838–1847. https://doi.org/10.1242/dev.128074

Bartel, D. P. (2004). MicroRNAs: Genomics, Biogenesis, Mechanism, and Function. *Cell*, *116*(2), 281–297. https://doi.org/10.1016/S0092-8674(04)00045-5

Bartel, D. P. (2018). Metazoan MicroRNAs. *Cell*, *173*(1), 20–51. https://doi.org/10.1016/j.cell.2018.03.006

Bartel, D. P., Sheng, M., Lau, L. F., & Greenberg, M. E. (1989). Growth factors and membrane depolarization activate distinct programs of early response gene expression: Dissociation of fos and jun induction. *Genes & Development*, *3*(3), 304–313. https://doi.org/10.1101/gad.3.3.304

Barth, A. L., Gerkin, R. C., & Dean, K. L. (2004). Alteration of Neuronal Firing Properties after In Vivo Experience in a FosGFP Transgenic Mouse. *The Journal of Neuroscience*, *24*(29), 6466–6475. https://doi.org/10.1523/JNEUROSCI.4737-03.2004

Barth, A. L., & Yassin, L. (2008). Activity-dependent Gene Transcription in Neurons: Defining the Plasticity Transcriptome. In S. M. Dudek (Ed.), *Transcriptional Regulation by Neuronal Activity: To the Nucleus and Back* (pp. 295–312). Springer US. https://doi.org/10.1007/978-0-387-73609-9_15

Batish, M., van den Bogaard, P., Kramer, F. R., & Tyagi, S. (2012). Neuronal mRNAs travel singly into dendrites. *Proceedings of the National Academy of Sciences*, *109*(12), 4645–4650. https://doi.org/10.1073/pnas.1111226109

Berg, M. G., Singh, L. N., Younis, I., Liu, Q., Pinto, A. M., Kaida, D., Zhang, Z., Cho, S., Sherrill-Mix, S., Wan, L., & Dreyfuss, G. (2012). U1 snRNP Determines mRNA Length and Regulates Isoform Expression. *Cell*, *150*(1), 53–64. https://doi.org/10.1016/j.cell.2012.05.029

Bhattacharyya, S. N., Habermacher, R., Martine, U., Closs, E. I., & Filipowicz, W. (2006). Relief of

microRNA-Mediated Translational Repression in Human Cells Subjected to Stress. *Cell*,

125(6), 1111–1124. https://doi.org/10.1016/j.cell.2006.04.031

Borghuis, B. G., Marvin, J. S., Looger, L. L., & Demb, J. B. (2013). Two-Photon Imaging of Nonlinear

Glutamate Release Dynamics at Bipolar Cell Synapses in the Mouse Retina. *The Journal of*

Neuroscience, *33*(27), 10972–10985. https://doi.org/10.1523/JNEUROSCI.1241-13.2013

Bravo-Egana, V., Rosero, S., Molano, R. D., Pileggi, A., Ricordi, C., Domínguez-Bendala, J., & Pastori, R.

L. (2008a). Quantitative differential expression analysis reveals miR-7 as major islet

microRNA. *Biochemical and Biophysical Research Communications*, *366*(4), 922–926.

https://doi.org/10.1016/j.bbrc.2007.12.052

Bravo-Egana, V., Rosero, S., Molano, R. D., Pileggi, A., Ricordi, C., Domínguez-Bendala, J., & Pastori, R.

L. (2008b). Quantitative differential expression analysis reveals miR-7 as major islet

microRNA. *Biochemical and Biophysical Research Communications*, *366*(4), 922–926.

https://doi.org/10.1016/j.bbrc.2007.12.052

Burns, M. E., & Augustine, G. J. (1995). Synaptic structure and function: Dynamic organization yields

architectural precision. *Cell*, *83*(2), 187–194. https://doi.org/10.1016/0092-8674(95)90160-4

Carson, J. H., Gao, Y., Tatavarty, V., Levin, M. K., Korza, G., Francone, V. P., Kosturko, L. D.,

Maggipinto, M. J., & Barbarese, E. (2008). Multiplexed RNA trafficking in oligodendrocytes

and neurons. *Biochimica Et Biophysica Acta*, *1779*(8), 453–458.

https://doi.org/10.1016/j.bbagrm.2008.04.002

Castellanos, F. X., Fine, E. J., Kaysen, D., Marsh, W. L., Rapoport, J. L., & Hallett, M. (1996).

Sensorimotor gating in boys with Tourette's syndrome and ADHD: Preliminary results.

Biological Psychiatry, *39*(1), 33–41. https://doi.org/10.1016/0006-3223(95)00101-8

Chen, B. J., Mills, J. D., Takenaka, K., Bliim, N., Halliday, G. M., & Janitz, M. (2016). Characterization of

circular RNAs landscape in multiple system atrophy brain. *Journal of Neurochemistry*, *139*(3),

485–496. https://doi.org/10.1111/jnc.13752

Chen, Y. T., Rettig, W. J., Yenamandra, A. K., Kozak, C. A., Chaganti, R. S., Posner, J. B., & Old, L. J.

(1990). Cerebellar degeneration-related antigen: A highly conserved neuroectodermal

marker mapped to chromosomes X in human and mouse. *Proceedings of the National

Academy of Sciences of the United States of America*, *87*(8), 3077–3081.

Chen, Y., & Wang, X. (2020). miRDB: An online database for prediction of functional microRNA

targets. *Nucleic Acids Research*, *48*(D1), D127–D131. https://doi.org/10.1093/nar/gkz757

Choudhury, N. R., de Lima Alves, F., de Andrés-Aguayo, L., Graf, T., Cáceres, J. F., Rappsilber, J., &

Michlewski, G. (2013). Tissue-specific control of brain-enriched miR-7 biogenesis. *Genes &

Development*, *27*(1), 24–38. https://doi.org/10.1101/gad.199190.112

Citri, A., & Malenka, R. C. (2008). Synaptic Plasticity: Multiple Forms, Functions, and Mechanisms.

Neuropsychopharmacology, *33*(1), Article 1. https://doi.org/10.1038/sj.npp.1301559

Cochran, B. H., Reffel, A. C., & Stiles, C. D. (1983). Molecular cloning of gene sequences regulated by

platelet-derived growth factor. *Cell*, *33*(3), 939–947. https://doi.org/10.1016/0092-

8674(83)90037-5

Cocquerelle, C., Daubersies, P., Majérus, M. A., Kerckaert, J. P., & Bailleul, B. (1992). Splicing with

inverted order of exons occurs proximal to large introns. *The EMBO Journal*, *11*(3), 1095–

1098.

Conn, S. J., Pillman, K. A., Toubia, J., Conn, V. M., Salmanidis, M., Phillips, C. A., Roslan, S., Schreiber,

A. W., Gregory, P. A., & Goodall, G. J. (2015). The RNA Binding Protein Quaking Regulates

Formation of circRNAs. *Cell*, *160*(6), 1125–1134. https://doi.org/10.1016/j.cell.2015.02.014

Correa-Medina, M., Bravo-Egana, V., Rosero, S., Ricordi, C., Edlund, H., Diez, J., & Pastori, R. L. (2009).

MicroRNA miR-7 is preferentially expressed in endocrine cells of the developing and adult

human pancreas. *Gene Expression Patterns: GEP*, *9*(4), 193–199.

https://doi.org/10.1016/j.gep.2008.12.003

Cortés-López, M., Gruner, M. R., Cooper, D. A., Gruner, H. N., Voda, A.-I., van der Linden, A. M., & Miura, P. (2018). Global accumulation of circRNAs during aging in Caenorhabditis elegans. *BMC Genomics*, *19*(1), 8. https://doi.org/10.1186/s12864-017-4386-y

Curran, T., & Morgan, J. I. (1987). Memories of fos. *BioEssays*, *7*(6), 255–258. https://doi.org/10.1002/bies.950070606

Darnell, R. B. (2010). RNA Regulation in Neurologic Disease and Cancer. *Cancer Research and Treatment*, *42*(3), 125–129. https://doi.org/10.4143/crt.2010.42.3.125

Deisseroth, K., Bito, H., & Tsien, R. W. (1996). Signaling from Synapse to Nucleus: Postsynaptic CREB Phosphorylation during Multiple Forms of Hippocampal Synaptic Plasticity. *Neuron*, *16*(1), 89–101. https://doi.org/10.1016/S0896-6273(00)80026-4

Dobin, A., Davis, C. A., Schlesinger, F., Drenkow, J., Zaleski, C., Jha, S., Batut, P., Chaisson, M., & Gingeras, T. R. (2013). STAR: Ultrafast universal RNA-seq aligner. *Bioinformatics (Oxford, England)*, *29*(1), 15–21. https://doi.org/10.1093/bioinformatics/bts635

Donato, A., Kagias, K., Zhang, Y., & Hilliard, M. A. (2019). Neuronal sub-compartmentalization: A strategy to optimize neuronal function. *Biological Reviews*, *94*(3), 1023–1037. https://doi.org/10.1111/brv.12487

Dudek, S. M. (Ed.). (2008). *Transcriptional Regulation by Neuronal Activity: To the Nucleus and Back*. Springer US. https://doi.org/10.1007/978-0-387-73609-9

Ebert, M. S., & Sharp, P. A. (2012). Roles for MicroRNAs in Conferring Robustness to Biological Processes. *Cell*, *149*(3), 515–524. https://doi.org/10.1016/j.cell.2012.04.005

El-Brolosy, M. A., & Stainier, D. Y. R. (2017). Genetic compensation: A phenomenon in search of mechanisms. *PLoS Genetics*, *13*(7), e1006780. https://doi.org/10.1371/journal.pgen.1006780

Eliscovich, C., Shenoy, S. M., & Singer, R. H. (2017). Imaging mRNA and protein interactions within neurons. *Proceedings of the National Academy of Sciences of the United States of America*, *114*(10), E1875–E1884. https://doi.org/10.1073/pnas.1621440114

Etherington, S. J., Atkinson, S. E., Stuart, G. J., & Williams, S. R. (2010). Synaptic Integration. In *ELS*. John Wiley & Sons, Ltd. https://doi.org/10.1002/9780470015902.a0000208.pub2

Farsi, Z., Walde, M., Klementowicz, A. E., Paraskevopoulou, F., & Woehler, A. (2021). Single synapse glutamate imaging reveals multiple levels of release mode regulation in mammalian synapses. *IScience*, *24*(1), 101909. https://doi.org/10.1016/j.isci.2020.101909

Fei, F., Rao, W., Zhang, L., Chen, B.-G., Li, J., Fei, Z., & Chen, Z. (2014). Downregulation of Homer1b/c improves neuronal survival after traumatic neuronal injury. *Neuroscience*, *267*, 187–194. https://doi.org/10.1016/j.neuroscience.2014.02.037

Fiore, R., Khudayberdiev, S., Christensen, M., Siegel, G., Flavell, S. W., Kim, T.-K., Greenberg, M. E., & Schratt, G. (2009). Mef2-mediated transcription of the miR379–410 cluster regulates activity-dependent dendritogenesis by fine-tuning Pumilio2 protein levels. *The EMBO Journal*, *28*(6), 697. https://doi.org/10.1038/emboj.2009.10

Flavell, S. W., & Greenberg, M. E. (2008). Signaling Mechanisms Linking Neuronal Activity to Gene Expression and Plasticity of the Nervous System. *Annual Review of Neuroscience*, *31*(1), 563–590. https://doi.org/10.1146/annurev.neuro.31.060407.125631

Flavell, S. W., Kim, T.-K., Gray, J. M., Harmin, D. A., Hemberg, M., Hong, E. J., Markenscoff-Papadimitriou, E., Bear, D. M., & Greenberg, M. E. (2008). Genome-wide analysis of MEF2 transcriptional program reveals synaptic target genes and neuronal activity-dependent polyadenylation site selection. *Neuron*, *60*(6), 1022–1038. https://doi.org/10.1016/j.neuron.2008.11.029

Fon, E. A., & Edwards, R. H. (2001). Molecular mechanisms of neurotransmitter release. *Muscle & Nerve*, *24*(5), 581–601. https://doi.org/10.1002/mus.1044

Fowler, T., Sen, R., & Roy, A. L. (2011). Regulation of Primary Response Genes. *Molecular Cell*, *44*(3), 348–360. https://doi.org/10.1016/j.molcel.2011.09.014

Gajda, E., Grzanka, M., Godlewska, M., & Gawel, D. (2021). The Role of miRNA-7 in the Biology of

Cancer and Modulation of Drug Resistance. *Pharmaceuticals*, *14*(2), 149.

https://doi.org/10.3390/ph14020149

Gallo, F. T., Katche, C., Morici, J. F., Medina, J. H., & Weisstaub, N. V. (2018). Immediate Early Genes,

Memory and Psychiatric Disorders: Focus on c-Fos, Egr1 and Arc. *Frontiers in Behavioral*

Neuroscience, *12*. https://www.frontiersin.org/articles/10.3389/fnbeh.2018.00079

Gansel, K. S. (2022). Neural synchrony in cortical networks: Mechanisms and implications for neural

information processing and coding. *Frontiers in Integrative Neuroscience*, *16*.

https://www.frontiersin.org/articles/10.3389/fnint.2022.900715

Glock, C., Biever, A., Tushev, G., Nassim-Assir, B., Kao, A., Bartnik, I., tom Dieck, S., & Schuman, E. M.

(2021). The translatome of neuronal cell bodies, dendrites, and axons. *Proceedings of the*

National Academy of Sciences, *118*(43), e2113929118.

https://doi.org/10.1073/pnas.2113929118

Gomes-Duarte, A., Venø, M. T., de Wit, M., Senthilkumar, K., Broekhoven, M. H., van den Herik, J.,

Heeres, F. R., van Rossum, D., Rybiczka-Tesulov, M., Legnini, I., van Rijen, P. C., van Eijsden,

P., Gosselaar, P. H., Rajewsky, N., Kjems, J., Vangoor, V. R., & Pasterkamp, R. J. (2022).

Expression of Circ_Satb1 Is Decreased in Mesial Temporal Lobe Epilepsy and Regulates

Dendritic Spine Morphology. *Frontiers in Molecular Neuroscience*, *15*.

https://www.frontiersin.org/articles/10.3389/fnmol.2022.832133

Gonzalez, O. J. A., Aerde, K. I. van, Mansvelder, H. D., Pelt, J. van, & Ooyen, A. van. (2014). Inter-

Network Interactions: Impact of Connections between Oscillatory Neuronal Networks on

Oscillation Frequency and Pattern. *PLOS ONE*, *9*(7), e100899.

https://doi.org/10.1371/journal.pone.0100899

Gruner, H., Cortés-López, M., Cooper, D. A., Bauer, M., & Miura, P. (2016). CircRNA accumulation in

the aging mouse brain. *Scientific Reports*, *6*(1), Article 1. https://doi.org/10.1038/srep38907

Guan, Z., Saraswati, S., Adolfsen, B., & Littleton, J. T. (2005). Genome-Wide Transcriptional Changes Associated with Enhanced Activity in the Drosophila Nervous System. *Neuron*, *48*(1), 91–107. https://doi.org/10.1016/j.neuron.2005.08.036

Gutierrez, R. C., Hung, J., Zhang, Y., Kertesz, A. C., Espina, F. J., & Colicos, M. A. (2009). Altered synchrony and connectivity in neuronal networks expressing an autism-related mutation of neuroligin 3. *Neuroscience*, *162*(1), 208–221. https://doi.org/10.1016/j.neuroscience.2009.04.062

Guzowski, J. F., Miyashita, T., Chawla, M. K., Sanderson, J., Maes, L. I., Houston, F. P., Lipa, P., McNaughton, B. L., Worley, P. F., & Barnes, C. A. (2006). Recent behavioral history modifies coupling between cell activity and Arc gene transcription in hippocampal CA1 neurons. *Proceedings of the National Academy of Sciences*, *103*(4), 1077–1082. https://doi.org/10.1073/pnas.0505519103

Hafner, A.-S., Donlin-Asp, P. G., Leitch, B., Herzog, E., & Schuman, E. M. (2019). Local protein synthesis is a ubiquitous feature of neuronal pre- and postsynaptic compartments. *Science*, *364*(6441), eaau3644. https://doi.org/10.1126/science.aau3644

Halliday, D. M., Rosenberg, J. R., Breeze, P., & Conway, B. A. (2006). Neural spike train synchronization indices: Definitions, interpretations,and applications. *IEEE Transactions on Biomedical Engineering*, *53*(6), 1056–1066. https://doi.org/10.1109/TBME.2006.873392

Hanan, M., Simchovitz, A., Yayon, N., Vaknine, S., Cohen-Fultheim, R., Karmon, M., Madrer, N., Rohrlich, T. M., Maman, M., Bennett, E. R., Greenberg, D. S., Meshorer, E., Levanon, E. Y., Soreq, H., & Kadener, S. (2020). A Parkinson's disease CircRNAs Resource reveals a link between circSLC8A1 and oxidative stress. *EMBO Molecular Medicine*, *12*(9), e11942. https://doi.org/10.15252/emmm.201911942

Hanniford, D., Ulloa-Morales, A., Karz, A., Berzoti-Coelho, M. G., Moubarak, R. S., Sánchez-Sendra, B., Kloetgen, A., Davalos, V., Imig, J., Wu, P., Vasudevaraja, V., Argibay, D., Lilja, K., Tabaglio, T., Monteagudo, C., Guccione, E., Tsirigos, A., Osman, I., Aifantis, I., & Hernando, E. (2020).

Epigenetic Silencing of CDR1as Drives IGF2BP3-Mediated Melanoma Invasion and Metastasis. *Cancer Cell*, *37*(1), 55-70.e15. https://doi.org/10.1016/j.ccell.2019.12.007

Hansen, T. B., Jensen, T. I., Clausen, B. H., Bramsen, J. B., Finsen, B., Damgaard, C. K., & Kjems, J. (2013). Natural RNA circles function as efficient microRNA sponges. *Nature*, *495*(7441), 384–388. https://doi.org/10.1038/nature11993

Hansen, T. B., Kjems, J., & Damgaard, C. K. (2013). Circular RNA and miR-7 in Cancer. *Cancer Research*, *73*(18), 5609–5612. https://doi.org/10.1158/0008-5472.CAN-13-1568

Hansen, T. B., Wiklund, E. D., Bramsen, J. B., Villadsen, S. B., Statham, A. L., Clark, S. J., & Kjems, J. (2011). miRNA-dependent gene silencing involving Ago2-mediated cleavage of a circular antisense RNA: MiRNA mediated cleavage of circular antisense RNA. *The EMBO Journal*, *30*(21), 4414–4422. https://doi.org/10.1038/emboj.2011.359

Henley, C. (2021). *Neurotransmitter Release*. https://openbooks.lib.msu.edu/neuroscience/chapter/neurotransmitter-release/

Herculano-Houzel, S. (2012). The remarkable, yet not extraordinary, human brain as a scaled-up primate brain and its associated cost. *Proceedings of the National Academy of Sciences*, *109*(supplement_1), 10661–10668. https://doi.org/10.1073/pnas.1201895109

Herdegen, T., & Leah, J. D. (1998). Inducible and constitutive transcription factors in the mammalian nervous system: Control of gene expression by Jun, Fos and Krox, and CREB/ATF proteins. *Brain Research Reviews*, *28*(3), 370–490. https://doi.org/10.1016/S0165-0173(98)00018-6

Herranz, H., & Cohen, S. M. (2010). MicroRNAs and gene regulatory networks: Managing the impact of noise in biological systems. *Genes & Development*, *24*(13), 1339–1344. https://doi.org/10.1101/gad.1937010

Hilgers, V., Perry, M. W., Hendrix, D., Stark, A., Levine, M., & Haley, B. (2011). Neural-specific elongation of 3' UTRs during Drosophila development. *Proceedings of the National Academy of Sciences*, *108*(38), 15864–15869. https://doi.org/10.1073/pnas.1112672108

Hsu, M.-T., & Coca-Prados, M. (1979). Electron microscopic evidence for the circular form of RNA in

the cytoplasm of eukaryotic cells. *Nature*, *280*(5720), Article 5720.

https://doi.org/10.1038/280339a0

Hsu, S.-D., Chu, C.-H., Tsou, A.-P., Chen, S.-J., Chen, H.-C., Hsu, P. W.-C., Wong, Y.-H., Chen, Y.-H.,

Chen, G.-H., & Huang, H.-D. (2008). miRNAMap 2.0: Genomic maps of microRNAs in

metazoan genomes. *Nucleic Acids Research*, *36*(Database issue), D165-169.

https://doi.org/10.1093/nar/gkm1012

Hunkler, H. J., Hoepfner, J., Huang, C.-K., Chatterjee, S., Jara-Avaca, M., Gruh, I., Bolesani, E.,

Zweigerdt, R., Thum, T., & Bär, C. (2020). The Long Non-coding RNA Cyrano Is Dispensable for

Pluripotency of Murine and Human Pluripotent Stem Cells. *Stem Cell Reports*, *15*(1), 13–21.

https://doi.org/10.1016/j.stemcr.2020.05.011

Ivanov, A., Memczak, S., Wyler, E., Torti, F., Porath, H. T., Orejuela, M. R., Piechotta, M., Levanon, E.

Y., Landthaler, M., Dieterich, C., & Rajewsky, N. (2015). Analysis of Intron Sequences Reveals

Hallmarks of Circular RNA Biogenesis in Animals. *Cell Reports*, *10*(2), 170–177.

https://doi.org/10.1016/j.celrep.2014.12.019

James, A. B., Conway, A.-M., & Morris, B. J. (2005). Genomic profiling of the neuronal target genes of

the plasticity-related transcription factor—Zif268. *Journal of Neurochemistry*, *95*(3), 796–810.

https://doi.org/10.1111/j.1471-4159.2005.03400.x

James, A. B., Conway, A.-M., & Morris, B. J. (2006). Regulation of the Neuronal Proteasome by Zif268

(Egr1). *Journal of Neuroscience*, *26*(5), 1624–1634. https://doi.org/10.1523/JNEUROSCI.4199-

05.2006

Jeck, W. R., Sorrentino, J. A., Wang, K., Slevin, M. K., Burd, C. E., Liu, J., Marzluff, W. F., & Sharpless, N.

E. (2013). Circular RNAs are abundant, conserved, and associated with ALU repeats. *RNA*,

19(2), 141–157. https://doi.org/10.1261/rna.035667.112

Jens, M., & Rajewsky, N. (2015). Competition between target sites of regulators shapes post-transcriptional gene regulation. *Nature Reviews Genetics*, *16*(2), 113–126. https://doi.org/10.1038/nrg3853

Jia, H., Gao, F., & Yu, D. (2021). Altered Temporal Structure of Neural Phase Synchrony in Patients With Autism Spectrum Disorder. *Frontiers in Psychiatry*, *12*, 618573. https://doi.org/10.3389/fpsyt.2021.618573

Jiang, C., Zeng, X., Shan, R., Wen, W., Li, J., Tan, J., Li, L., & Wan, R. (2020). The Emerging Picture of the Roles of CircRNA-CDR1as in Cancer. *Frontiers in Cell and Developmental Biology*, *8*. https://www.frontiersin.org/articles/10.3389/fcell.2020.590478

Kaech, S., & Banker, G. (2006). Culturing hippocampal neurons. *Nature Protocols*, *1*(5), 2406–2415. https://doi.org/10.1038/nprot.2006.356

Kandel, E. R. (2001). The Molecular Biology of Memory Storage: A Dialogue Between Genes and Synapses. *Science*, *294*(5544), 1030–1038. https://doi.org/10.1126/science.1067020

Kandel, E. R., Koester, J. D., Mack, S. H., & Siegelbaum, S. A. (2021). *Principles of Neural Science, Sixth Edition*. McGraw Hill Professional.

Karres, J. S., Hilgers, V., Carrera, I., Treisman, J., & Cohen, S. M. (2007). The Conserved microRNA MiR-8 Tunes Atrophin Levels to Prevent Neurodegeneration in Drosophila. *Cell*, *131*(1), 136–145. https://doi.org/10.1016/j.cell.2007.09.020

Kasper, S., & McEwen, B. S. (2008). Neurobiological and clinical effects of the antidepressant tianeptine. *CNS Drugs*, *22*(1), 15–26. https://doi.org/10.2165/00023210-200822010-00002

Kim, J., Abdelmohsen, K., Yang, X., De, S., Grammatikakis, I., Noh, J. H., & Gorospe, M. (2016). LncRNA OIP5-AS1/cyrano sponges RNA-binding protein HuR. *Nucleic Acids Research*, *44*(5), 2378–2392. https://doi.org/10.1093/nar/gkw017

Kleaveland, B., Shi, C. Y., Stefano, J., & Bartel, D. P. (2018). A Network of Noncoding Regulatory RNAs Acts in the Mammalian Brain. *Cell*, *174*(2), 350-362.e17. https://doi.org/10.1016/j.cell.2018.05.022

Köhrmann, M., Luo, M., Kaether, C., DesGroseillers, L., Dotti, C. G., & Kiebler, M. A. (1999). Microtubule-dependent Recruitment of Staufen-Green Fluorescent Protein into Large RNA-containing Granules and Subsequent Dendritic Transport in Living Hippocampal Neurons. *Molecular Biology of the Cell*, *10*(9), 2945–2953.

Korać, P., Antica, M., & Matulić, M. (2021). MiR-7 in Cancer Development. *Biomedicines*, *9*(3), 325. https://doi.org/10.3390/biomedicines9030325

Koshkin, F. A., Chistyakov, D. A., Nikitin, A. G., Konovalov, A. N., Potapov, A. A., Usachyov, D. Y., Pitskhelauri, D. I., Kobyakov, G. L., Shishkina, L. V., & Chekhonin, V. P. (2014). Profile of microRNA expression in brain tumors of different malignancy. *Bulletin of Experimental Biology and Medicine*, *157*(6), 794–797. https://doi.org/10.1007/s10517-014-2669-8

Kosik, K. S. (2006). The neuronal microRNA system. *Nature Reviews. Neuroscience*, *7*(12), 911–920. https://doi.org/10.1038/nrn2037

Kredo-Russo, S., Ness, A., Mandelbaum, A. D., Walker, M. D., & Hornstein, E. (2012). Regulation of pancreatic microRNA-7 expression. *Experimental Diabetes Research*, *2012*, 695214. https://doi.org/10.1155/2012/695214

Kristensen, L. S., Andersen, M. S., Stagsted, L. V. W., Ebbesen, K. K., Hansen, T. B., & Kjems, J. (2019). The biogenesis, biology and characterization of circular RNAs. *Nature Reviews Genetics*, *20*(11), 675–691. https://doi.org/10.1038/s41576-019-0158-7

Kristensen, L. S., Hansen, T. B., Venø, M. T., & Kjems, J. (2018). Circular RNAs in cancer: Opportunities and challenges in the field. *Oncogene*, *37*(5), Article 5. https://doi.org/10.1038/onc.2017.361

Lafourcade, C. A., Fernández, A., Ramírez, J. P., Corvalán, K., Carrasco, M. Á., Iturriaga, A., Bátiz, L. F., Luarte, A., & Wyneken, U. (2020). A Role for mir-26a in Stress: A Potential sEV Biomarker and Modulator of Excitatory Neurotransmission. *Cells*, *9*(6), 1364. https://doi.org/10.3390/cells9061364

Lanahan, A., & Worley, P. (1998). Immediate-early genes and synaptic function. *Neurobiology of Learning and Memory*, *70*(1–2), 37–43. https://doi.org/10.1006/nlme.1998.3836

Landgraf, P., Rusu, M., Sheridan, R., Sewer, A., Iovino, N., Aravin, A., Pfeffer, S., Rice, A., Kamphorst, A. O., Landthaler, M., Lin, C., Socci, N. D., Hermida, L., Fulci, V., Chiaretti, S., Foà, R., Schliwka, J., Fuchs, U., Novosel, A., … Tuschl, T. (2007). A mammalian microRNA expression atlas based on small RNA library sequencing. *Cell*, *129*(7), 1401–1414. https://doi.org/10.1016/j.cell.2007.04.040

LaPierre, M. P., Lawler, K., Godbersen, S., Farooqi, I. S., & Stoffel, M. (2022). MicroRNA-7 regulates melanocortin circuits involved in mammalian energy homeostasis. *Nature Communications*, *13*(1), Article 1. https://doi.org/10.1038/s41467-022-33367-w

LaPierre, M. P., & Stoffel, M. (2017). MicroRNAs as stress regulators in pancreatic beta cells and diabetes. *Molecular Metabolism*, *6*(9), 1010–1023. https://doi.org/10.1016/j.molmet.2017.06.020

Latreille, M., Hausser, J., Stützer, I., Zhang, Q., Hastoy, B., Gargani, S., Kerr-Conte, J., Pattou, F., Zavolan, M., Esguerra, J. L. S., Eliasson, L., Rülicke, T., Rorsman, P., & Stoffel, M. (2014). MicroRNA-7a regulates pancreatic β cell function. *The Journal of Clinical Investigation*, *124*(6), 2722–2735. https://doi.org/10.1172/JCI73066

Lebedeva, S., Jens, M., Theil, K., Schwanhäusser, B., Selbach, M., Landthaler, M., & Rajewsky, N. (2011). Transcriptome-wide analysis of regulatory interactions of the RNA-binding protein HuR. *Molecular Cell*, *43*(3), 340–352. https://doi.org/10.1016/j.molcel.2011.06.008

Li, Q., Lee, J.-A., & Black, D. L. (2007). Neuronal regulation of alternative pre-mRNA splicing. *Nature Reviews Neuroscience*, *8*(11), Article 11. https://doi.org/10.1038/nrn2237

Li, X., & Carthew, R. W. (2005). A microRNA mediates EGF receptor signaling and promotes photoreceptor differentiation in the Drosophila eye. *Cell*, *123*(7), 1267–1277. https://doi.org/10.1016/j.cell.2005.10.040

Li, X., Cassidy, J. J., Reinke, C. A., Fischboeck, S., & Carthew, R. W. (2009). A MicroRNA Imparts Robustness against Environmental Fluctuation during Development. *Cell*, *137*(2), 273–282. https://doi.org/10.1016/j.cell.2009.01.058

Licatalosi, D. D., & Darnell, R. B. (2006). Splicing regulation in neurologic disease. *Neuron*, *52*(1), 93–101. https://doi.org/10.1016/j.neuron.2006.09.017

Licatalosi, D. D., & Darnell, R. B. (2010). RNA processing and its regulation: Global insights into biological networks. *Nature Reviews Genetics*, *11*(1), Article 1. https://doi.org/10.1038/nrg2673

Lin, S.-P., Ye, S., Long, Y., Fan, Y., Mao, H.-F., Chen, M.-T., & Ma, Q.-J. (2016). Circular RNA expression alterations are involved in OGD/R-induced neuron injury. *Biochemical and Biophysical Research Communications*, *471*(1), 52–56. https://doi.org/10.1016/j.bbrc.2016.01.183

Lodish, U. H., Lodish, H., Berk, A., Kaiser, C. A., Kaiser, C., Krieger, M., Kaiser, U. C. A., Scott, M. P., Bretscher, A., Ploegh, H., Matsudaira, P., Ploegh, U. H., & Matsudaira, U. P. (2008). *Molecular Cell Biology*. W. H. Freeman.

Lugli, G., Larson, J., Martone, M. E., Jones, Y., & Smalheiser, N. R. (2005). Dicer and eIF2c are enriched at postsynaptic densities in adult mouse brain and are modified by neuronal activity in a calpain-dependent manner. *Journal of Neurochemistry*, *94*(4), 896–905. https://doi.org/10.1111/j.1471-4159.2005.03224.x

Lukiw, W. J. (2013). Circular RNA (circRNA) in Alzheimer's disease (AD). *Frontiers in Genetics*, *4*. https://doi.org/10.3389/fgene.2013.00307

Lyons, M. R., & West, A. E. (2011). Mechanisms of specificity in neuronal activity-regulated gene transcription. *Progress in Neurobiology*, *94*(3), 259–295. https://doi.org/10.1016/j.pneurobio.2011.05.003

Marie, H., Morishita, W., Yu, X., Calakos, N., & Malenka, R. C. (2005). Generation of silent synapses by acute in vivo expression of CaMKIV and CREB. *Neuron*, *45*(5), 741–752. https://doi.org/10.1016/j.neuron.2005.01.039

Marini, F., & Binder, H. (2019). pcaExplorer: An R/Bioconductor package for interacting with RNA-seq principal components. *BMC Bioinformatics*, *20*(1), 331. https://doi.org/10.1186/s12859-019-2879-1

Martin, K. C., & Ephrussi, A. (2009). mRNA Localization: Gene Expression in the Spatial Dimension. *Cell*, *136*(4), 719–730. https://doi.org/10.1016/j.cell.2009.01.044

Marvin, J. S., Borghuis, B. G., Tian, L., Cichon, J., Harnett, M. T., Akerboom, J., Gordus, A., Renninger, S. L., Chen, T.-W., Bargmann, C. I., Orger, M. B., Schreiter, E. R., Demb, J. B., Gan, W.-B., Hires, S. A., & Looger, L. L. (2013). An optimized fluorescent probe for visualizing glutamate neurotransmission. *Nature Methods*, *10*(2), Article 2. https://doi.org/10.1038/nmeth.2333

Mayr, C. (2016). Evolution and Biological Roles of Alternative 3'UTRs. *Trends in Cell Biology*, *26*(3), 227–237. https://doi.org/10.1016/j.tcb.2015.10.012

Memczak, S., Jens, M., Elefsinioti, A., Torti, F., Krueger, J., Rybak, A., Maier, L., Mackowiak, S. D., Gregersen, L. H., Munschauer, M., Loewer, A., Ziebold, U., Landthaler, M., Kocks, C., le Noble, F., & Rajewsky, N. (2013). Circular RNAs are a large class of animal RNAs with regulatory potency. *Nature*, *495*(7441), 333–338. https://doi.org/10.1038/nature11928

Mendonsa, S., von Kügelgen, N., Dantsuji, S., Ron, M., Breimann, L., Baranovskii, A., Lödige, I., Kirchner, M., Fischer, M., Zerna, N., Bujanic, L., Mertins, P., Ulitsky, I., & Chekulaeva, M. (2023). Massively parallel identification of mRNA localization elements in primary cortical neurons. *Nature Neuroscience*, 1–12. https://doi.org/10.1038/s41593-022-01243-x

Middleton, S. A., Eberwine, J., & Kim, J. (2019). Comprehensive catalog of dendritically localized mRNA isoforms from sub-cellular sequencing of single mouse neurons. *BMC Biology*, *17*(1), 5. https://doi.org/10.1186/s12915-019-0630-z

miRNA gene family: Mir-7 (43 sequences). (2007, September 29). https://web.archive.org/web/20070929111655/http://microrna.sanger.ac.uk/cgi-bin/sequences/mirna_summary.pl?fam=MIPF0000022

Miura, P., Shenker, S., Andreu-Agullo, C., Westholm, J. O., & Lai, E. C. (2013). Widespread and extensive lengthening of 3' UTRs in the mammalian brain. *Genome Research*, *23*(5), 812–825. https://doi.org/10.1101/gr.146886.112

Moore, M. J., Scheel, T. K. H., Luna, J. M., Park, C. Y., Fak, J. J., Nishiuchi, E., Rice, C. M., & Darnell, R. B. (2015). MiRNA–target chimeras reveal miRNA 3'-end pairing as a major determinant of Argonaute target specificity. *Nature Communications*, *6*(1), Article 1. https://doi.org/10.1038/ncomms9864

Morales-Martínez, M., & Vega, M. I. (2022). Role of MicroRNA-7 (MiR-7) in Cancer Physiopathology. *International Journal of Molecular Sciences*, *23*(16), Article 16. https://doi.org/10.3390/ijms23169091

Morris, K. V., & Mattick, J. S. (2014). The rise of regulatory RNA. *Nature Reviews Genetics*, *15*(6), Article 6. https://doi.org/10.1038/nrg3722

Nigro, J. M., Cho, K. R., Fearon, E. R., Kern, S. E., Ruppert, J. M., Oliner, J. D., Kinzler, K. W., & Vogelstein, B. (1991). Scrambled exons. *Cell*, *64*(3), 607–613. https://doi.org/10.1016/0092-8674(91)90244-s

Onitsuka, T., Oribe, N., & Kanba, S. (2013). Neurophysiological findings in patients with bipolar disorder. In *Supplements to Clinical Neurophysiology* (Vol. 62, pp. 197–206). Elsevier. https://doi.org/10.1016/B978-0-7020-5307-8.00013-2

Pan, Q., Shai, O., Lee, L. J., Frey, B. J., & Blencowe, B. J. (2008). Deep surveying of alternative splicing complexity in the human transcriptome by high-throughput sequencing. *Nature Genetics*, *40*(12), 1413–1415. https://doi.org/10.1038/ng.259

Pereira, L. A., Munita, R., González, M. P., & Andrés, M. E. (2017). Long 3'UTR of Nurr1 mRNAs is targeted by miRNAs in mesencephalic dopamine neurons. *PLOS ONE*, *12*(11), e0188177. https://doi.org/10.1371/journal.pone.0188177

Perillo, M., Paganos, P., Mattiello, T., Cocurullo, M., Oliveri, P., & Arnone, M. I. (2018). New Neuronal Subtypes With a "Pre-Pancreatic" Signature in the Sea Urchin Stongylocentrotus purpuratus. *Frontiers in Endocrinology*, *9*, 650. https://doi.org/10.3389/fendo.2018.00650

Piwecka, M., Glažar, P., Hernandez-Miranda, L. R., Memczak, S., Wolf, S. A., Rybak-Wolf, A., Filipchyk, A., Klironomos, F., Cerda Jara, C. A., Fenske, P., Trimbuch, T., Zywitza, V., Plass, M., Schreyer,

L., Ayoub, S., Kocks, C., Kühn, R., Rosenmund, C., Birchmeier, C., & Rajewsky, N. (2017). Loss of a mammalian circular RNA locus causes miRNA deregulation and affects brain function. *Science (New York, N.Y.)*, *357*(6357), eaam8526. https://doi.org/10.1126/science.aam8526

Pollock, A., Bian, S., Zhang, C., Chen, Z., & Sun, T. (2014). Growth of the Developing Cerebral Cortex Is Controlled by MicroRNA-7 through the p53 Pathway. *Cell Reports*, *7*(4), 1184–1196. https://doi.org/10.1016/j.celrep.2014.04.003

Powell, S. B., Weber, M., & Geyer, M. A. (2012). Genetic Models of Sensorimotor Gating: Relevance to Neuropsychiatric Disorders. *Current Topics in Behavioral Neurosciences*, *12*, 251–318. https://doi.org/10.1007/7854_2011_195

Proudfoot, N. J., & Brownlee, G. G. (1976). 3' Non-coding region sequences in eukaryotic messenger RNA. *Nature*, *263*(5574), Article 5574. https://doi.org/10.1038/263211a0

Quattrone, A., Pascale, A., Nogues, X., Zhao, W., Gusev, P., Pacini, A., & Alkon, D. L. (2001). Posttranscriptional regulation of gene expression in learning by the neuronal ELAV-like mRNA-stabilizing proteins. *Proceedings of the National Academy of Sciences*, *98*(20), 11668–11673. https://doi.org/10.1073/pnas.191388398

Raj, A., van den Bogaard, P., Rifkin, S. A., van Oudenaarden, A., & Tyagi, S. (2008). Imaging individual mRNA molecules using multiple singly labeled probes. *Nature Methods*, *5*(10), 877–879. https://doi.org/10.1038/nmeth.1253

Rajman, M., & Schratt, G. (2017). MicroRNAs in neural development: From master regulators to fine-tuners. *Development*, *144*(13), 2310–2322. https://doi.org/10.1242/dev.144337

Reznikov, L. R., Fadel, J. R., & Reagan, L. P. (2009). Glutamate-Mediated Neuroplasticity Deficits in Mood Disorders. In J. A. Costa e Silva, J. P. Macher, & J. P. Olié (Eds.), *Neuroplasticity: New Biochemical Mechanisms* (pp. 13–26). Springer Healthcare Ltd. https://doi.org/10.1007/978-1-908517-18-0_2

Rienecker, K. D. A., Poston, R. G., & Saha, R. N. (2020). Merits and Limitations of Studying Neuronal

    Depolarization-Dependent Processes Using Elevated External Potassium. *ASN Neuro*, *12*,

    1759091420974807. https://doi.org/10.1177/1759091420974807

Rodrigues, D. C., Kim, D.-S., Yang, G., Zaslavsky, K., Ha, K. C. H., Mok, R. S. F., Ross, P. J., Zhao, M.,

    Piekna, A., Wei, W., Blencowe, B. J., Morris, Q., & Ellis, J. (2016). MECP2 Is Post-

    transcriptionally Regulated during Human Neurodevelopment by Combinatorial Action of

    RNA-Binding Proteins and miRNAs. *Cell Reports*, *17*(3), 720–734.

    https://doi.org/10.1016/j.celrep.2016.09.049

Rybak-Wolf, A., Stottmeister, C., Glažar, P., Jens, M., Pino, N., Giusti, S., Hanan, M., Behm, M., Bartok,

    O., Ashwal-Fluss, R., Herzog, M., Schreyer, L., Papavasileiou, P., Ivanov, A., Öhman, M.,

    Refojo, D., Kadener, S., & Rajewsky, N. (2015). Circular RNAs in the Mammalian Brain Are

    Highly Abundant, Conserved, and Dynamically Expressed. *Molecular Cell*, *58*(5), 870–885.

    https://doi.org/10.1016/j.molcel.2015.03.027

Saetrom, P., Heale, B. S. E., Snøve, O., Aagaard, L., Alluin, J., & Rossi, J. J. (2007). Distance constraints

    between microRNA target sites dictate efficacy and cooperativity. *Nucleic Acids Research*,

    35(7), 2333–2342. https://doi.org/10.1093/nar/gkm133

Salzman, J., Gawad, C., Wang, P. L., Lacayo, N., & Brown, P. O. (2012). Circular RNAs Are the

    Predominant Transcript Isoform from Hundreds of Human Genes in Diverse Cell Types. *PLoS*

    ONE, *7*(2), e30733. https://doi.org/10.1371/journal.pone.0030733

Sambandan, S., Akbalik, G., Kochen, L., Rinne, J., Kahlstatt, J., Glock, C., Tushev, G., Alvarez-Castelao,

    B., Heckel, A., & Schuman, E. M. (2017). Activity-dependent spatially localized miRNA

    maturation in neuronal dendrites. *Science*, *355*(6325), 634–637.

    https://doi.org/10.1126/science.aaf8995

Schratt, G. (2009). MicroRNAs at the synapse. *Nature Reviews Neuroscience*, *10*(12), 842–849.

    https://doi.org/10.1038/nrn2763

Schratt, G. M., Tuebing, F., Nigh, E. A., Kane, C. G., Sabatini, M. E., Kiebler, M., & Greenberg, M. E. (2006). A brain-specific microRNA regulates dendritic spine development. *Nature*, *439*(7074), 283–289. https://doi.org/10.1038/nature04367

Shi, Z., Chen, T., Yao, Q., Zheng, L., Zhang, Z., Wang, J., Hu, Z., Cui, H., Han, Y., Han, X., Zhang, K., & Hong, W. (2017). The circular RNA ciRS-7 promotes APP and BACE1 degradation in an NF-κB-dependent manner. *The FEBS Journal*, *284*(7), 1096–1109. https://doi.org/10.1111/febs.14045

Smith, K. N., Starmer, J., Miller, S. C., Sethupathy, P., & Magnuson, T. (2017). Long Noncoding RNA Moderates MicroRNA Activity to Maintain Self-Renewal in Embryonic Stem Cells. *Stem Cell Reports*, *9*(1), 108–121. https://doi.org/10.1016/j.stemcr.2017.05.005

Spruston, N. (2008). Pyramidal neurons: Dendritic structure and synaptic integration. *Nature Reviews Neuroscience*, *9*(3), Article 3. https://doi.org/10.1038/nrn2286

Suenkel, C., Cavalli, D., Massalini, S., Calegari, F., & Rajewsky, N. (2020). A Highly Conserved Circular RNA Is Required to Keep Neural Cells in a Progenitor State in the Mammalian Brain. *Cell Reports*, *30*(7), 2170-2179.e5. https://doi.org/10.1016/j.celrep.2020.01.083

Swerdlow, N. R., & Light, G. A. (2018). Sensorimotor gating deficits in schizophrenia: Advancing our understanding of the phenotype, its neural circuitry and genetic substrates. *Schizophrenia Research*, *198*, 1–5. https://doi.org/10.1016/j.schres.2018.02.042

Tessmar-Raible, K., Raible, F., Christodoulou, F., Guy, K., Rembold, M., Hausen, H., & Arendt, D. (2007). Conserved sensory-neurosecretory cell types in annelid and fish forebrain: Insights into hypothalamus evolution. *Cell*, *129*(7), 1389–1400. https://doi.org/10.1016/j.cell.2007.04.041

Tischmeyer, W., & Grimm, R. (1999). Activation of immediate early genes and memory formation. *Cellular and Molecular Life Sciences CMLS*, *55*(4), 564–574. https://doi.org/10.1007/s000180050315

Tyssowski, K. M., DeStefino, N. R., Cho, J.-H., Dunn, C. J., Poston, R. G., Carty, C. E., Jones, R. D., Chang, S. M., Romeo, P., Wurzelmann, M. K., Ward, J. M., Andermann, M. L., Saha, R. N., Dudek, S. M., & Gray, J. M. (2018). Different Neuronal Activity Patterns Induce Different Gene Expression Programs. *Neuron*, *98*(3), 530-546.e11. https://doi.org/10.1016/j.neuron.2018.04.001

Ule, J., Ule, A., Spencer, J., Williams, A., Hu, J.-S., Cline, M., Wang, H., Clark, T., Fraser, C., Ruggiu, M., Zeeberg, B. R., Kane, D., Weinstein, J. N., Blume, J., & Darnell, R. B. (2005). Nova regulates brain-specific splicing to shape the synapse. *Nature Genetics*, *37*(8), 844–852. https://doi.org/10.1038/ng1610

Ulitsky, I., Shkumatava, A., Jan, C. H., Sive, H., & Bartel, D. P. (2011). Conserved Function of lincRNAs in Vertebrate Embryonic Development despite Rapid Sequence Evolution. *Cell*, *147*(7), 1537–1550. https://doi.org/10.1016/j.cell.2011.11.055

Vasudevan, S., Tong, Y., & Steitz, J. A. (2007). Switching from Repression to Activation: MicroRNAs Can Up-Regulate Translation. *Science*, *318*(5858), 1931–1934. https://doi.org/10.1126/science.1149460

Venø, M. T., Hansen, T. B., Venø, S. T., Clausen, B. H., Grebing, M., Finsen, B., Holm, I. E., & Kjems, J. (2015). Spatio-temporal regulation of circular RNA expression during porcine embryonic brain development. *Genome Biology*, *16*(1), 245. https://doi.org/10.1186/s13059-015-0801-3

Vo, N., Klein, M. E., Varlamova, O., Keller, D. M., Yamamoto, T., Goodman, R. H., & Impey, S. (2005). A cAMP-response element binding protein-induced microRNA regulates neuronal morphogenesis. *Proceedings of the National Academy of Sciences of the United States of America*, *102*(45), 16426–16431. https://doi.org/10.1073/pnas.0508448102

Weng, W., Wei, Q., Toden, S., Yoshida, K., Nagasaka, T., Fujiwara, T., Cai, S., Qin, H., Ma, Y., & Goel, A. (2017). Circular RNA ciRS-7-A Promising Prognostic Biomarker and a Potential Therapeutic Target in Colorectal Cancer. *Clinical Cancer Research: An Official Journal of the American*

Association for Cancer Research, *23*(14), 3918–3928. https://doi.org/10.1158/1078-0432.CCR-16-2541

Westholm, J. O., Miura, P., Olson, S., Shenker, S., Joseph, B., Sanfilippo, P., Celniker, S. E., Graveley, B. R., & Lai, E. C. (2014). Genome-wide Analysis of Drosophila Circular RNAs Reveals Their Structural and Sequence Properties and Age-Dependent Neural Accumulation. *Cell Reports*, *9*(5), 1966–1980. https://doi.org/10.1016/j.celrep.2014.10.062

Wu, W., Ji, P., & Zhao, F. (2020). CircAtlas: An integrated resource of one million highly accurate circular RNAs from 1070 vertebrate transcriptomes. *Genome Biology*, *21*(1), 101. https://doi.org/10.1186/s13059-020-02018-y

Xia, S., Feng, J., Lei, L., Hu, J., Xia, L., Wang, J., Xiang, Y., Liu, L., Zhong, S., Han, L., & He, C. (2017). Comprehensive characterization of tissue-specific circular RNAs in the human and mouse genomes. *Briefings in Bioinformatics*, *18*(6), 984–992. https://doi.org/10.1093/bib/bbw081

Xu, H., Guo, S., Li, W., & Yu, P. (2015). The circular RNA Cdr1as, via miR-7 and its targets, regulates insulin transcription and secretion in islet cells. *Scientific Reports*, *5*(1), 12453. https://doi.org/10.1038/srep12453

Xu, K., Chen, D., Wang, Z., Ma, J., Zhou, J., Chen, N., Lv, L., Zheng, Y., Hu, X., Zhang, Y., & Li, J. (2018). Annotation and functional clustering of circRNA expression in rhesus macaque brain during aging. *Cell Discovery*, *4*. https://doi.org/10.1038/s41421-018-0050-1

Xu, K., Zhang, Y., Xiong, W., Zhang, Z., Wang, Z., Lv, L., Liu, C., Hu, Z., Zheng, Y.-T., Lu, L., Hu, X.-T., & Li, J. (2020). CircGRIA1 shows an age-related increase in male macaque brain and regulates synaptic plasticity and synaptogenesis. *Nature Communications*, *11*(1), Article 1. https://doi.org/10.1038/s41467-020-17435-7

Yang, H., Wang, H., Shang, H., Chen, X., Yang, S., Qu, Y., Ding, J., & Li, X. (2019). Circular RNA circ_0000950 promotes neuron apoptosis, suppresses neurite outgrowth and elevates inflammatory cytokines levels via directly sponging miR-103 in Alzheimer's disease. *Cell Cycle*, *18*(18), 2197–2214. https://doi.org/10.1080/15384101.2019.1629773

Yoshimoto, R., Rahimi, K., Hansen, T. B., Kjems, J., & Mayeda, A. (2020). Biosynthesis of Circular RNA

ciRS-7/CDR1as Is Mediated by Mammalian-wide Interspersed Repeats. *IScience*, *23*(7),

101345. https://doi.org/10.1016/j.isci.2020.101345

You, X., Vlatkovic, I., Babic, A., Will, T., Epstein, I., Tushev, G., Akbalik, G., Wang, M., Glock, C.,

Quedenau, C., Wang, X., Hou, J., Liu, H., Sun, W., Sambandan, S., Chen, T., Schuman, E. M., &

Chen, W. (2015). Neural circular RNAs are derived from synaptic genes and regulated by

development and plasticity. *Nature Neuroscience*, *18*(4), 603–610.

https://doi.org/10.1038/nn.3975

Zappulo, A., van den Bruck, D., Ciolli Mattioli, C., Franke, V., Imami, K., McShane, E., Moreno-Estelles,

M., Calviello, L., Filipchyk, A., Peguero-Sanchez, E., Müller, T., Woehler, A., Birchmeier, C.,

Merino, E., Rajewsky, N., Ohler, U., Mazzoni, E. O., Selbach, M., Akalin, A., & Chekulaeva, M.

(2017). RNA localization is a key determinant of neurite-enriched proteome. *Nature

Communications*, *8*(1), Article 1. https://doi.org/10.1038/s41467-017-00690-6

Zeldenrust, F., Wadman, W. J., & Englitz, B. (2018). Neural Coding With Bursts—Current State and

Future Perspectives. *Frontiers in Computational Neuroscience*, *12*, 48.

https://doi.org/10.3389/fncom.2018.00048

Zhang, L., Li, Z., Mao, L., & Wang, H. (2022). Circular RNA in Acute Central Nervous System Injuries: A

New Target for Therapeutic Intervention. *Frontiers in Molecular Neuroscience*, *15*.

https://www.frontiersin.org/articles/10.3389/fnmol.2022.816182

Zhang, N., Gao, Y., Yu, S., Sun, X., & Shen, K. (2020). Berberine attenuates Aβ42-induced neuronal

damage through regulating circHDAC9/miR-142-5p axis in human neuronal cells. *Life

Sciences*, *252*, 117637. https://doi.org/10.1016/j.lfs.2020.117637

Zhang, X.-O., Wang, H.-B., Zhang, Y., Lu, X., Chen, L.-L., & Yang, L. (2014). Complementary Sequence-

Mediated Exon Circularization. *Cell*, *159*(1), 134–147.

https://doi.org/10.1016/j.cell.2014.09.001

Zhang, Y., Zhang, X.-O., Chen, T., Xiang, J.-F., Yin, Q.-F., Xing, Y.-H., Zhu, S., Yang, L., & Chen, L.-L.

(2013). Circular Intronic Long Noncoding RNAs. *Molecular Cell*, *51*(6), 792–806.

https://doi.org/10.1016/j.molcel.2013.08.017

Zhao, W., Hirose, T., Ishikawa, M., Oshima, Y., Hirai, S.-I., Ohno, S., & Taniguchi, H. (2007). Neonatal

pancreatic cells redifferentiate into both neural and pancreatic lineages. *Biochemical and*

Biophysical Research Communications, *352*(1), 84–90.

https://doi.org/10.1016/j.bbrc.2006.10.179

Zhao, Y., Alexandrov, P. N., Jaber, V., & Lukiw, W. J. (2016). Deficiency in the Ubiquitin Conjugating

Enzyme UBE2A in Alzheimer's Disease (AD) is Linked to Deficits in a Natural Circular miRNA-7

Sponge (circRNA; ciRS-7). *Genes*, *7*(12), E116. https://doi.org/10.3390/genes7120116

Acknowledgements